EVIDENCE FOR REGIONAL EXTENSIONAL FAULTING AT GREY ROCKS RIDGE, EASTERN KLAMATH MOUNTAINS, CALIFORNIA

By

Emily C. Fudge

A Thesis

Presented to

The Faculty of Humboldt State University.

In Partial Fulfillment

Of the Requirements for the Degree of

Master of Environmental Systems:

Geology

October, 2008

EVIDENCE FOR REGIONAL EXTENSIONAL FAULTING AT

GREY ROCKS RIDGE,

EASTERN KLAMATH MOUNTAINS,

CALIFORNIA

By

Emily C. Fudge

Approved by the Masters Thesis Committee:

Dr. Susan Cashman, Major Professor	Date
Dr. Brandon Schwab, Committee Member	Date
Dr. Harvey Kelsey, Committee Member	Date
Dr. Chris Dugaw, Graduate Coordinator	Date
Chris Hopper, Interim Dean, Research, Graduate Studies, and International Programs	

ABSTRACT

Geologic mapping of the Grey Rocks Ridge area identified three klippes of Devonian Copley Greenstone separated from the underlying Trinity terrane by an undulating extensional fault and preserved by oblique down-dropping on NW-NE striking faults. The Grey Rocks klippe and the Horse Heaven Meadows klippe dip shallowly (5 to10 degrees) to the N-NE and have convex boundaries. The basal fault is associated with regional extensional faulting that extends across the Eastern Klamath Mountains.

Geochemical analysis links the greenstone pillows of the Grey Rocks and Panther Rock klippes to the Copley Greenstone of the Redding terrane. The Horse Heaven Meadows klippe is comprised mainly of fractured slate with minor amounts of volcanic breccias and tuffs, forming a localized lens within the Copley Greenstone. A similar metasedimentary and metavolcanic lens is located in the southern section of the Grey Rocks klippe.

The three klippes form the hanging wall of a regional extensional fault that juxtaposes the three klippes over the underlying Trinity terrane. The undeformed greenstone pillows of Grey Rocks and Panther Rock klippes and the fractured metavolcanic and metasedimentary units of the Horse Heaven Meadows klippe clearly contrast with the mylonite and fault breccia at the contact and with the serpentinized mafic/ultramafic complex (Trinity terrane) of the footwall. Geochemical values of fault zone mylonite indicate elevated values of Al_2O_3 and depleted values of MgO when

compared to ultramafic compositional values, supporting a mixing of upper and lower plate components.

Fault outcrop characteristics include mylonite, foliated fault breccia zones, and parallel foliation observed in proximal greenstone and ultramafic rocks. Quartz veins run both parallel and perpendicular to foliation, suggesting that injection of hydrothermal fluids accompanied faulting and accommodated extensional deformation of more coherent rock. In thin section, fault proximal rocks in the upper and lower plate exhibit shear microstructures including foliation, s-c fabrics, planar mineral alignment, sigma clasts, pull-apart clasts, and perpendicular to foliation quartz veining.

Felsic dikes intrude the fault breccia at the base of the Horse Heaven Meadows klippe and intrude parallel to the fault zone at the base of the Grey Rocks klippe. Emplacement of the parallel dike is interpreted to be syntectonic with the extensional faulting event based on shear and extensional microstructures such as anastomosing foliation and perpendicular to foliation quartz veining.

ACKNOWLEDGEMENTS

I am grateful to the many individuals who led to the completion of this thesis. My advisors were key in me attaining my degree. Dr. Sue Cashman answered questions, contributed ideas, read endless versions of my paper, and provided funding for the thin-sections. Dr. Brandon Schwab provided the use of a photomicrograph camera, access to petrographic resource materials, and helpful review comments. Dr. Harvey Kelsey provided constructive comments that improved the manuscript and aided in the final push to finish.

Thank you to those who volunteered to accompany me in the field and generated discussion. Field assistants Tim Glidden, Mort Larsen, Nick Graehl, Julianne Fudge, and Emily Hobelmann accompanied me on adventures around Grey Rocks, collected data, battled the elements, and helped keep me sane. Don Elder and Juan de la Fuente shared their expertise in the field and contributed to stimulating discussions of Grey Rocks and Klamath Mountain geology. Don Elder provided additional background information. Juan de la Fuente and the Shasta-Trinity National Forest provided access to air photos of the field area. Peter Masson shared unpublished geologic maps and photographs of Grey Rocks.

I thank Scott North for geochemical analyses from the Humboldt State University Geology Department's XRF lab. In addition, Dr. Keith Putirka generously provided access to the XRF machine at CSU Fresno and Gerardo Torrez analyzed samples for my project.

I am very thankful for financial support from the U.S. Geological Survey, EdMap program for geological mapping, and from the Northern California Geological Society for travel to the Geological Society of America meeting in Alaska to present research results. Thank you to Humboldt State University and the Geology Department for additional financial assistance and access to resources like the thin-section lab and the XRF machine.

Lastly, thanks to all those who made HSU a memorable experience: Emily Hobelmann, Stephanie Oliveira, Julianne Fudge, my family, teachers, and all of my friends…you know who you are.

TABLE OF CONTENTS

TABLE OF TABLES

TABLE PAGE

TABLE OF FIGURES

FIGURE PAGE

INTRODUCTION

At Grey Rocks ridge, located in the Klamath and Trinity Mountains of northern California, three small bodies of greenstone and fine-grained metasedimentary rocks overlie the Trinity ultramafic complex. The "Grey Rocks outlier" (Irwin, 1966) occupies a key position in the tectonic evolution of the Klamath Mountains provenance. Conflicting interpretations on the structural relations and stratigraphic affiliation of the Grey Rocks outliers include: formation as part of a classic ophiolitic sequence (Brouxel and Lapierre, 1988), formation in an island arc (Irwin, 1981; Albers and Bain, 1985; Doe et. al, 1985), formation in a suprasubduction zone (Wallin and Metcalf, 1998), remnant of a thrust plate (Irwin, 1966; Brouxel et al., 1989), and tectonic emplacement by extensional faulting (Schweickert and Irwin, 1989; Masson, 2002; Cashman and Elder, 2002).

The project concentrates on mapping three klippes in the Grey Rocks area (Plate 1), identifying the nature of the contact between the Trinity ultramafic complex and the structurally overlying metasedimentary and metavolcanic units, and geochemically and descriptively correlating the geologic units with known formations using x-ray fluorescence analysis.

The three klippes are termed the Panther Rock klippe, the Horse Heaven Meadows klippe, and the Grey Rocks klippe. To maintain continuity the term greenstone will relate to both hydrothermally altered basalts and basalts altered in the greenschist facies. The term mylonite refers to fine-grained fault rocks that form as a result of ductile

deformation at temperatures between 250 ^{o}C – 350 ^{o}C and depths of 10 to 15 km. Mylonitic texture includes a planar foliation and recrystallization of minerals (Twiss and Moores, 1992).

Geologic Setting

Regional Geology

The Klamath Mountains Province is comprised of a series of arcuate, accreted terranes resulting from Paleozoic to Mesozoic subduction along the western plate boundary of the North American plate (Irwin, 1960; 1963; 1966; 1972; 1994). Terranes young to the west and are separated by major north-south-striking, east-dipping thrust faults (Irwin, 1966; 1972; 1994). Mesozoic plutons and dikes intrude the terranes (Irwin, 1966; 1994). N-S Tertiary extensional faulting cuts across all terranes of the Eastern Klamath Mountains (Schweickert and Irwin, 1989; Cashman and Elder, 2002).

Eastern Klamath Belt

The study site is located within the Eastern Klamath Belt, which is the oldest and eastern-most accreted terrane (Fig. 1). The Eastern Klamath Belt is subdivided into the Trinity, Yreka, and Redding terranes based on distinctive stratigraphic successions, magmatic histories, and age relations of rock units (Irwin, 1966; 1972; 1994). Mesozoic post-amalgamation plutons, including the Shasta Bally batholith, Castle Crags pluton, and Craggy Peak pluton area, have intruded all three terranes within the Eastern Klamath Belt (Irwin, 1994).

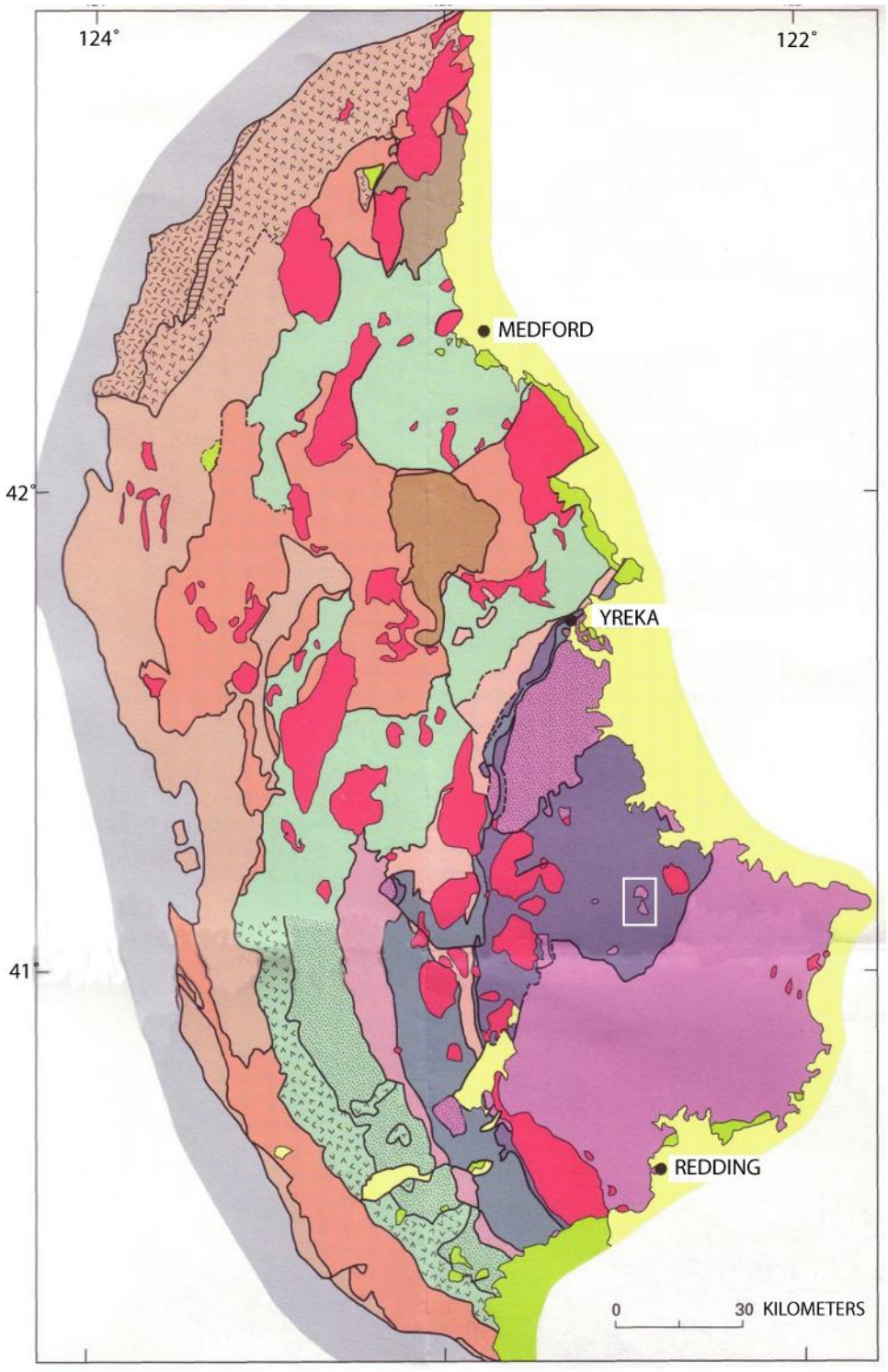

Figure 1A: Geologic Map of the Klamath and Trinity Mountains, Northern California, compiled by Irwin (1994). Bounding box shows the location of the Grey Rocks study area.

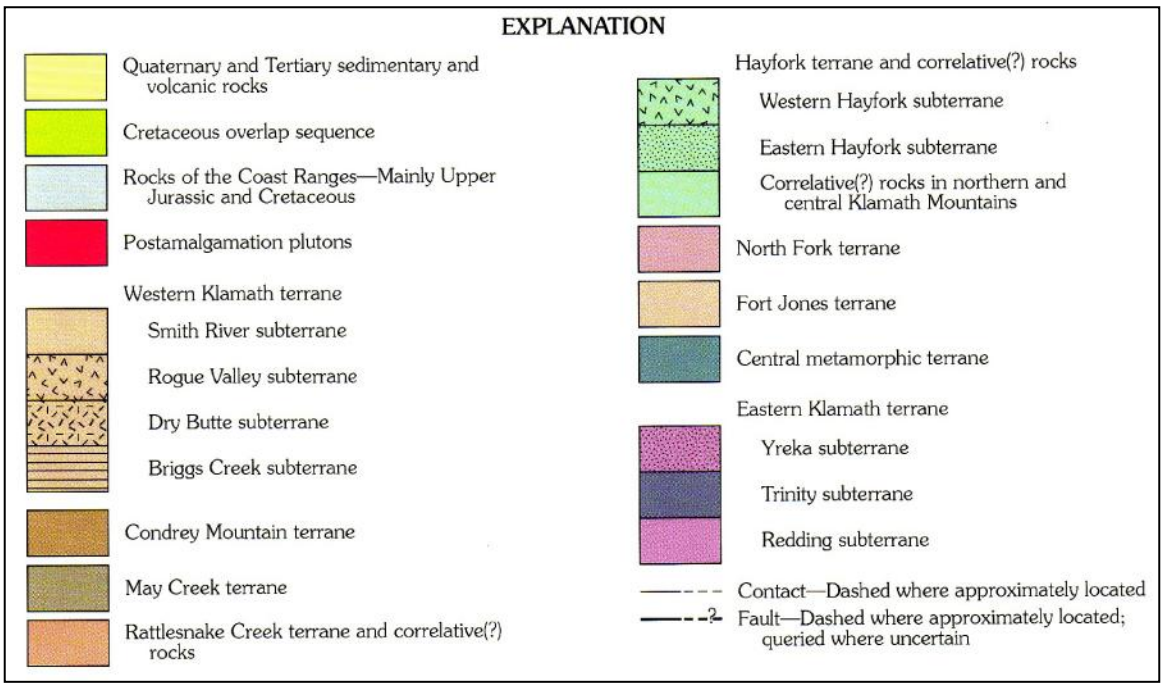

Figure 1B: Legend for the geologic map in Figure 1A (Irwin, 1994).

Trinity Terrane. The Trinity terrane, at the center of the Eastern Klamath Belt, is the oldest of the three terranes dating from Vendian to Siluro-Devonian (Jacobsen et al., 1984; Lindsley-Griffin et al., 2006), and is stratigraphically the lowest terrane in the Eastern Klamath Belt (Irwin and Lipman, 1962). The Trinity terrane is estimated to be between 6.5 and 8 km thick based on models combining seismic, gravity, and aeromagnetic data (Zucca et al., 1986).

The polygenetic Trinity terrane consists of tectonically foliated, ultramafic packages and two crustal sequences, one Vendian and one Siluro-Devonian with minor associated Siluro-Devonian volcanic rocks (Lindsley-Griffin, 1977; 1991; Quick, 1981; Irwin, 1994; Metcalf et. al., 2000; Lindsley-Griffin et al., 2006). One tectonically foliated ultramafic package contains the Vendian gabbroic to felsic plutonic suite and represents an ophiolitic crustal sequence (Lindsley-Griffin et al., 2006). Ordovician felsic dikes and plutons intrude the tectonically foliated, ultramafic packages and the Vendian sequence (Mattinson and Hopson, 1972; Lindsley-Griffin et al., 2006). The Siluro-Devonian gabbroic to felsic plutonic suites intrude units throughout the Trinity terrane and part of the Yreka terrane. The Siluro-Devonian suites are cogenetic with the Yreka terrane Siluro-Devonian volcanic flows and the Siluro-Devonian Redding volcanics (Wallin et al., 1991; Wallin and Metcalf, 1998; Metcalf, et al. 2000; Lindsley-Griffin et al., 2006).

Yreka Terrane. The Yreka terrane is structurally and stratigraphically complex, and consists of thin, fault-bounded slices of Vendian to Devonian shale, sandstone, phylite, schist, greenstone, and mélange units (Lindsley-Griffin, 1977; Potter et al., 1977; Lindsley-Griffin et al., 1991; Irwin, 1994; Lindsley-Griffin et al., 2006). Volcanic flows

within the Yreka terrane are the extrusive component of the Siluro-Devonian intrusive suite found within the Trinity terrane (Wallin and Metcalf, 1998). The Trinity-Yreka contact is faulted in all locations (Lindsley-Griffin, 1977; 1991; Potter et al., 1977; Schweickert and Irwin, 1989; Miller and Harwood, 1990; Lindsley Griffin et al., 1991; Cashman and Elder, 2002; Lindsley-Griffin et al., 2006).

Redding Terrane. The Redding terrane consists of Devonian to Jurassic volcanic and marine sedimentary units (Kinkel et al., 1956; Miller, 1989; Miller and Harwood, 1990; Irwin, 1994). The Devonian Copley Greenstone comprises the oldest stratigraphic layer of the Redding terrane and consists of pillow lavas, tuffs, volcanic flows and breccias, and some shales (Kinkel et al., 1956; Lapierre et al., 1985; Brouxel et al., 1988). Massive flows dominate the lower half of the unit, whereas the upper half is characterized by pillow lavas and interbedded pyroclastic deposits (Kinkel et al., 1956). Near Redding the upper Copley Greenstone is dominated by pillow lavas with minor amounts of "tuffaceous slaty sediments and sandstones with granitic debris" (Lapierre et al., 1985).

The Copley Greenstone is estimated to be at least 1800 meters thick (Diller, 1905; Lapierre et al., 1985; Brouxel et al., 1988). The contact between the Devonian Copley Greenstone and the Ordovician Trinity terrane is faulted at all locations (Wagner and Saucedo, 1987; Schweickert and Irwin, 1989; Irwin, 1994; Cashman and Elder, 2002). Overlying and interfingering with the Copley Greenstone are the Devonian Balaklala Rhyolite, dated by a Devonian fish fossil plate (Boucot et al. 1974), the mid-Devonian Kennett Formation, and the Mississippian Bragdon Formation (Kinkel et al., 1956).

The Mississippian Bragdon Formation consists mainly of argillite with minor amounts of conglomerate, silt, and sandstone, and rare fossiliferous units in the upper section (Kinkel et al., 1956; Miller 1989; Miller and Harwood, 1990). Chert pebble conglomerate is a distinctive unit within the formation and used for identification (Albers and Robertson, 1961). The majority of the conglomerate beds are located in the lower section of the Bragdon Formation, within 165 to 500 meters from the base. The conglomerates form lenticular beds that range up to several hundred meters thick and contain large portions of chert and limestone clasts (Kinkel et al., 1956; Albers and Robertson, 1961). The upper portion of the Bragdon Formation (structurally upper-most 2800 m) is dominated by sand-rich turbidites (Watkins, 1986; Miller and Cui, 1989). Sedimentary lithics dominate clast compositions throughout the formation, with some beds containing minor amounts of epiclastic volcanic lithics mixed in heterogeneously with the sedimentary clasts, and fewer beds with reworked pyroclastic debris (Miller and Cui, 1989). Internal deformation skews thickness measurements, but stratigraphic thickness estimates range from 900 m (Diller, 1905) to >2000 m (Watkins, 1986). Structural thickness estimates range up to 4400 meters thick (Watkins, 1986). In some locations, the Bragdon Formation conformably overlies the Balaklala Rhyolite and Kennett Formations, but elsewhere, the Bragdon Formation unconformably overlies the Kennett Formation (Kinkel et al., 1956) or Devonian Copley Greenstone (Kinkel et al., 1956; Albers and Robertson, 1961), or is faulted against the Balaklala Rhyolite or Copley Greenstone (Kinkel et al., 1956). The upper contact conformably grades into the

overlying Baird Formation, which contains Mississippian fish fossils (Watkins 1986; Miller and Cui, 1989).

Contact Relations. Faults bound the Trinity terrane both with the overlying Yreka terrane in the north (Potter et al., 1977; Miller and Harwood, 1990; Cashman and Elder, 2002; Lindsley-Griffin et al., 2006) and with the overlying Redding terrane in the south (Wagner and Saucedo, 1987; Schweickert and Irwin, 1989; Irwin 1994; Cashman and Elder, 2002). The structurally complex Yreka terrane contains multiple fault slices that displace Yreka fault blocks with the underlying Trinity terrane (Potter et al., 1977; Lindsley-Griffin, 1977). Outliers observed in the Callahan and Cecilville/Richter mine areas contain upper plate Yreka units with low-angle basal faults (Cashman and Elder, 2002).

The faults in the south, including the La Grange, Carrville, and Deer Creek faults, separate the Redding terrane from the underlying Trinity terrane and have been identified as low-angle, extensional faults (Schweickert and Irwin, 1989; Goldstein, 1997; Cashman and Elder, 2002). The Deer Creek and Carrville faults separate Devonian Copley Greenstone from the underlying Trinity terrane (Goldstein, 1997; Cashman and Elder, 2002); a similar relationship of greenstone overlying Trinity terrane mafic and ultramafic rocks is observed at Grey Rocks. Earlier interpretations have identified faults that bound the Trinity terrane with the Redding and Yreka terranes and underlie various outliers as thrust faults, including the basal contacts of the klippes at Grey Rocks (Irwin, 1966; Potter et al., 1977; Harwood and Miller, 1990; Charvet et al., 1990; Lindsley-Griffin,

1991). The significance of these faults as extensional faults is that they record an extensional event within a classically compressive zone.

The ambiguous nature of the contact between the Grey Rocks, Panther Rock, and Horse Heaven Meadows klippes and the underlying Trinity ultramafic complex has resulted in multiple conflicting interpretations. Depositional and tectonic hypotheses for the origin of Grey Rocks greenstone and metasedimentary bodies include: 1) part of a single, complete ophiolite sequence formed along a slow spreading ridge (Lindsley-Griffin, 1977; Brouxel and Lapierre, 1988; Boudier et al., 1989), 2) part of a single, complete ophiolite displaced by Paleozoic thrust faulting (Charvet et al., 1990), 3) part of a polygenetic ophiolite (Wallin et al., 1988; Lindsley-Griffin, 1991; Lindsley-Griffin et al., 2006), 4) the extrusive component of the Siluro-Devonian intrusive suite depositionally overlying a polygenetic Trinity terrane (Wallin and Metcalf, 1998; Metcalf et al., 2000), and 5) an upper plate remnant of Yreka and/or Redding terrane resulting from Tertiary detachment faulting (Schweickert and Irwin, 1989; Masson, 2002; Cashman and Elder, 2002).

Greenstone units at Grey Rocks and Panther Rock klippes were mapped as "Trinity basalts" and interpreted as part of a complete ophiolitic suite by Brouxel and Lapierre (1988). Boudier et al. (1989) suggest the Trinity ophiolite formed at a slow spreading ridge citing spatial relations between ultramafic rocks, cumulate gabbros, dikes, and pillow basalts as evidence. In this interpretation, the basal contacts of the Grey Rocks greenstone and metasedimentary units were identified as depositional and the

structurally high location of the greenstone and metasedimentary units as evidence for their position in a classic ophiolitic sequence.

The basal contacts of greenstone, metavolcanic, and metasedimentary rocks at Grey Rocks, Panther Rock, and Horse Heaven Meadows have been described as partially depositional and partially tectonic (Charvet et al., 1990). According to this interpretation, Grey Rocks and Panther Rock klippe greenstones represent part of an ophiolite that has experienced Paleozoic thrust faulting. The basal contacts of the Grey Rocks and Panther Rock klippes are described as thrust faults. The faulting event occurred after the greenstone pillows formed, but predated deposition of sedimentary rocks at Horse Heaven Meadows klippe. The Horse Heaven Meadows klippe is interpreted by Charvet et al. (1990) as an in-place section of Mississippian Bragdon shale with a depositional basal contact.

In contrast, geochronological analysis of metagabbro, gabbro, and tonalite in the Trinity terrane shows that the Trinity terrane consists of two ophiolitic sequences, one Vendian and one Siluro-Devonian in age, and formed over a period of 180 m.y. (Wallin et al., 1988; Lindsley-Griffin, 1991; Wallin et al., 1991; Wallin et al., 1995; Metcalf et al., 2000). These data, combined with mapping and description of the Yreka and Trinity terranes (Quick, 1981; Lindsley-Griffin, 1991; Lindsley-Griffin et al., 2006) indicate a complex polygenetic history for the Trinity terrane, which is the basis for the most recent interpretations of the Eastern Klamath Belt. Wallin and Metcalf (1998) indicate that the basal contact of greenstones at Grey Rocks could be faulted but interpret this contact as depositional.

First to suggest that the contact between the Trinity terrane and the Redding terrane is a low-angle detachment fault were Schweickert and Irwin (1989). They extended their observation of a low-angle normal fault at the La Grange mine, southwest of the Trinity terrane, to speculate that the imbricate faulting observed in the Yreka terrane may represent the break-away region of a south moving Redding terrane block that forms the upper plate of a regional-scale detachment fault. Masson (2002) identified a possible fault beneath the Grey Rocks klippe. According to Masson's (2002) interpretation, metasedimentary rocks at the Horse Heaven Meadows klippe depositionally overlie Trinity terrane peridotite and a deeper fault cuts through the peridotite, juxtaposing Trinity terrane against Trinity terrane. Cashman and Elder (2002) support a low-angle normal fault interpretation through identification of several klippes with low-angle basal faults separating Yreka and Redding terrane units with the underlying Trinity terrane.

The purpose of this study is to identify the nature of the basal contacts of the Grey Rocks, Panther Rock, and Horse Heaven Meadows klippes, and to utilize detailed mapping, petrography, and XRF analysis to associate each of the three klippes with a known rock assemblage (Plate 1).

PETROGRAPHY

The following rock descriptions, listed from oldest to youngest, describe the units observed at Grey Rocks, Horse Heaven Meadows, Panther Rock, and surrounding area (Plate 1). Unit names follow those of Irwin (1994) and Lindsley-Griffin et al. (2006). For locations mentioned in text, refer to Figure 2.

Trinity Terrane

Rock units of the Trinity terrane observed within the study area include 1) the Ordovician Trinity ultramafic sheet (Oum), termed the "Trinity peridotite" (Quick, 1981), and 2) various Ordovician to Siluro-Devonian gabbroic and dioritic suites (O/SDgb) (Irwin, 1994). Undated hornblende porphyry dikes (SDd) are also described here; these may be related to the Siluro-Devonian volcanic suite described by Lindsley-Griffin (1991) and Lindsley-Griffin et al. (2006). These units are mapped together here as Trinity ultramafic complex, (Ouc), with the exception of mappable dikes (SDd) near contacts with the Horse Heaven Meadows, Grey Rocks, and Panther Rock klippes. Lindsley-Griffin (1991) and Wallin et al. (1988) have used the Trinity ultramafic complex (Ouc) description to refer to the combination of the Trinity ultramafic sheet (Oum) and various intrusive suites (O/SDgb).

Mapping the extent of the O/SDgb intrusions is complex and beyond the scope of this project. For a detailed description of the various intrusions, refer to Lindsley-Griffin (1977; 1991), Lindsley-Griffin and Griffin (1983), Quick (1981), Cannat and Lecuyer (1991), Boudier et al. (1989), Metcalf et al. (2000), and Lindsley-Griffin et al. (2006).

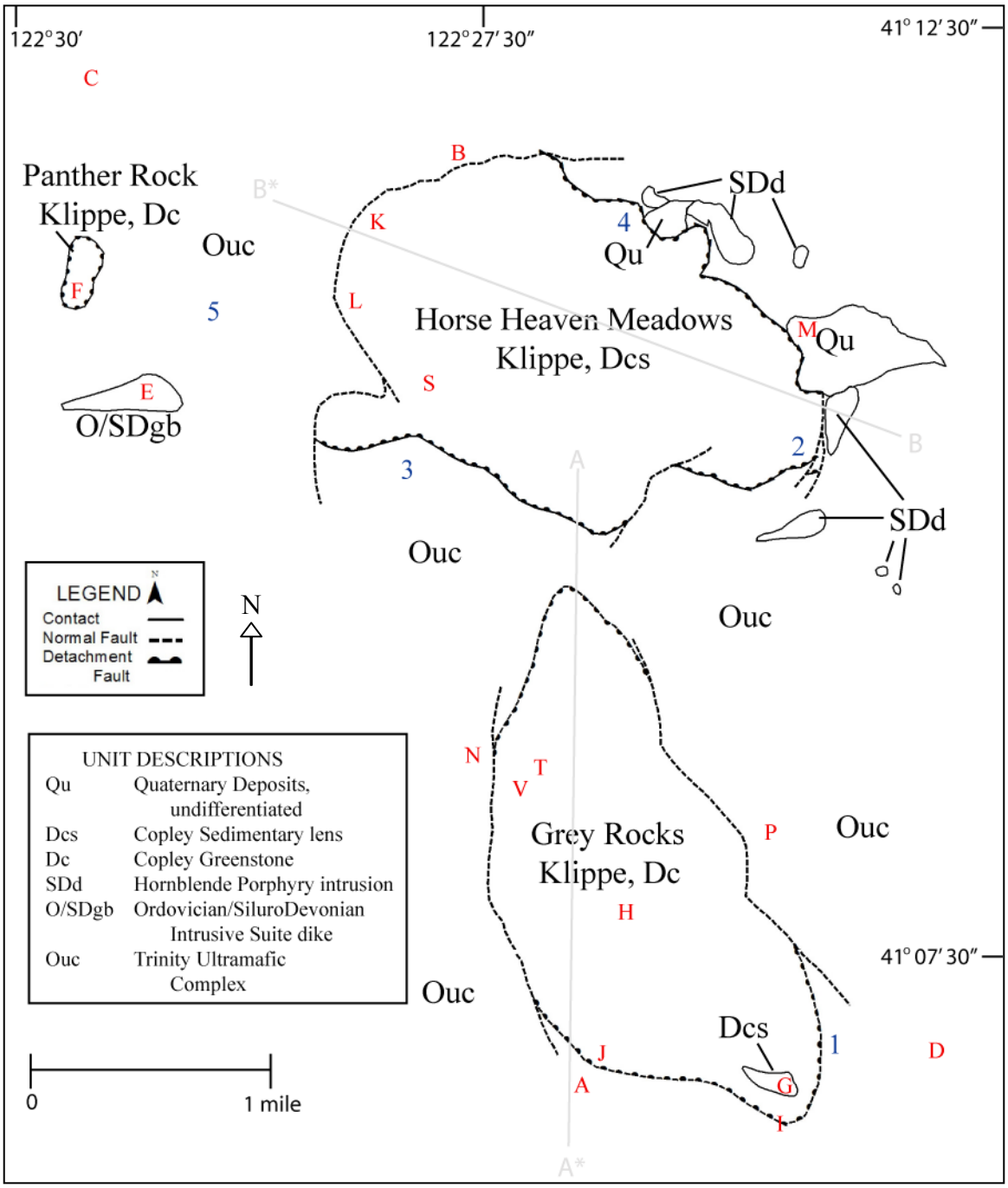

Figure 2: Location Map. Letters refer to sites noted within text. Numbers refer to samples listed in Table 1.

The three Trinity units comprising the Trinity ultramafic complex in the study area are described and listed in order of known ages, oldest to youngest.

Ultramafic Rocks (Oum)

The Trinity ultramafic unit, comprised mainly of serpentinite, is the oldest, most abundant unit in the mapped area and corresponds with the Trinity ultramafic sheet (Oum). The majority of the Trinity ultramafic sheet is Ordovician in age (Jacobsen et al., 1984), although minor sections of the northwest Trinity terrane near the Yreka terrane are dated as Vendian (Wallin et al., 1988; Wallin, 1990; Lindsley-Griffin, 1991; Wallin et al., 1995; Lindsley-Griffin et al., 2006). The majority of geologic mapping of the Trinity ultramafic sheet details the northern boundary adjacent to the overlying Yreka terrane. There, the ultramafic unit includes Ordovician feldspathic harzburgite, lherzolite, and dunite and Vendian plagiogranite and metagabbro (Lindsley-Griffin, 1977; 1991; Quick, 1981; Brouxel and Lapierre, 1988; Wallin et al., 1988; Boudier et al., 1989; Wallin et al. 1995; Lindsley-Griffin et al., 2006). Further east, in the Mt. Eddy area, the Ordovician units collectively termed the "Trinity peridotite" are 20 to 50% serpentinized with serpentinization increasing near intrusions (Quick, 1981). However, serpentinization in the western and northwestern parts of the Trinity ultramafic unit (Lindsley-Griffin, 1991), and within the Grey Rocks area (this project), is more extensive ranging up to complete serpentinization.

Location A (Fig. 2) near the southern contact of the Grey Rocks klippe, exhibits the complexity and altered nature of the Trinity ultramafic sheet. Undeformed dark to blackish green serpentinitized peridotite is layered within pale green serpentinite,

possibly representing a layered peridotite. Fractures parallel the layering in the serpentinite, striking N75W and dipping 50NE (Fig. 3).

The dark to blackish green serpentinized peridotite has undergone complete psuedomorphic alteration to serpentine and opaque magnetite forming serpentinite (Fig. 4). The opaque magnetite, which is faintly aligned in hand sample, preserves the original grain boundaries and idiomorphic granular texture. The dark to blackish green serpentinized peridotite can be observed in the north at Location B (Fig. 2).

A range of mafic to intermediate discontinuous dikes and plutons of the Ordovician to Siluro-Devonian intrusive suites O/SDgb have intruded the Trinity ultramafic sheet (Oum) and caused alteration zones near intrusion contacts. Along the steep banks of Castle Creek, serpentine country rock displays local metamorphism, shearing, and development of schistose at intrusive contacts (Fig. 5). In other locations, for example Helen Lake at Location C (Fig. 2), the intrusion-serpentinite contacts are broadly gradational. The integrated, gradational, and discontinuous nature of the contact zones are reasons for ambiguity and variation on different published maps.

Mafic Intrusive Rocks (O/SDgb and unofficial SDd)

The Ordovician and Siluro-Devonian intrusive suites include plutons and dikes of tonalite, plagiogranite, diabase, diorite, aplite, basalt, gabbro, and pyroxenite that have been described and mapped in detail throughout the Trinity terrane (Lindsley-Griffin, 1977; 1991; Quick, 1981; Brouxel and Lapierre, 1988; Wallin et al., 1988; Boudier et al., 1989; Metcalf, et al., 2000). A detailed description of the Trinity ultramafic complex (Ouc), specifically the intrusive suites, is presented in Quick (1981) and Lindsley-Griffin

Figure 3: Photograph of pervasive parallel fractures, striking N75W and dipping 50NE, in the massive light green serpentinite of the Trinity ultramafic sheet (Oum), SW of Grey Rocks klippe, Location A (Fig. 2). The fractures parallel 15 cm thick sections of dark to blackish green serpentinite (Oum), interpreted as a layered peridotite. View is to the NW.

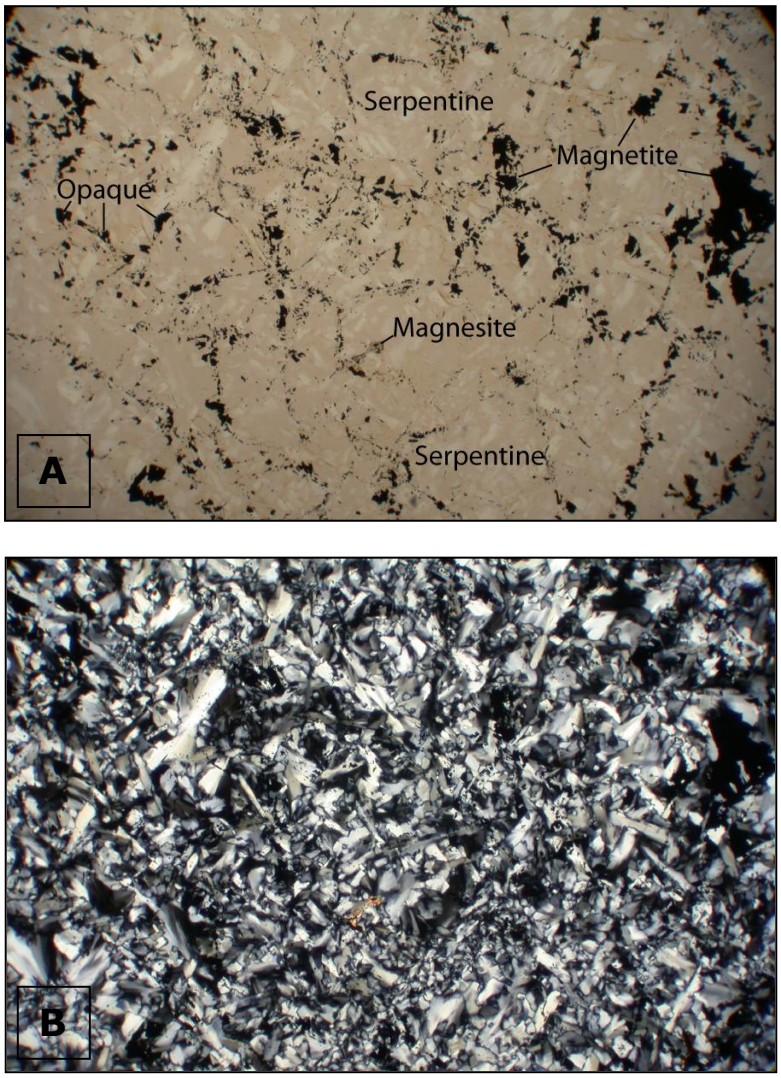

Figure 4: Photomicrographs of dark to blackish green serpentinite unit of the Trinity ultramafic sheet (Oum). Sample UM-2, Location A (Fig. 2), width of image is 1.75 mm, A) in plane polarized light and B) in cross polarized light. Serpentinite is comprised mainly of serpentine, opaque magnetite, and minor magnesite. Psuedomorphic alteration of pyroxene and olivine preserve the original idiomorphic granular texture, large equant grains outlined by smaller opaque minerals.

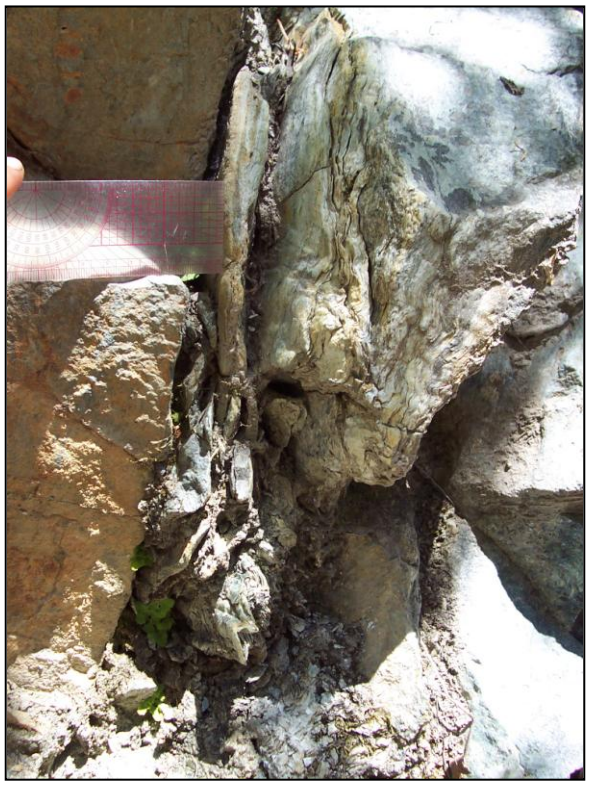

Figure 5: Photograph of dike-serpentinite contact. Intrusion of an aphanitic basalt dike (O/SDgb) causes contact metamorphism and localized foliation zones within the massive serpentinite of the Trinity ultramafic sheet (Oum). Foliated zone is approximately 8 cm thick. Photo location is from Castle Creek near Location 4 (Fig. 2), view is to the NE. Local zones of schistosity within the serpentinite are commonly observed adjacent to dikes and plutons.

(1991). The Trinity ultramafic unit is described as polygenetic with several dikes ranging in composition from plagiogranite to gabbric and ages spanning from Ordovician to Siluro-Devonian (Wallin et al., 1988; Wallin et al., 1991; Wallin et al., 1995; Wallin and Metcalf, 1998). Tonalitic plutons and dikes are dated as Ordovician, ranging from 455 to 485 Ma (Mattinson and Hopson, 1972). The Siluro-Devonian gabbroic and dioritic suite, dated by Jacobsen et al. (1984), includes a characteristic pegmatitic gabbro along with intrusions of pyroxenite, gabbro, diorite, and aplite (Quick, 1981; Lindsley-Griffin, 1991). Cannat and Lecuyer (1991) mapped basalt dikes and plutons south of Grey Rocks klippe at Tamarack Lake and northeast of Horse Heaven Meadows klippe at Castle Lake.

Within the Grey Rocks study area, small plutons of fine-grained diabase, diorite, and gabbro intrude the Trinity ultramafic sheet (i.e., Locations D and E, Fig. 2). Composition, grain-size, and texture are variable from pluton to pluton and given the multitude and variety of intrusions, a detailed description is beyond the scope of this project. Observable at several locations, the diabase, diorite and gabbro grade into each other and are intruded by the pegmatitic hornblende gabbro (i.e., Location D, Fig. 2). All felsic to gabbroic dikes and plutons within the study area are small and discontinuous with the exception of the pegmatitic hornblende gabbro (O/SDgb) that covers large areas to the north of Horse Heaven Meadows klippe and east of Grey Rocks klippe.

Pegmatitic Hornblende Gabbro (O/SDgb). The pegmatitic hornblende gabbro, comprising the area near Helen Lake (Location C, Fig. 2) and Boulder Peak, the eastern side of Grey Rocks Basin and Mears Ridge area (Location D, Fig. 2), and the Seven Lakes Basin area, corresponds to the younger plutonic component of O/SDgb in Irwin

(1994) and Silurian gabbroic suite of Lindsley-Griffin (1991). The pegmatitic gabbro is comprised primarily of aggregates of coarse-grained (0.5 to 5 cm) pyroxene, hornblende, plagioclase, and quartz. Unlike the smaller dikes and sills, this unit forms large plutons. Near Helen Lake (Location C, Fig. 2), the irregular and complex O/SDgb pluton boundary with the Trinity ultramafic sheet (Oum) can be observed, displaying a zone of O/SDgb intrusions interfingering with hydrothermally altered Trinity ultramafic sheet. Other units associated with the pegmatitic hornblende gabbro include intrusions of pyroxenite, gabbro, diorite of various compositions, and aplite (Lindsley-Griffin, 1991).

Porphyritic Hornblende Andesite. (SDd). Small discontinuous hypabyssal plutons of porphyritic hornblende andesite intrude Trinity terrane ultramafic rocks on the southeastern side of the Horse Heaven Meadows klippe, near Locations 4 and 2 (Fig. 2). These plutons are irregularly shaped, appear undeformed, and are up to 1700 m in diameter. In the field, the andesite is lavender grey with black hornblende phenocrysts up to 3 mm in length. In thin-section, the andesite contains euhedral hornblende crystals about 3mm in length (locally altered to fine-grained amphiboles, chlorite, and calcite), euhedral 1mm plagioclase phenocrysts altered to saussurite and fine-grained clay; and minor pyrite phenocrysts. The fine-grained groundmass consists of microcrystalline quartz, plagioclase, chlorite, and small laths of clinozoisite.

Devonian Copley Greenstone (Dc and Dcs)

The Devonian Copley Greenstone is the basal unit of the Redding terrane (Kinkel et al., 1956; Miller and Harwood, 1990; Irwin, 1994). Massive greenstone and pillow

greenstone of Panther Rock and Grey Rocks klippes have been mapped as Copley Greenstone based on petrographic characteristics (Wagner and Saucedo, 1987; Irwin, 1994) and as "Trinity ophiolitic basalts" based on petrographic and geochemical characteristics (Brouxel and Lapierre, 1988; Brouxel et al., 1988).

Panther Rock Klippe: Greenstone Pillows (Dc)

Greenstone caps Panther Rock klippe (Location F, Fig. 2) and exhibits classic pillow structures, aphanitic texture, and irregular quartz veins. Only the very top of Panther Rock contains in-place pillow structures with float comprised solely of greenstone blocks blanketing the slopes. The basal contact between the pillows and the underlying Trinity ultramafic complex is obscured; however, based on map relations, the minimum unit thickness is estimated at 27 meters.

The greenstone of Panther Rock klippe is aphanitic, comprised of radial, fibrous actinolite, chlorite, plagioclase, fine-grained microcrystalline and larger quartz, euhedral clinozoisite, square 0.5 mm relict pyroxenes that are being replaced by chlorite, and fine-grained clays (Fig. 6). The intergranular texture is overprinted by alteration minerals.

Grey Rocks Klippe

Greenstone Pillows (Dc). Greenstone pillows form the majority of Grey Rocks klippe. A minor metavolcanic/metasedimentary lens (Dcs) is interstratified with pillow greenstone in the southern section of the klippe (Location H, Fig. 2; and Fig. 7). In outcrop, classic aphanitic, green to reddish brown pillow structures are apparent (Fig. 8). The greenstone unit is coherent and lacks a pervasive tectonic fabric, only exhibiting a faint foliation near the basal contacts with the Trinity ultramafic complex, (Location I

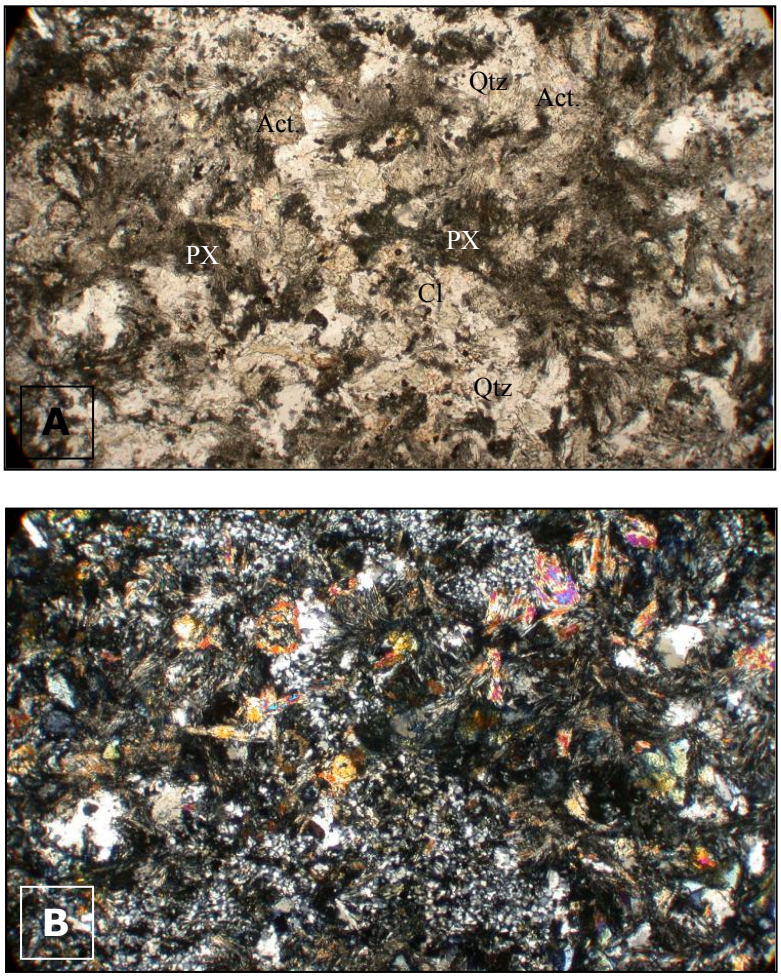

Figure 6: Photomicrographs of Panther Rock greenstone pillows, Dc. Sample PR-1, Location F (Fig. 2), width of image is 3.2 mm, A) in plane polarized light and B) in cross polarized light. Mineralogy includes radial, fiberous actinolite (Act.), chlorite (Cl), quartz (Qtz.), euhedral clinozoisite, square 0.5mm relict pyroxene (PX) replaced by chlorite, and fine-grained clay.

A). Grey Rocks Klippe Stratigraphy Location 1

B). Horse Heaven Meadows Klippe Stratigraphy, Location 2

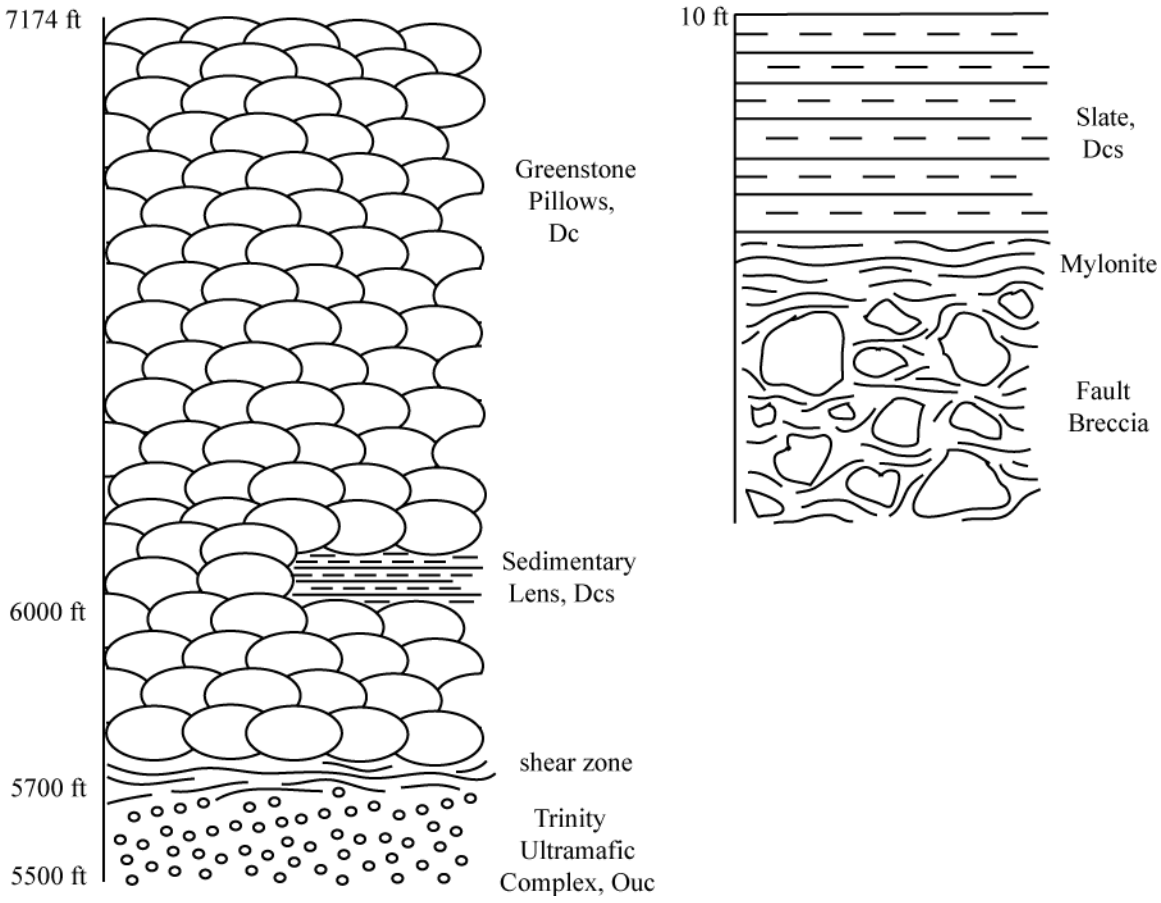

Figure 7: Stratigraphic columns of Grey Rocks klippe (Location 1, Fig. 2), and Horse Heaven Meadows klippe (Location 2, Fig. 2).

along Mears Ridge and in the saddle at Location J, Fig. 2). The basal contact of the greenstone is a fault and will be further discussed in the Structure section. The minimum thickness of the Grey Rocks klippe greenstone is 340 meters.

The greenstone pillows of Grey Rock klippe have a fine-grained intergranular texture and are comprised mainly of chlorite, plagioclase, microcrystalline quartz, clinozoisite, opaque minerals, relict clinopyroxene altering to actinolite and chlorite, and fine-grained clays (Fig. 9). Plagioclase display sparrow-tail edges and are altering to epidote group minerals and clays. The intergranular texture is consistent with pillow basalts and the sparrow-tail plagioclase laths are indicative of rapid cooling. Based on the mineral assemblage: albite-actinolite-chlorite-epidote observed in the Panther Rock and Grey Rocks greenstones, these rocks have been metamorphosed to greenschist facies.

Meta-Volcanic/Sedimentary unit (Dcs). The Grey Rocks klippe metasedimentary/metavolcanic lens, Dcs, consists of both fine-grained slate and volcaniclastic tuffaceous beds that are discontinuous, conformable, and syndepositional with the greenstone unit (Location G, Fig. 2). An exact thickness was not determined because of the lenticular nature of the unit, but the maximum thickness of the metasedimentary/metavolcanic lens is less than 60 meters thick. The fissile slate is dark reddish brown to dark brown and fine-grained. The dark brown tuffaceous medium pebble breccia is a massive, unsorted, angular, polymictic, clast-supported volcanic medium pebble breccia with a fine-grained quartz, chlorite, and clay matrix (Fig. 10). Clast sizes range up to 0.75 cm. Clast compositions include a) microcrystalline quartz, b) aligned fine-grained plagioclase, epidote, and chlorite, and c) single grain clasts of quartz

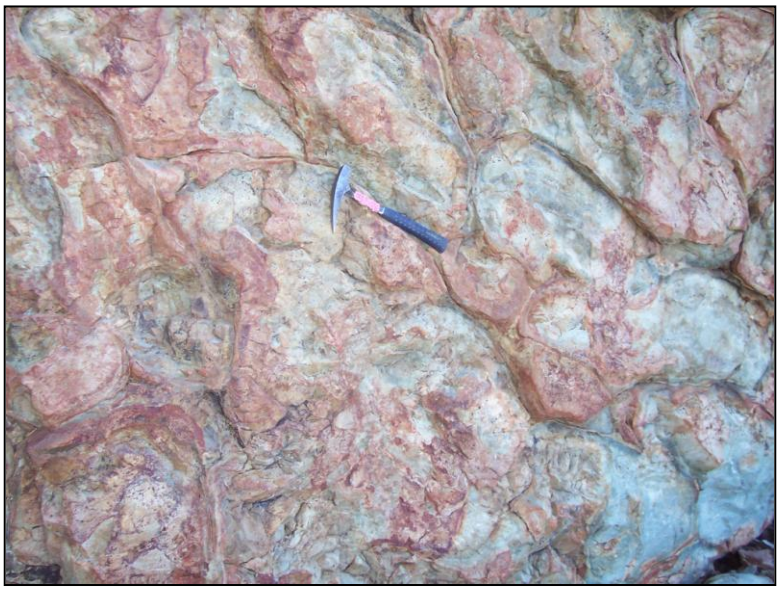

Figure 8: Photograph of greenstone from the Grey Rocks klippe, Dc (Location H, Fig. 2). Photograph depicts the classic pillow structure typical of greenstone in the study area. View is to the NW. Hammer for scale.

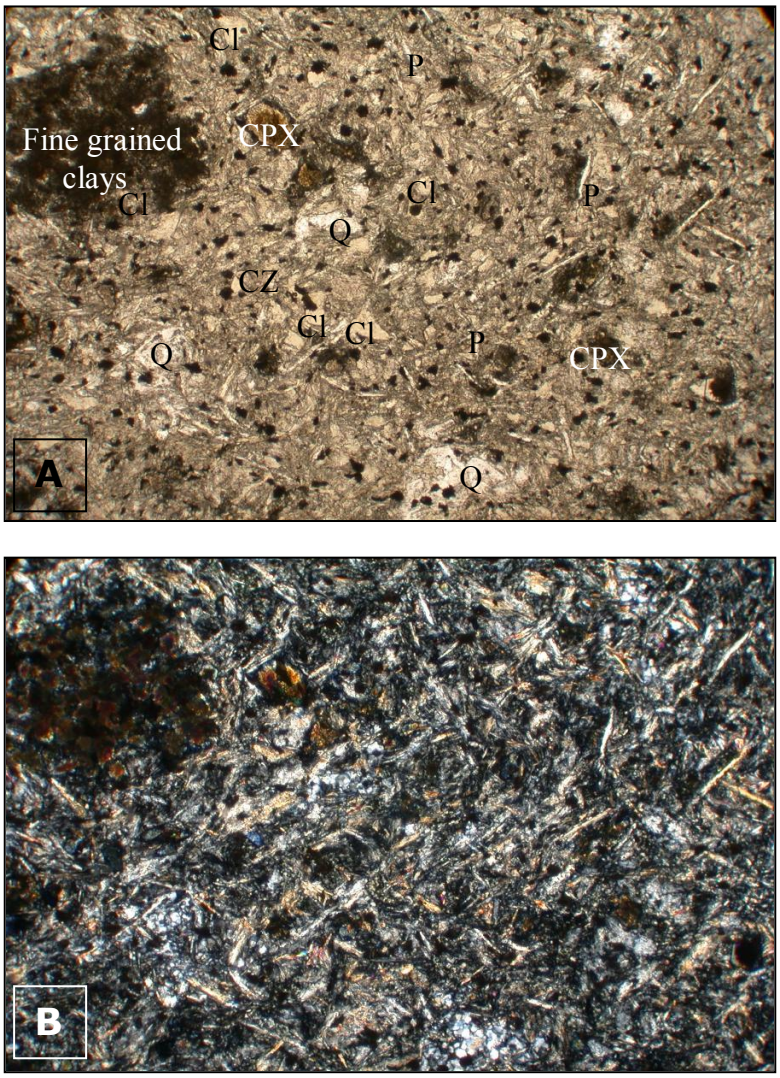

Figure 9: Photomicrographs of greenstone from Grey Rocks klippe, Dc. Sample GR-6, Location H (Fig. 2), width of image is 3.2 mm, A) in plane polarized light and B) in cross polarized light. Mineralogy includes microcrystalline quartz (Q), relict plagioclase crystals degrading to saussurite (P), large unidentified minerals degrading to fine-grain clay, and relict clinopyroxenes (CPX) rimmed with chlorite. Secondary alteration minerals include clinozoisite (CZ), saussurite, chlorite (Cl), and fine-grained clay. Plagioclase crystals display swallow-tail textures typical of pillow basalts.

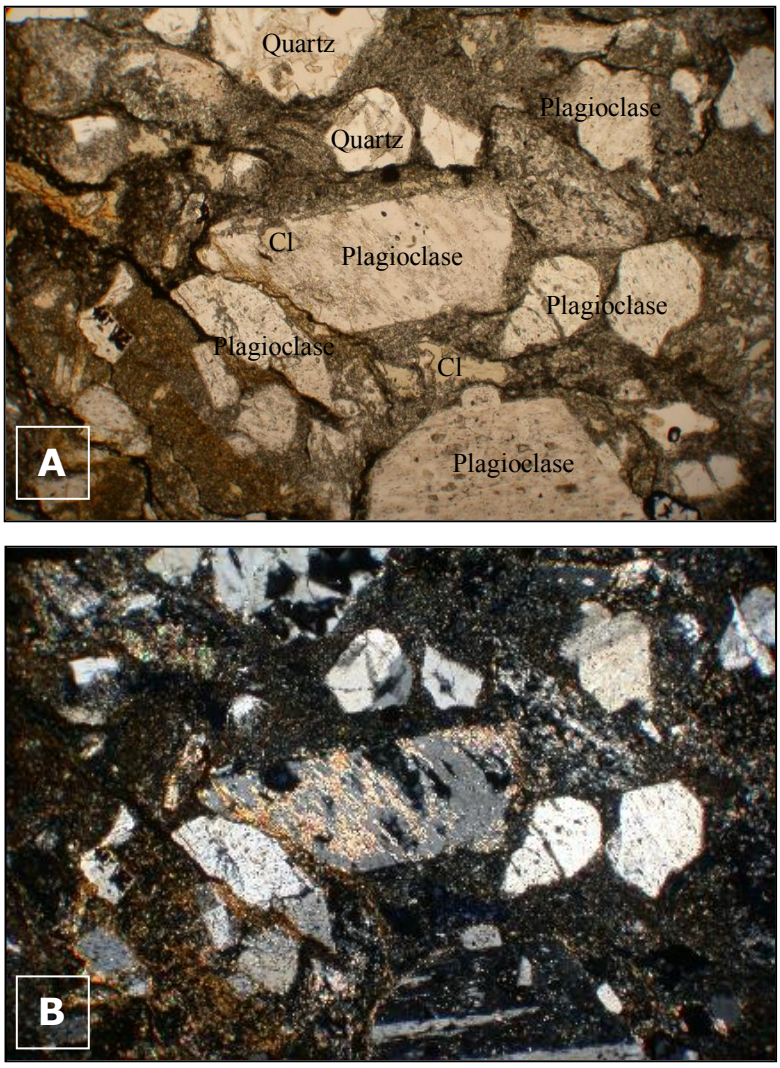

Figure 10: Photomicrographs of tuffaceous breccia, from the Grey Rocks klippe metasedimentary unit, Dcs. Sample SV-6, Location G (Fig. 2), width of image is 3.2 mm, A) in plane polarized light and B) in cross polarized light. Poorly-sorted, angular, polymictic, clast-supported tuffaceous medium pebble breccia with a fine-grained quartz, chlorite, and clay matrix. Pebble to sand sized clasts include: clasts of microcrystalline quartz; diorite clasts comprised of aligned fine-grain plagioclase, epidote, and chlorite (not photographed); and single grain clasts of quartz, plagioclase, and chlorite (Cl). Large sections of the matrix appear to have been recrystallized into chlorite, possibly replacing volcanic glass.

plagioclase, and chlorite (originally clasts of volcanic glass). Large sections of the matrix appear to have been recrystallized into chlorite, possibly replacing original volcanic glass.

Horse Heaven Meadows Klippe: Slate, Tuff, and Volcanic Breccia (Dcs)

Horse Heaven Meadows klippe consists of tilted, highly fractured, fine-grained dark reddish brown to dark brown slate with minor amounts of interbedded tuffs and volcanic breccias. The metasedimentary unit is juxtaposed with the Trinity ultramafic complex by faults at all contacts. An accurate thickness is hard to determine because the klippe is tilted, has irregular bedding, and is highly fractured. At the western edge (Location K, Fig. 2), a coherent section approximately 20 meters thick is exposed; however, the sedimentary unit appears to be at least 60 meters thick based on dip measurements, exposure width, and topography.

Tuffs and volcanic breccias display maximum clast sizes ranging from sand to cobbles. An example of a coarse tuff is exposed at Location K (Fig. 2) and in Figure 11. This glass-rich, matrix-supported unit exhibits poorly sorted, angular to sub-rounded clasts of volcanic glass, single grains of subhedral and microcrystalline quartz, and subhedral relict grains now comprised of actinolite. The fine-grained matrix is composed of chlorite, micas, volcanic glass, and fine-grained clays.

The pyroclastic breccia (Location L, Fig. 2) is a discontinuous, unsorted, angular, polymictic, matrix-supported metavolcanic unit with clasts ranging up to cobble size and a chlorite, microcrystalline quartz, epidote, and fine-grained clay matrix (Fig. 12). Clasts are volcanic, containing a) epidote and quartz, b) microcrystalline quartz, c)

Figure 11: Tilted shale and sandy tuff beds from the NW margin of the Horse Heaven Meadows klippe, Location K (Fig. 2). View is to the SE with rock hammer for scale.

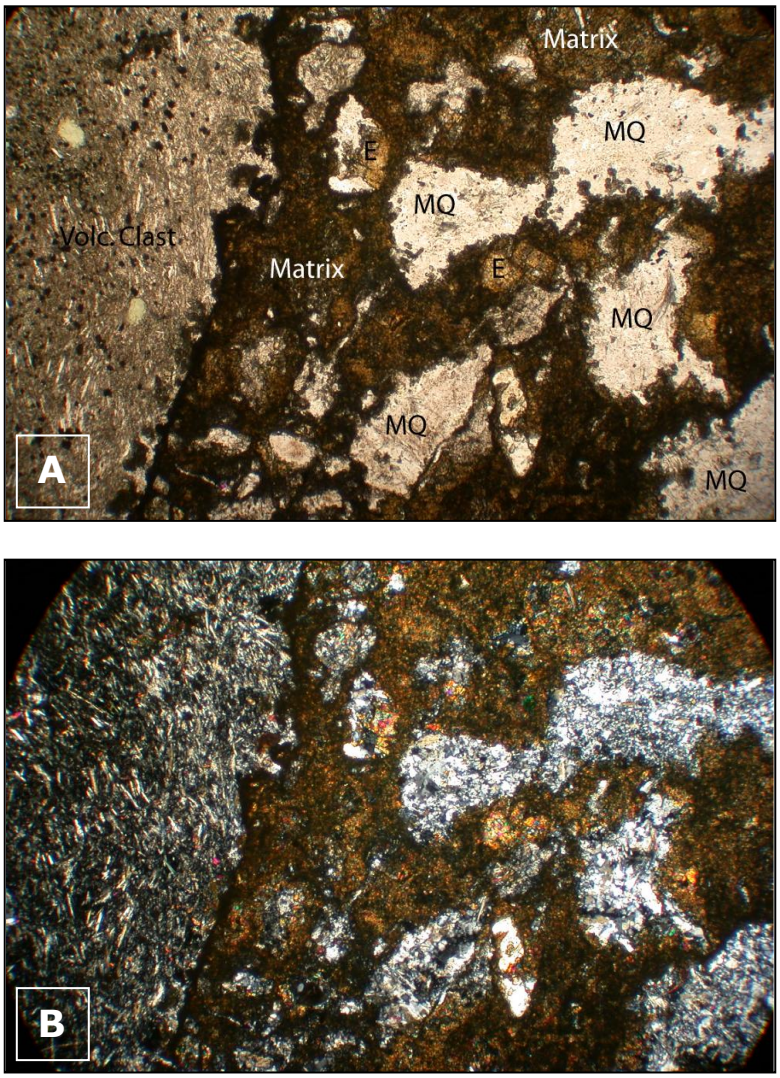

Figure 12: Photomicrographs of pyroclastic breccia of the Horse Heaven Meadows klippe, Dcs. Sample SV-2, Location L (Fig. 2), width of image is 3.2 mm, A) in plane polarized light and B) in cross polarized light. Unsorted, angular, polymictic, matrix supported pyroclastic breccia with a chlorite, microcrystalline quartz (MQ), epidote (E), and fine-grained clay matrix. Clasts consist of 1) epidote and quartz; 2) microcrystalline quartz; 3) microcrystalline quartz with chlorite, plagioclase laths, and opaque minerals; and 4) fiberous actinolite, microcrystalline quartz, chlorite, epidote, and saussurite.

microcrystalline quartz with chlorite, plagioclase laths, and opaque minerals, and d) fibrous actinolite, microcrystalline quartz, chlorite, epidote, and saussurite (relict plagioclase). At the outcrop scale, clast boundaries are faint but become more distinguishable in thin-section. The blending of clast boundaries is likely due to the aphanitic and epidote overgrowths that have overprinted the unit and original grain boundaries.

Felsic Dikes

Two felsic dikes cross-cut the foliation in fault breccia at the base of the Horse Heaven Meadows klippe (Location 2, Fig. 2), and a third intrudes parallel to foliation in fault rocks in the shear zone at the base of the Grey Rocks klippe (Location 1, Fig. 2). The dikes are fine-grained, felsic, and only observed in the lower plate and fault zone rocks. The dikes have not been dated.

The two felsic dikes that intrude fault breccia (Location 2, Fig. 2) are 4 meters apart, 1.3 meters thick, strike parallel at N32E, dip 76N, and are similar in composition and texture. The allotriomorphic granular grano-dioritic dike consists mainly of <0.5 mm quartz, 1 to 1.25 mm mantled, poikilitic plagioclase with epidote group inclusions, and minor orthoclase feldspar (Fig. 13). Other minerals include chlorite, saussurite, and reddish brown opaque minerals.

The aphanitic rhyolite dike, classified based on the Jensen cation plot (Jensen, 1976), consists mainly of microcrystalline to <0.4 mm quartz, <0.5mm poikilitic plagioclase with epidote group inclusions, and minor anorthoclase feldspar (Fig.14).

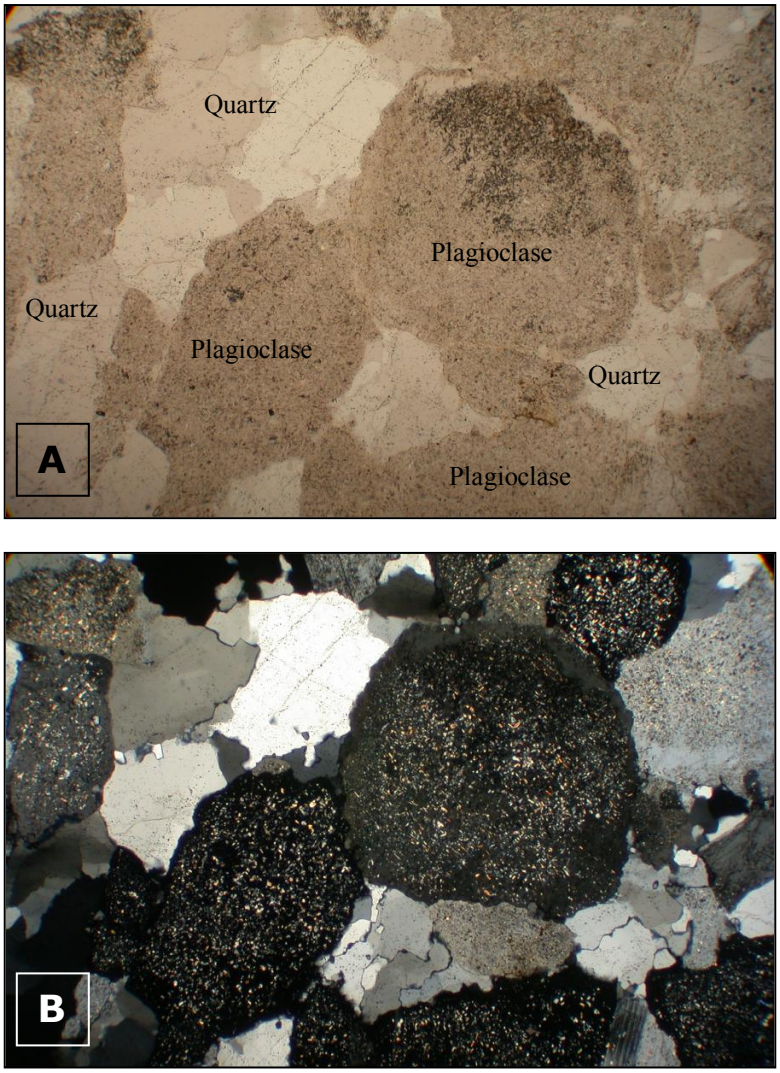

Figure 13: Photomicrographs of allotriomorphic granular grano-diorite dike. Sample D-2, Location 2 (Fig. 2), width of image is 3.2 mm, A) in plane polarized light and B) in cross polarized light. Dike is comprised mainly of coarse (1.25 to 1mm), mantled, poikilitic plagioclase, orthoclase, and quartz. Plagioclase contains epidote group inclusions and has altered to saussurite and chlorite.

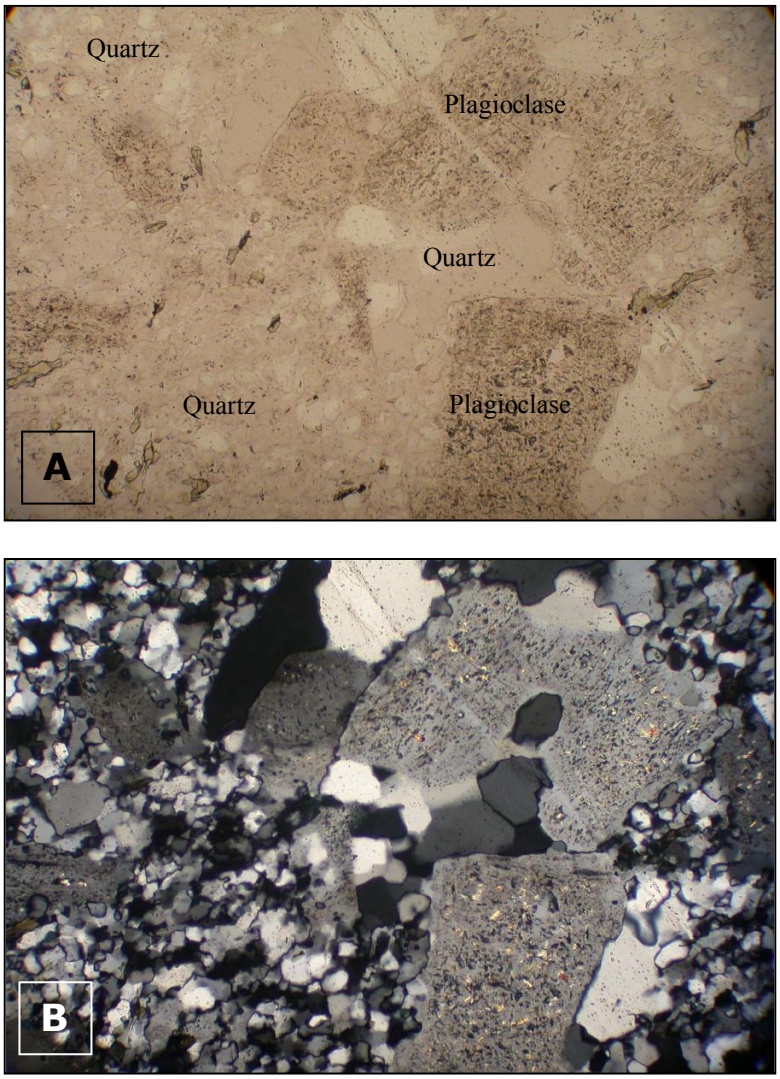

Figure 14: Photomicrographs of aphanitic rhyolite dike. Sample D-1, Location 2 (Fig. 2), width of image 1.37 mm, A) in plane polarized light and B) in cross polarized light. Dike is comprised of fine-grain (0.5 mm) plagioclase, anorthoclase feldspar, and coarse grain to microcrystalline quartz, with some secondary alteration to chlorite and saussurite. Plagioclase crystals display mantled edges and poikilitic texture with epidote group inclusions.

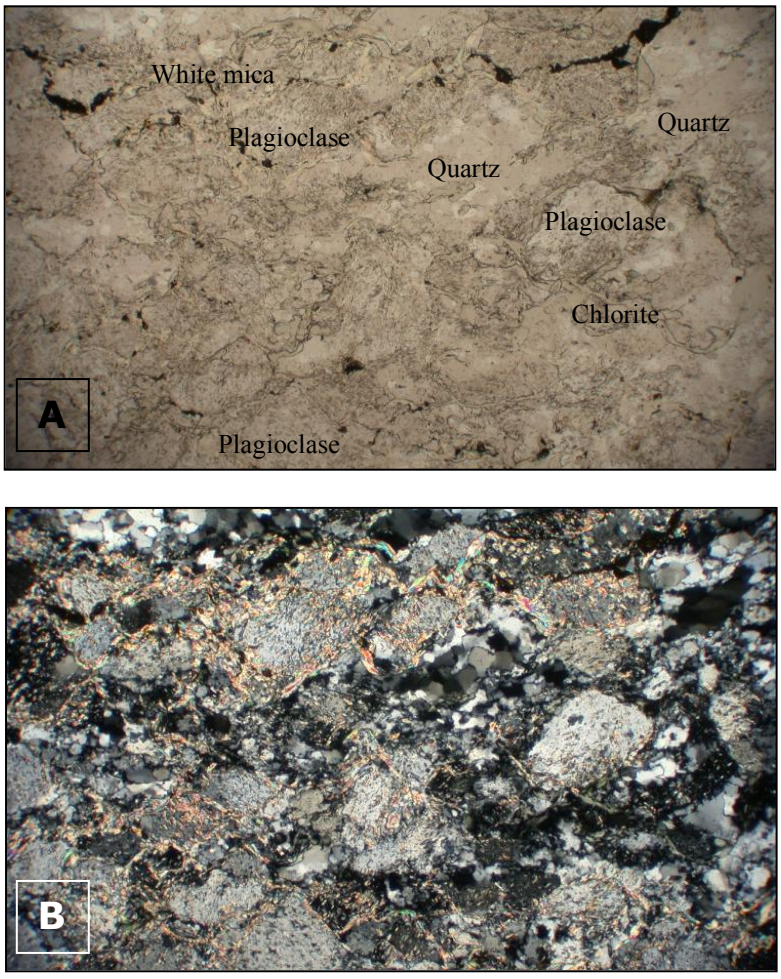

Figure 15: Photomicrograph of aphanitic rhyolite dike intruding parallel to the basal fault of Grey Rocks klippe. Sample SHZD-8, Location 1 (Fig. 2), width of image 3.2 mm, A) in plane polarized light and B) in cross polarized light. Dike consists mainly of strongly aligned, poikilitic plagioclase containing fine-grain epidote group inclusions, minor amounts of orthoclase feldspar, and quartz, in a groundmass of chlorite, fine-grained white mica, saussurite, and fine-grained clay. Dike displays anastomosing, moderately rough foliation (~horizontal in this photomicrograph) defined by thin bands of white mica and quartz that flow around the plagioclase crystals creating augens.

Some feldspar crystals exhibit mantling, myrmekite texture, and grid like twinning typical of anorthoclase feldspar in hypabyssal intrusive rocks. Secondary minerals include chlorite, saussurite, and reddish brown opaque minerals. The rhyolite dike displays chilled margins.

The third aphanitic rhyolite dike, classified based on the Jensen cation plot (Jensen, 1976), is about 1 meter thick and intrudes parallel to the fault zone in the Grey Rocks klippe basal shear zone (Location 1, Fig. 2). Microscopic shear fabric, observed in thin-section, shows that the sheared rhyolite consists mainly of strongly aligned, poikilitic plagioclase containing fine-grained epidote group inclusions and quartz, with lesser amounts of orthoclase feldspar, chlorite, fine-grained white micas, saussurite, and fine-grained clays. An anastomozing and moderately rough foliation, defined by thin bands of white mica and quartz, flows around the plagioclase crystals creating augens (Fig. 15). Quartz veins cross-cut the dike approximately perpendicular to foliation.

Quaternary Deposits

Quaternary deposits in the Grey Rocks, Panther rock, and Horse Heaven Meadows area include glacial moraines and till, alluvial deposits, and a variety of landslides including debris slides and slumps. Because the glacial history is beyond the scope of this project, only the large landslide deposits near bedrock contacts were mapped (Plate 1 and Fig. 2).

The surficial deposits in the area are apparent in airphotos, where massive landslides (i.e. Location M), glacial moraines (i.e. Location N), glacial erratics (i.e. near

Location 3), and poorly sorted glacial till (everywhere) cover the landscape. Grey Rocks ridge has been carved out, creating cirques, and glacial erratics have collected on the slopes below.

Large Quaternary landslide and slump deposits (Qu) occur along the eastern edge of the Horse Heaven Meadows klippe (near Locations 4 and M, Fig. 2) where they obscure the fault contact (Fig. 16). The landslides and scarps start within the slate and the toes extend to and locally fill Castle Creek valley. The coherent slump block at Location M (Fig. 2) is about 20 meters high and consists of slate. This coherent block is surrounded by a debris flow deposit consisting of an incoherent mixture of metasedimentary blocks, Trinity mafic and ultramafic blocks, and indiscernible soil.

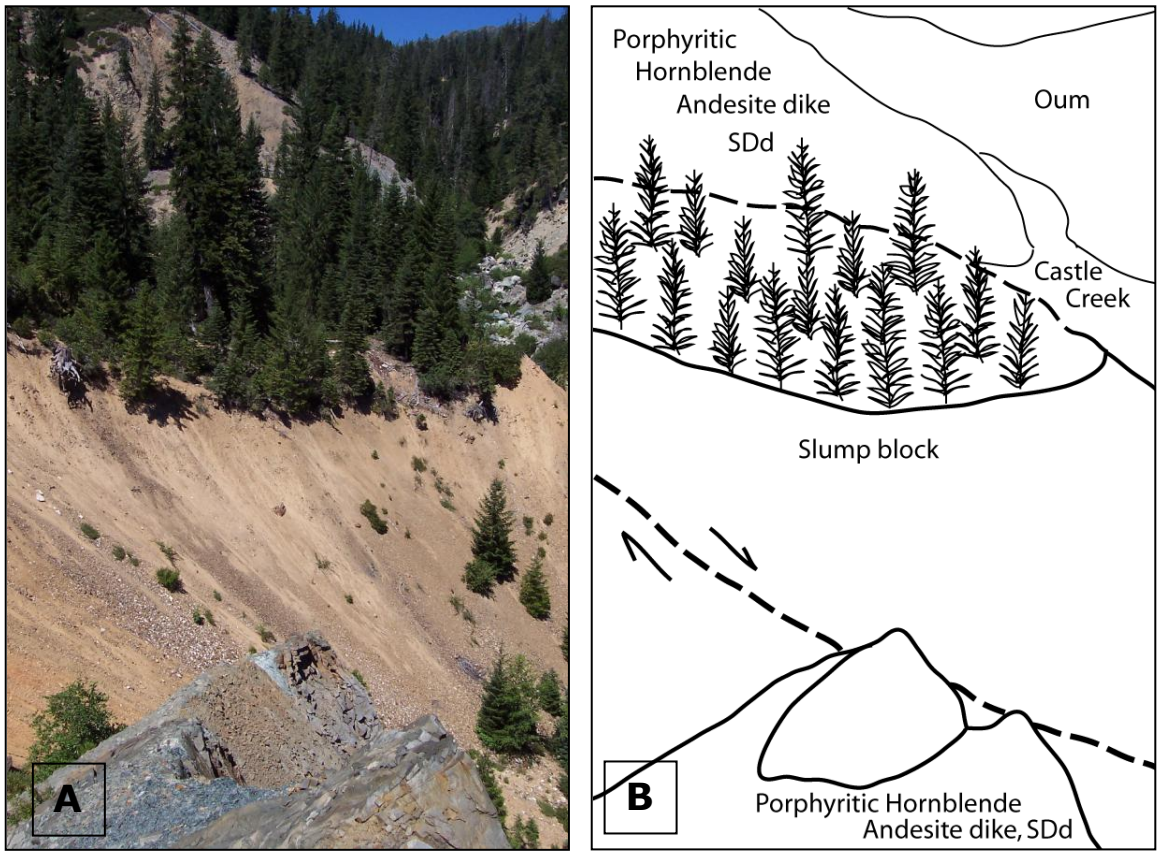

Figure 16: Photograph looking north upstream of Castle Creek at northeast margin of Horse Heaven Meadows klippe (Location 4, Fig. 2). A) Photograph and B) sketch depict a slump block of upper plate shale that has slid into Castle Creek.

GEOCHEMISTRY

Geochemical studies have proved useful for determining the origin and metamorphic history of rocks within the Eastern Klamath Belt (e.g. Lapierre et al., 1985; Brouxel et al., 1987; Brouxel and Lapierre, 1988; Brouxel et al., 1988; Metcalf, et al., 2000). The geochemical analyses conducted in this project were designed to test proposed stratigraphic correlations between 1) the greenstones of the Grey Rocks and Panther Rock klippes and the Copley Greenstone, and 2) felsic dikes in the Grey Rocks project area and felsic dikes found at the other fault contacts in the Klamath Mountains Provenance (e.g. Cashman and Elder, 2002). Geochemical analyses also were used to look for evidence of the incorporation of upper and lower plate components in fault zone samples.

GREENSTONE ANALYSES

Rocks from a similar source will display similar geochemical signatures (Rollinson, 1993). To determine whether the greenstones of Panther Rock and Grey Rocks klippes were derived from the same source as the Copley Greenstone, samples from the three greenstones were crushed, powdered, and analyzed using x-ray fluorescence spectrometry (Table 1, Fig. 2).

Pillow basalts typically undergo hydrothermal alteration during formation, as heated water circulates through the fresh basalt (Humphris and Thompson, 1978a). In the process of hydrothermal alteration, both major and trace element compositions are commonly altered. Bulk elements Al_2O_3, TiO_2, and P_2O_5 are typically more stable than

other major elements. However, the relative abundances of some more mobile elements, such as CaO and MgO, can be used to determine the extent of hydrothermal alteration (Humphris and Thompson, 1978a).

Humphris and Thompson (1978a) found a pattern of 1:1 CaO replacement by MgO in hydrothermally altered basalts. Circulating water deposits MgO and removes CaO. Graphing CaO against MgO content from fresh and altered basalts results in a negative trend that signifies an increase in hydrothermal alteration. Samples displaying extensive hydrothermal alteration no longer reflect original composition. To determine whether Panther Rock klippe, Grey Rocks klippe, and Copley Greenstone have been too altered for comparison, their CaO and MgO content have been plotted with both fresh and altered samples from Humphris and Thompson (1978a) (Fig. 17).

The replacement trend of MgO for CaO is defined by basalt samples from Humphris and Thompson (1978a) and outlined by the dashed line (Fig. 17). Greenstone samples from Grey Rocks klippe, Panther Rock klippe, and the Copley Greenstone exhibit generally varying extents of hydrothermal alteration, plotting both within and outside the defined trend. Sample GR-6 is the only greenstone sample that plots near fresh basalts, indicating the least amount of hydrothermal alteration. This particular greenstone sample is from a site located the farthest from the basal fault zone (Location H, Fig 2). The other greenstone samples are located closer to fault zones (Fig. 2) and have experienced increased hydrothermal alteration.

Samples plotting with values outside the dashed line in Figure 17 have been left out of further comparisons of bulk and trace compositional values. Other studies that

Table 1. Geochemical values of samples from Grey Rocks project. *Data from petrology lab at CSU Fresno. (page 1 of 6)

SAMPLE NUMBER	LOC	NAME	MAP UNIT	SiO_2	TiO_2	Al_2O_3	FeO	MnO	MgO	CaO	Na_2O	K_2O	P_2O_5	H_2O
Upper Plate														
SV-1	L	Copley	Dcs	57.11	0.695	14.60	8.38	0.10	6.33	8.61	4.11	0.02	0.043	7.68
SV-2	L	Copley	Dcs	55.74	0.719	16.59	7.49	0.09	4.88	8.87	5.52	0.07	0.033	8.12
SV-3	K	Copley	Dcs											
SV-4	S	Copley	Dcs	78.64	0.165	11.15	2.38	0.05	1.11	3.43	0.53	2.50	0.033	8.31
SV-5	S	Copley	Dcs	76.33	0.273	12.36	3.19	0.07	1.79	2.19	2.04	1.72	0.044	8.32
SV-6	G	Copley	Dcs	57.09	0.872	20.44	11.31	0.10	6.07	0.07	2.16	1.80	0.092	12.57
GR-1	T	Copley	Dc	61.66	0.497	12.10	6.61	0.10	9.57	8.01	0.55	0.84	0.065	7.25
GR-2	T	Copley	Dc	58.30	0.591	14.64	5.95	0.09	11.46	4.36	4.45	0.04	0.112	10.22
GR-3	T	Copley	Dc	56.08	0.805	14.92	7.92	0.12	8.49	8.76	2.66	0.17	0.065	7.93
GR-4	V	Copley	Dc	49.31	0.877	17.73	8.76	0.13	12.79	6.61	2.63	1.08	0.078	9.82
GR-5	V	Copley	Dc	57.97	0.579	12.74	6.34	0.11	6.72	15.17	0.01	0.33	0.032	6.69
GR-6	H	Copley	Dc	55.17	0.678	14.07	7.74	0.13	8.45	10.56	3.07	0.03	0.087	8.42
PR-1	F	Copley	Dc	65.75	0.476	11.14	5.51	0.09	7.48	6.75	2.73	0.04	0.021	3.14
PR-2	F	Copley	Dc	44.70	0.582	13.50	9.51	0.24	17.45	13.23	0.68	0.07	0.044	8.76
PR-3	F	Copley	Dc	50.33	0.460	13.56	7.06	0.23	14.69	10.95	2.09	0.60	0.034	12.9
PR-4	F	Copley	Dc	45.56	0.649	13.33	9.30	0.24	18.22	11.65	0.79	0.23	0.022	8.96
PR-5	F	Copley	Dc	62.74	0.571	14.02	5.87	0.08	9.12	3.51	3.93	0.09	0.077	8.9
PR-6	F	Copley	Dc	53.31	0.633	13.96	8.19	0.13	13.76	7.99	1.08	0.92	0.033	8.22
PR-7	F	Copley	Dc	57.77	0.567	12.32	6.51	0.11	11.58	7.87	1.44	1.82	0.021	6.44
COP-1		Copley	Dc	58.45	0.486	15.32	9.38	0.28	9.93	3.76	2.06	0.31	0.033	9.36
COP-3		Copley	Dc	54.21	0.844	15.10	9.21	0.16	9.32	7.72	3.00	0.36	0.078	9.83
COP-4		Copley	Dc	58.25	0.776	14.02	8.77	0.13	7.92	6.91	3.04	0.10	0.078	9.69
COP-5		Copley	Dc	52.85	0.555	17.48	11.20	0.33	12.45	2.89	1.88	0.33	0.034	11.46
COP-6		Copley	Dc	50.54	0.474	12.92	6.93	0.13	10.67	15.27	2.96	0.06	0.049	17.66
COP-7		Copley	Dc	54.36	0.540	13.07	7.98	0.11	12.41	8.02	3.44	0.03	0.033	9.05
COP-8		Copley	Dc	50.62	0.471	12.92	6.93	0.13	10.59	15.26	2.96	0.07	0.048	17.15
COP-9		Copley	Dc	52.29	0.809	16.42	7.62	0.14	9.58	6.85	4.60	1.62	0.069	13.34
COP-10		Copley	Dc	53.46	0.794	15.89	8.24	0.16	10.10	5.60	5.37	0.28	0.093	14.27
COP-11		Copley	Dc	55.11	0.666	14.88	7.39	0.15	9.78	6.21	5.56	0.18	0.079	11.26

Table 1 continued. (page 2 of 6)

SAMPLE NUMBER	LOC	NAME	MAP UNIT	Ba	Ce	Cl	Co	Cr	Cs	Cu	F	Ga	Hf	La	Nd	Ni	Pb
Upper Plate																	
SV-1	L	Copley	Dcs														
SV-2	L	Copley	Dcs	16.3	0	33.3	32.2	143.9	2	321.4	100.7	17.7	3.9	22.9	19	33.3	0.1
SV-3	K	Copley	Dcs														
SV-4	S	Copley	Dcs	4064.1	362.2	15.1	0	154.3	4.4	18.1	0	8.6	7.1	31.9	22.9	29.6	10.6
SV-5	S	Copley	Dcs	932.8	73.3	20.5	4.7	105.5	4.1	26.6	0	10.9	7.5	43.3	26	27.7	4
SV-6	G	Copley	Dcs	577.5	64.3	33.3	63.5	76.8	2.3	29.7	752.5	18.2	4.4	45.6	53.8	37.6	8.9
GR-1	T	Copley	Dc	37.2	0	26.1	31.5	321	2.3	130.2	139.6	11.4	4.2	10.6	8.8	91.1	0
GR-2	T	Copley	Dc	45.5	1.3	24.1	36.5	270.2	3.2	20.7	136.1	5.2	5.4	33.9	26.4	115.5	0
GR-3	T	Copley	Dc	18	0	20.8	39.5	214.8	1.9	22.7	157	15.6	3.8	15.1	14.5	33.7	0.05
GR-4	V	Copley	Dc	64.1	7.8	25.1	50.9	312.8	1.9	9.7	136.5	16.6	3.6	21.8	25.1	95.3	0
GR-5	V	Copley	Dc	0	0	19.3	16.4	376.6	1.6	98.5	86.1	15.6	3	0	0	73.1	0
GR-6	H	Copley	Dc	0	0	30.2	35.5	347.3	1.7	24.9	233.3	15.2	3.2	7.9	5.1	73.7	0
PR-1	F	Copley	Dc	1.4	0	19.9	28.8	567.1	2.9	11.8	155.4	10.6	4.6	11	9	140.5	2.3
PR-2	F	Copley	Dc	0	0	21.4	54.3	536.8	0.9	0	251.1	12.9	1.9	0.3	7.9	151.2	0
PR-3	F	Copley	Dc	34.6	0	29.6	37.1	429.4	2.4	27	0	5.3	4.1	8.2	12.7	112.8	0
PR-4	F	Copley	Dc	0	0	25.3	55	557.8	1.2	41.9	249.7	10.1	2.4	11.3	10.2	149.7	1.9
PR-5	F	Copley	Dc	35.8	0	29.3	33.3	347.2	3.4	41	0	4.8	5.4	29.3	28	124.3	0
PR-6	F	Copley	Dc	39	0	33.6	45.2	336.5	2	38	82	9.2	3.8	15.4	12.2	107.8	0.6
PR-7	F	Copley	Dc	78.5	0	36	31.2	289.5	2.5	43.8	8	8.1	4.2	7.4	7.7	89.3	0
COP-1		Copley	Dc	59.3	5.9	21.2	56.8	158.7	2.1	281.4	499.9	14.6	4.1	26.2	36.1	40.7	0.8
COP-3		Copley	Dc	60.9	7.3	31.4	49.1	215.2	1.7	41.9	323	16.2	3.6	19.4	22.5	36.6	2.6
COP-4		Copley	Dc	50.4	0.6	22.5	45.8	254.4	2	58.3	193.4	16.9	4	21.8	22.2	42.3	7.1
COP-5		Copley	Dc	68.3	9.1	22.4	69.7	151.5	1.7	432.4	603.9	17.6	3.8	39.1	42.9	40.7	0.4
COP-6		Copley	Dc	15.2	0	50.3	29.7	367.8	2.6	27.4	282.4	5.1	4.4	11.8	0	120.2	0.3
COP-7		Copley	Dc	10.7	0	32.4	46.3	769.4	2.2	62	413.4	11	3.9	19.5	22.2	155.7	0
COP-8		Copley	Dc	8.7	0	52.3	29.8	373	2.6	26	301.5	5.6	4.2	12.3	0	122.1	0
COP-9		Copley	Dc	362.0	28.3	28.4	36.9	155.7	2.4	76.5	64.1	13.5	4.2	17.3	21.5	59.5	3.8
COP-10		Copley	Dc	77.4	7.5	28.9	45.9	73.3	2.4	109.5	44.9	14.5	4.0	26.5	23.9	35.2	0.0
COP-11		Copley	Dc	45.1	2.0	31.7	41.0	52.6	2.6	91.4	173.6	13.2	4.3	20.7	22.0	43.0	0.7

Table 1 continued. (page 3 of 6)

SAMPLE NUMBER	Rb	S	Sc	Sr	Ta	Th	U	V	Zn	Zr
Upper plate										
SV-1										
SV-2	3.5	24.5	27.2	172.9	0.8	8.2	1.4	295.9	41.9	66.9
SV-3										
SV-4	54.3	28.8	9.3	49.5	1.5	30.1	4.8	0	24.1	139.2
SV-5	49.2	106.9	7.4	122.6	1.6	30.5	5.1	15.1	29.5	163.9
SV-6	54.9	41.3	7.4	80.4	0.9	10.7	1.6	214.8	177.7	100.2
GR-1	15.7	55.9	22.3	56.6	0.9	11.9	1.9	302	46.5	32.4
GR-2	12.4	22.2	14.6	106.5	1.3	18.9	3.4	107.1	50.4	48.5
GR-3	5	23.5	25	311.5	0.7	7.9	1.4	226.8	48	78.2
GR-4	13.7	24.1	19.8	116.5	0.7	6.7	1.1	242.8	67.5	56.6
GR-5	4.2	21.6	40	41.9	0.6	5.1	0.8	220.6	29.8	28.6
GR-6	2	23.5	28.9	65.3	0.7	5.9	0.9	265.3	49.5	32.8
PR-1	10	25.5	22.6	39.7	1.1	16.8	2.7	215.2	37.3	26.2
PR-2	0	20.8	36.5	161	0.4	0	0	198.7	66.9	30.5
PR-3	14.5	21.9	28.4	45.3	0.9	11.2	2	174.5	60.9	23.2
PR-4	0.2	18.6	33.1	96.5	0.4	0.3	0	182.1	70.5	26.5
PR-5	13.9	25.4	12.7	51.6	1.3	19.7	3.5	122.1	53.4	40.3
PR-6	16.4	23.8	22.7	180.2	0.8	7.6	1.3	163.6	54.9	49.4
PR-7	33.9	21.1	22.7	125.7	1	12.1	2.1	160.1	49.7	42.9
COP-1	9.5	28.3	14.5	121.4	0.9	8.5	1.5	206.7	247.3	51.8
COP-3	5	32.9	22.9	236.6	0.7	5.7	1	246.8	66.9	72.3
COP-4	3.5	26.7	20.8	256.2	0.8	7.8	1.3	245.7	62.5	71.9
COP-5	6.6	29.8	13	89.6	0.8	5.2	0.8	214.5	321.5	49.9
COP-6	8.2	78.1	35.6	57.8	0.9	13.4	2.3	168.8	48.7	31.8
COP-7	4.5	27.5	23.4	70.9	0.9	9.6	1.6	188.1	49	35.5
COP-8	7.6	80.3	35.8	58.2	0.9	13	2.3	164.1	49	32.1
COP-9	20.5	65.3	20.8	141.7	0.9	10.9	1.9	236.2	52.1	58.7
COP-10	7.6	57.3	18.8	57.3	0.9	11.4	1.9	272.0	64.2	46.1
COP-11	8.1	41.0	19.6	132.6	1.0	13.1	2.2	218.6	54.9	49.1

Table 1 continued. (page 4 of 6) **Data obtained from Petrology lab at CSU Fresno*

SAMPLE NUMBER	LOC	NAME	MAP UNIT	SiO_2	TiO_2	Al_2O_3	FeO	MnO	MgO	CaO	Na_2O	K_2O	P_2O_5	H_2O	TOTAL
Fault Rocks															
COP-12*		Copley	Dc	62.08	0.921	17.96	8.61	0.26	6.41	0.08	1.76	1.84	0.083		100.80
COP-13*		Copley	Dc	50.88	0.410	12.09	29.14	0.06	7.13	0.02	0.22	0.03	0.013		103.30
C0P-14*		Copley	Dc	60.94	0.403	14.85	6.98	0.06	2.48	13.76	0.39	0.12	0.022		100.06
SHZ-1*	4	Copley	Dcs	58.14	0.090	3.14	6.75	0.14	27.35	4.10	0.25	0.03	0.013		100.26
SHZ-2	2	Copley	Dcs												
SHZ-3*	2		Fault	54.75	0.050	4.68	10.01	0.19	23.85	6.05	0.36	0.04	0.024		100.27
SHZ-4*	4		Fault	55.83	0.120	2.57	5.01	0.12	24.28	11.29	0.68	0.08	0.026		100.33
SHZ-5*	3		Fault	61.35	0.050	1.36	4.50	0.04	27.63	4.79	0.25	0.02	0.014		100.73
SHZ-6*	1		Fault	66.28	0.734	13.02	7.08	0.09	7.52	3.57	1.59	0.04	0.070		100.24
SHZ-7*	1		Fault	53.11	0.070	6.24	9.76	0.12	20.92	9.44	0.29	0.03	0.016		100.63
SHZD-8*	1	Undated	Dike	80.41	0.201	11.04	2.24	0.04	0.84	0.34	4.58	0.27	0.040		99.67
Lower Plate				SiO_2	TiO_2	Al_2O_3	FeO	MnO	MgO	CaO	Na_2O	K_2O	P_2O_5	H_2O	TOTAL
D-4		Trinity	Ogd	50.01	0.575	13.78	8.81	0.16	16.83	6.64	3.14	0.02	0.045	11.14	
D-1	2	Undated	O?d	76.91	0.087	12.39	1.53	0.01	1.39	0.37	7.14	0.14	0.033	7.87	
D-2	2	Undated	O?d												
D-3	4	Trinity	SDgb												
SHZ-9	2		Fault	59.08	0.561	14.01	5.78	0.13	13.36	2.54	4.42	0.03	0.079	10.72	
SHZ-10	2		Fault												
UM-1		Trinity	Oum	44.70	0.131	9.41	7.68	0.15	30.81	6.95	0.15	0.00	0.022	8.09	
UM-2*	A	Trinity	Oum	46.57	0.030	1.04	9.52	0.07	42.47	0.19	0.03	0.07	0.018		99.85
UM-3	B	Trinity	Oum	45.63	0.034	1.47	7.40	0.13	45.24	0.09	0.00	0.00	0.000	12.04	
UM-4	B	Trinity	Oum	45.09	0.045	1.70	7.46	0.13	45.49	0.08	0.00	0.00	0.000	10.49	

Table 1 continued. (page 5 of 6)

NEW NAME	LOC	NAME	MAP UNIT	Ba	Ce	Cl	Co	Cr	Cs	Cu	F	Ga	Hf	La	Nd	Ni	Pb
Fault Rocks																	
COP-12		Copley	Dc	318.8			300.2	17.9				27.0	4.4	57.8	27.9	19.3	
COP-13		Copley	Dc	79.2			647.4	18.1				20.4	15.4	94.8	28.8	19.2	
C0P-14		Copley	Dc				229.7	17.9				20.9	4.4	63.6	27.8	19.5	
SHZ-1	4	Copley	Dcs				326.0	19.7				22.9	5.4	72.4	28.2	37.1	
SHZ-2	2	Copley	Dcs														
SHZ-3	2		Fault				523.4	21.2				22.2	3.1	80.2	28.4	41.1	
SHZ-4	4		Fault				272.6	18.4				22.6	4.2	64.3	28.1	35.3	
SHZ-5	3		Fault				243.2	18.8				28.6	4.4	77.3	28.2	32.5	
SHZ-6	1		Fault				286.7	17.9				22.4	2.9	63.3	28.0	21.4	
SHZ-7	1		Fault				360.7	19.9				20.9	2.9	76.9	28.4	32.6	
SHZD-8	1	Undated	Dike	40.3			141.0	17.9				25.2	9.5	54.5	28.1	19.6	
Lower Plate				**Ba**	**Ce**	**Cl**	**Co**	**Cr**	**Cs**	**Cu**	**F**	**Ga**	**Hf**	**La**	**Nd**	**Ni**	**Pb**
D-4		Trinity	Ogd														
D-1	2	Undated	O?d	165.5	17.9	63	0.8	145.1	4.8	58.7	0	11	8.3	60.5	38.7	59.9	36.2
D-2	2	Undated	O?d														
D-3	4		SDgb														
SHZ-9	2		Fault	81.2	13.2	48.6	44.4	258.1	3.7	453.8	7.8	8.5	6.4	31.3	35.4	244.7	3.9
SHZ-10	2		Fault														
UM-1		Trinity	Oum	0	0	35	64.9	1716.5	2.7	0	0	6.7	4.6	15.5	50.9	1387.2	0.4
UM-2	A	Trinity	Oum				486.4	19.6				23.7	4.4	76.0	28.1	53.5	
UM-3	B	Trinity	Oum	61.2	21.8	17.6	94.8	2021.4	4.1	0	0	0.7	6.7	59.8	73.4	2163.8	0
UM-4	B	Trinity	Oum	62.2	22.5	26.1	90.8	2695.8	4.2	1.9	0	3.1	6.7	64.5	82.9	2213.1	3

Table 1 continued. (page 6 of 6)

SAMPLE NUMBER	Rb	S	Sc	Sr	Ta	Th	U	V	Zn	Zr	Y	Nb	Sm	Eu	Tb	Yb
Fault Rocks																
COP-12	95.4		43.3	108.3	3.8			234.1	219.9	105.5	38.9	23.1	7.8	2.4	1.1	3.0
COP-13	42.8		51.1	97.0	3.2			157.9	148.5	66.1	32.4	41.1	5.1	1.9	1.1	3.0
C0P-14	42.2		35.3	96.3	3.8			113.7	87.0	58.1	31.2	68.1	7.6	1.9	1.1	3.0
SHZ-1	40.5		28.9	96.0	3.8			34.4	87.8	57.4	31.2	65.3	6.7	2.1	1.1	3.1
SHZ-2																
SHZ-3	41.8		35.0	95.8	3.9			48.4	86.2	57.8	31.0	67.0	6.1	2.1	1.1	3.1
SHZ-4	40.2		30.3	95.8	3.8			24.3	87.8	58.1	31.2	67.0	7.0	2.0	1.1	3.1
SHZ-5	25.9		24.6	100.3	3.8			27.2	132.6	61.4	32.6	6.2	7.3	1.9	1.1	3.1
SHZ-6	39.9		37.6	97.5	3.8			144.5	88.3	60.1	31.2	67.5	8.4	2.0	1.1	3.0
SHZ-7	42.5		31.6	95.9	3.8			40.2	87.8	57.3	31.0	68.1	5.0	2.0	1.1	3.1
SHZD-8	40.5		21.9	97.5	3.8			23.8	91.8	67.9	31.8	66.4	9.1	1.8	1.1	3.0
Lower Plt.	**Rb**	**S**	**Sc**	**Sr**	**Ta**	**Th**	**U**	**V**	**Zn**	**Zr**	**Y**	**Nb**	**Sm**	**Eu**	**Tb**	
D-4																
D-1	26.2	29.5	3.7	63.8	2	37.8	6.6	8.3	12.7	88.8						
D-2																
D-3																
SHZ-9	14.7	29.1	11.1	51.5	1.5	23	4	145.6	49.7	79.5						
SHZ-10																
UM-1	6.8	21.4	20.1	6.3	1.2	12.8	2.2	90.4	65.2	26.2						
UM-2	42.2		30.9	96.1	3.9			22.0	92.4	57.4	31.2	65.3	6.6	1.9	1.1	3.2
UM-3	16.4	110.2	4	16.4	1.9	24.5	4.4	34	38.5	14.6						
UM-4	16.4	92	4.1	16.5	2	25.5	4.6	35.8	59.6	14.6						

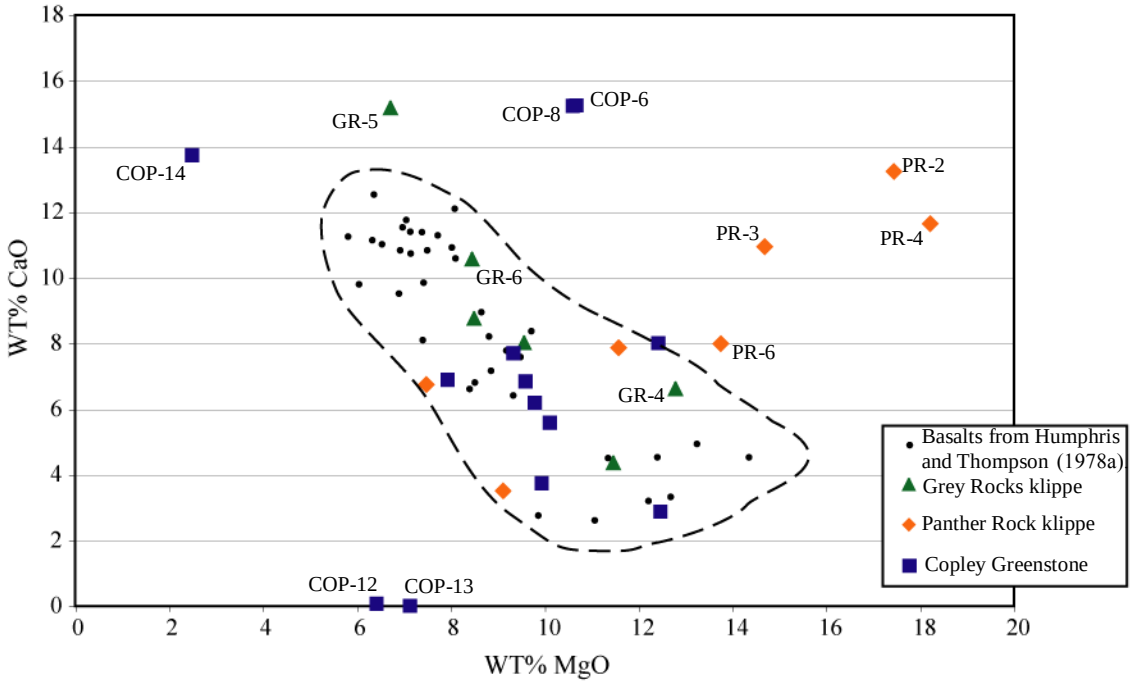

Figure 17: Plot of CaO vs. MgO in Greenstones from Grey Rocks and Panther Rock klippes, and the Copley Greenstone. Values are compared to those from fresh and altered basalts (Humphris and Thompson, 1978a). Dashed outline represents hydrothermally altered basalts.

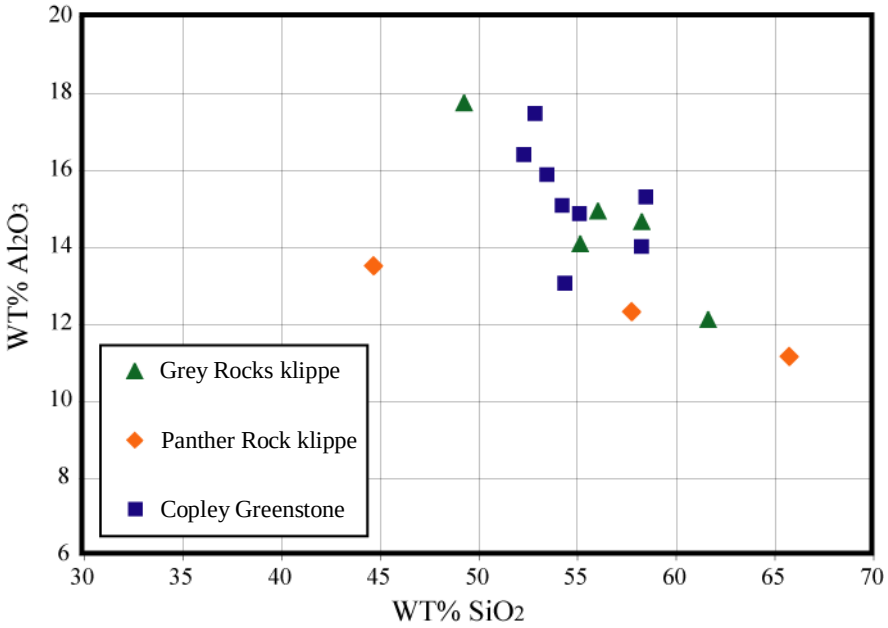

Figure 18: Plot of Al_2O_3 vs. SiO_2 for greenstone samples from Grey Rocks, Panther Rock, and Copley Greenstone.

have used data from Humphris and Thompson (1978a) have interpreted data that lie outside the trend as either being from another magma source or as experiencing increased alteration (Barrow and Metcalf, 2006). The samples from this study are unlikely to be from different sources, as samples from similar locations lie both within and outside the field of fresh and hydrothermally altered basalts (Fig. 17) (i.e., GR-4 and GR-5). The samples that plot outside the dashed area are interpreted to have experienced increased levels of alteration and are not reliable for comparison.

Bulk Rock Composition Comparison

Humphris and Thompson (1978a) found that bulk SiO_2 can be depleted or enhanced as SiO_2 is leached from the altered rock and then precipitated in veins within pillow rims. SiO_2 comprises the major portion of the bulk composition, so variation in SiO_2 affects the rest of the bulk composition values. Harker diagrams have been used to eliminate scatter due to variations in SiO_2. The diagrams typically exhibit negative trends between bulk elements and percent SiO_2.

Plotting values from this project on Harker diagrams displayed only weak trends and inconclusive results, with the best correlation between Al_2O_3 and SiO_2 (Fig. 18). Because of the lack of clearly defined trends, correlation of the trace elements between the greenstones was used for further classification and identification.

Trace Element Composition Comparison

Some trace elements are more mobile than others and can be enhanced or removed during alteration. Minor and trace elements that are more stable under greenschist facies alteration include Cr, Zr, and REEs (Humphris and Thompson, 1978b).

To compare the trace elements of all three greenstones, spider diagrams have been plotted using MORB normalization values of Pearce (1983) (Fig. 19a), and chondrite normalization values of Thompson (1982) (Fig. 19b).

From the trace element patterns exhibited in these two diagrams, the greenstones of the Panther Rock and Grey Rocks klippes are geochemically related to the Copley Greenstone of the Redding terrane. This interpretation supports other interpretations of a cogenetic link between "Trinity basalts" (Brouxel 1988) and the Copley Greenstone (Wallin and Metcalf, 1998). Wallin and Metcalf (1998) interpret the Siluro-Devonian intrusive suite within the Trinity terrane as cogenetic with the Copley Greenstone. They compared data of "Trinity terrane" gabbros, dikes, pillow basalts and Copley Greenstone samples compiled from Lapierre et al. (1985), Brouxel et al. (1988), Brouxel and Lapierre (1988), Brouxel et al. (1989), Brouxel et al. (1991), Cannat and Lecuyer (1991), Petersen et al. (1991), and Gruau et al. (1995). Wallin and Metcalf (1998) interpret the geochemical similarity, spatial relations, and age relations between these units as indicative of a cogenetic system. Data from this project further supports this cogenetic interpretation.

Felsic Dikes Analyses

Numerous dikes are observed intruding mafic and ultramafic rocks of the Trinity terrane. Although none of the dikes are observed intruding the upper plate klippes, three felsic dikes are observed intruding fault rocks. Two felsic dikes intrude fault zone rocks at the base of the Horse Heaven Meadows klippe (D-1, D-2) and a third tectonized felsic

A. Comparison of greenstones from Grey Rocks and Panther Rock klippes and Copley Greenstone samples, normalized to MORB.

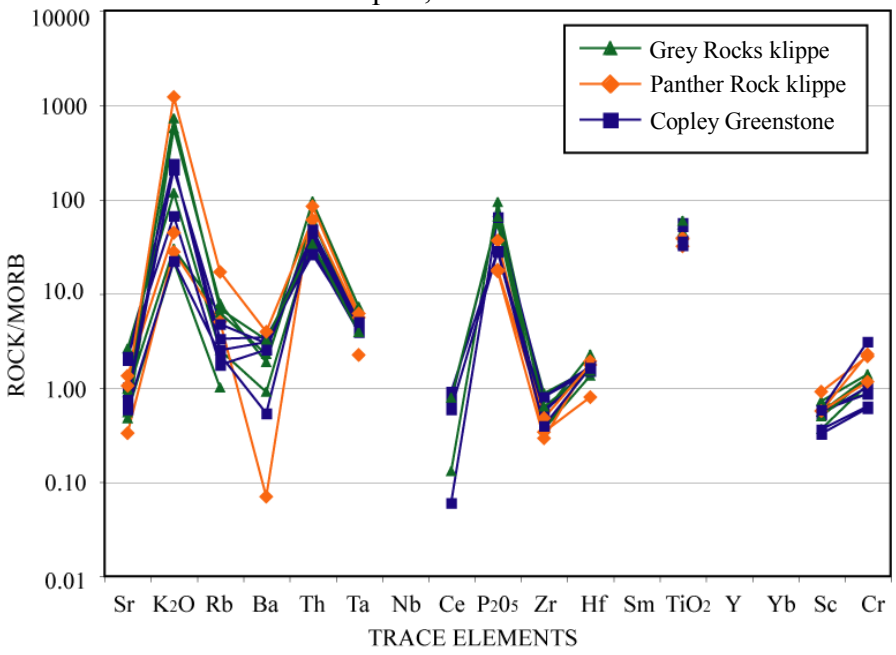

B) Comparison of greenstones from Grey Rocks and Panther Rock klippes and Copley Greenstone samples, normalized to chondrite values.

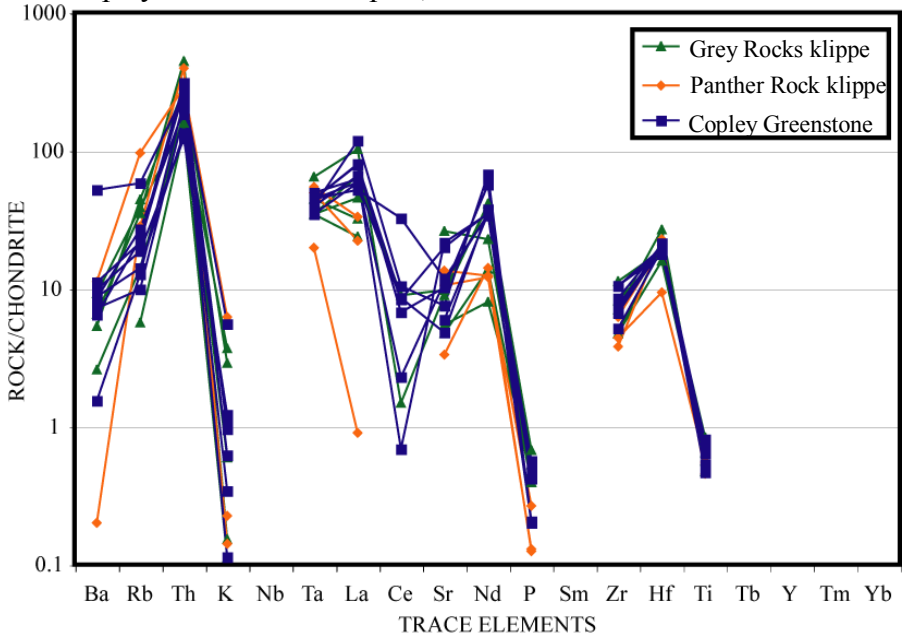

Figure 19: REE patterns of greenstones from Grey Rocks and Panther Rock klippes and Copley Greenstone samples using A) MORB (Pearce, 1983) and B) chondrite (Thompson, 1982) values.

dike (SHZD-8) intrudes parallel to the fault zone at the base of the Grey Rocks klippe (Locations 2 and 1, Fig. 2). The mineralogy and bulk composition of the felsic dikes support an affinity between the two dikes sets from this project (Table 2); however, the structural relations of the two dike sets indicates a timing difference of emplacement that also constrains timing for part of the basal faulting event. Sample D-1 and sample SHZD-8 are both rhyolite dikes categorized by the Jensen cation plot (Jensen, 1976). Similarly, the bulk compositional values reflect comparable elemental percentages (Table 2). The structural relations of the dikes dates the fault parallel dike at Location 1 as syntectonic with the basal fauting indicated by the shear microstructures (Fig. 15) and the other two dikes at Location 2 as post-basal faulting by cross-cutting the fault breccia (Fig. 2). The difference in emplacement timing between the dike sets could constrain the timing of faulting if dated.

Fault parallel, felsic dikes (muscovite-bearing dacite, muscovite-bearing rhyolite, and plagioclase porphyry) were mapped intruding detachment faults between the Copley Greenstone and Trinity terrane mafic and ultramafic rocks at Deer Creek (Mt. Shasta area) and along the Carrville fault (Trinity Lake area) (Table 2 and Fig. 20) (Goldstein, 1997; Cashman and Elder, 2002). Geochemical analyses were conducted to test correlation between felsic dikes at Locations 1 and 2 (Fig. 2) and those observed at Mt. Shasta area and Trinity Lake by Cashman and Elder (2002). Felsic dikes from Cashman and Elder (2002) and the two rhyolite dikes (D-1, SHZD-8) were plotted on a TAS diagram (Fig. 20); however, the plot yielded inconclusive results as to whether the dikes are from a similar source.

Table 2. Chemical Analyses of Felsic dikes that intrude faults that form the upper contact of the Trinity terrane. Values are weight percent. Samples have been normalized to 100 percent.

SAMPLE #	LOCATION	SiO2	TiO2	Al2O3	FeO	MnO	MgO	CaO	Na2O	K2O	P205
SHZD-8	Grey Rocks klippe, LOC 1	80.41	0.201	11.04	2.24	0.04	0.84	0.34	4.58	0.27	0.040
D-1	Horse Heaven Meadows klippe, LOC 2	76.91	0.087	12.39	1.53	0.01	1.39	0.37	7.14	0.14	0.033
96-HG-8AM*	MT. SHASTA	69.09	0.235	16.26	3.45	0.06	1.28	1.22	4.85	3.52	0.032
96-HG-8B*	MT. SHASTA	71.06	0.224	15.13	2.92	0.05	1.57	0.45	5.52	3.05	0.021
94-28*	TRINITY LAKE	66.38	0.563	15.84	4.15	0.09	3.53	1.13	3.82	4.33	0.174
94-29A*	TRINITY LAKE	72.09	0.137	16.00	1.91	0.05	0.55	0.67	5.19	3.34	0.063
93-31M*	TRINITY LAKE	66.04	0.500	16.06	4.39	0.10	3.86	0.63	4.76	3.46	0.198
94-95*	TRINITY LAKE	71.09	0.148	17.07	1.95	0.06	0.49	0.42	5.58	3.15	0.042
94-20M*	TRINITY LAKE	68.30	0.399	17.18	3.37	0.05	1.61	1.03	4.57	3.34	0.147
94-35M*	TRINITY LAKE	69.10	0.449	15.52	3.48	0.07	1.76	1.12	3.64	4.59	0.265
94-29B*	TRINITY LAKE	70.53	0.150	14.83	3.40	0.07	0.72	0.70	6.25	3.26	0.090
94-35BM*	TRINITY LAKE	67.68	0.485	16.05	4.38	0.11	3.01	0.13	5.17	2.81	0.169

*From Cashman and Elder, 2002.

Table 3. Chemical Analyses of Shear Zone rocks from Grey Rocks and Horse Heaven Meadows klippes shear zones with Upper Plate rocks from Grey Rocks klippe and Lower Plate rocks from the Trinity terrane.

Location/Descr.	Sample #	SiO_2	TiO_2	Al_2O_3	Fe_2O_3	MnO	MgO	CaO	Na_2O	K_2O	P_2O_5
Gray Rocks klippe Loc. H - greenstone	GR-6	55.17	0.68	14.07	7.74	0.13	8.45	10.56	3.07	0.03	0.09
Grey Rocks klippe Loc. 1 - sheared greenstone	SHZ-6	66.28	0.73	13.02	7.08	0.09	7.52	3.57	1.59	0.04	0.07
Grey Rocks klippe Loc. 1 - mylonite	SHZ-7	53.11	0.07	6.24	9.76	0.12	20.92	9.44	0.29	0.03	.016
Trinity ultramafic sheet Loc. A - serpentinite	UM-2	46.57	0.03	1.04	9.52	0.07	42.47	0.19	0.03	0.07	0.018
Horse Heaven Meadows klippe Loc. 4 - mylonite	SHZ 1	55.83	0.12	2.57	5.01	0.12	24.28	11.29	0.68	0.08	0.026
Horse Heaven Meadows klippe Loc. 2 - mylonite	SHZ-3	54.75	0.05	4.68	10.01	0.19	23.85	6.05	0.36	0.04	0.024

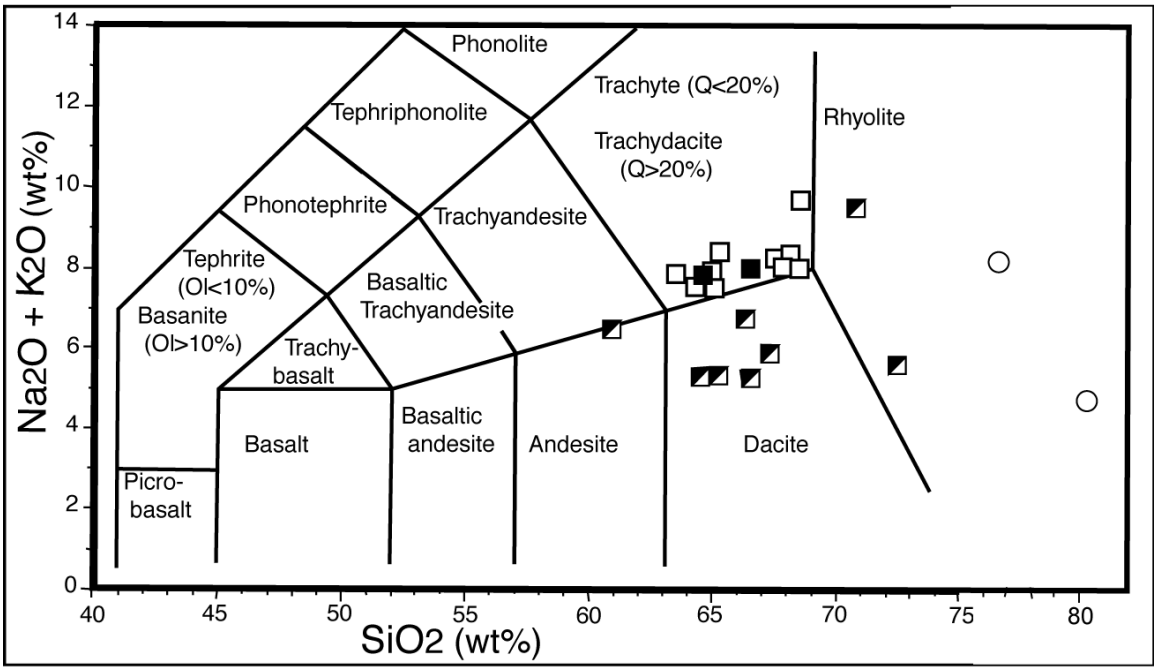

Figure 20: Total alkalis vs. silica plot (TAS) from LeBas et al. (1986). Circles - dikes from Location 1 and 2 (this project). Black squares – Deer Creek; Half-white squares – Cecilville; White squares – Trinity Lake (Cashman and Elder, 2002).

Fault Rocks Analyses

Grey Rocks Klippe Basal Shear Zone

The shear zone exposed at the southeast contact of the Grey Rocks klippe (Location 1, Fig. 2) is a nine-meter thick zone of coherent and sheared layers that incorporate both upper and lower plate units. Rock types observed in the shear zone are mylonite (SHZ-7), greenstone (SHZ-6), and rhyolite (SHZD-8). Bulk compositions of shear zone samples were measured to determine the origin of fine-grained material in the shear zone and to assess the relative importance of components from the upper and lower plates of the fault.

Comparing bulk compositions of upper plate and lower plate samples with those of shear zone samples indicates a mixing of upper and lower plate rock components in the shear zone. The greenstone sample GR-6 from the upper plate and Trinity ultramafic sheet sample UM-2 from the lower plate are used as limits, representing upper and lower plate values of rock units proximal to the exposed shear zone near Grey Rocks basin, (Table 3 and Location 1, Fig. 2). The shear zone mylonite, sample SHZ-7, has bulk composition values that fall between the upper and lower plate values (Table 3 and Fig. 21A). A comparison of shear zone sample SHZ-7 with lower plate sample UM-2, indicates increased amounts of Al_20_3 and depleted amounts of MgO in the shear zone. This shift in bulk composition is interpreted as evidence for incorporation of Al_20_3-rich upper plate material in the shear zone during faulting.

More coherent sections of the shear zone are comprised of greenstone, represented by sample SHZ-6, and resemble upper plate greenstone (GR-6) samples rather than lower plate (UM-2) and mylonite (SHZ-7) samples of the shear zone. Sample SHZ-6 exhibits lower MgO, higher SiO_2, and higher Al_2O_3 values than the lower plate sample UM-2 and the mylonite SHZ-7 (Table 3).

In comparison with the upper plate greenstone (GR-6), coherent greenstone sections in the shear zone (SHZ-6) have higher SiO_2 and lower CaO content. The coherent greenstone sections (SHZ-6) exhibit extensive quartz veining that accounts for the elevated SiO_2 content. The quartz veining is also interpreted as accommodating some of the extension within the shear zone. Other greenstone samples close to the fault zone have exhibited low CaO content due to increased hydrothermal alteration. The lower CaO content in sample SHZ-6 is interpreted as resulting from increased hydrothermal alteration along the fault zone. An affinity of the coherent sections with upper plate greenstone is expected as the lower plate is comprised of units that more readily deform and would more likely exhibit extreme shearing.

Horse Heaven Meadows Klippe Shear Zone:

Shear zone exposures of the mylonitic basal contact of the Horse Heaven Meadows klippe are located at Locations 2 and 4 (Fig. 2). The shear zone exposed at the southeast contact of the Horse Heaven Meadows klippe (Location 2, Fig. 2) is the clearest exposure, displaying a direct contact between slate of the upper plate and mylonite of the fault zone. Here, the shear zone is at least 3 meters thick and is comprised of mylonite (SHZ-3), fault breccia (SHZ-9), and felsic dikes (D-1 and D-2). Bulk compositions of

mylonite samples from basal shear zones of Horse Heaven Meadows (SHZ-3, SHZ-4) and Grey Rocks (SHZ-7) klippes are compared to determine whether the mylonite samples are uniform.

Based on the geochemical affinity of the bulk compositions of the three mylonite samples, the mylonitic layer observed at the base of Horse Heaven Meadows klippe consists of the same mylonite as occurs at the base of the Grey Rocks klippes (Fig. 21B and Table 3). All samples are enriched in Al_2O_3 and SiO_2 and are depleted in MgO compared to ultramafic samples observed in the lower plate (UM-3, UM-2).

A. Bulk composition comparison of mylonite Grey Rocks basal shear zone with upper and lower plate units.

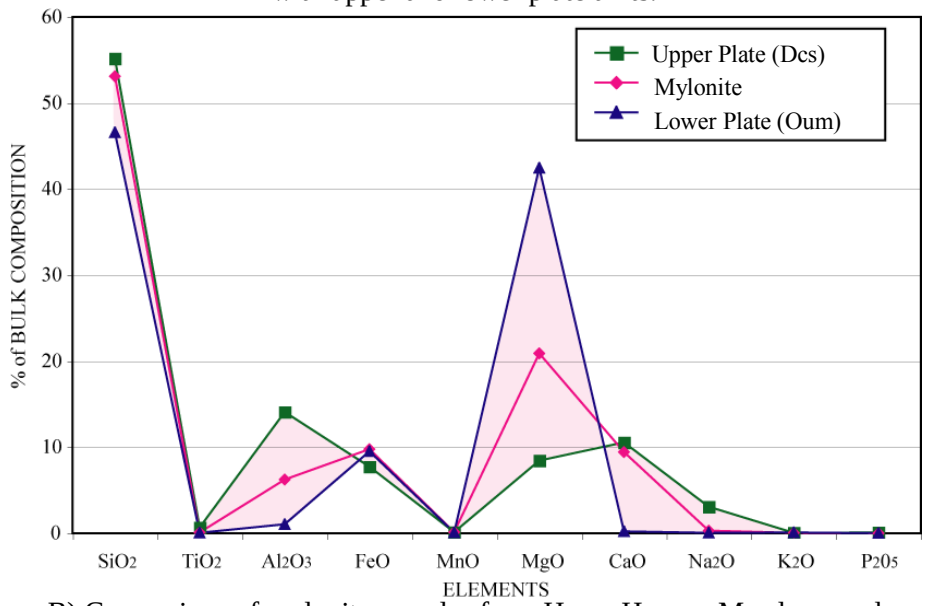

B) Comparison of mylonite samples from Horse Heaven Meadows and Grey Rocks klippe basal fault zones.

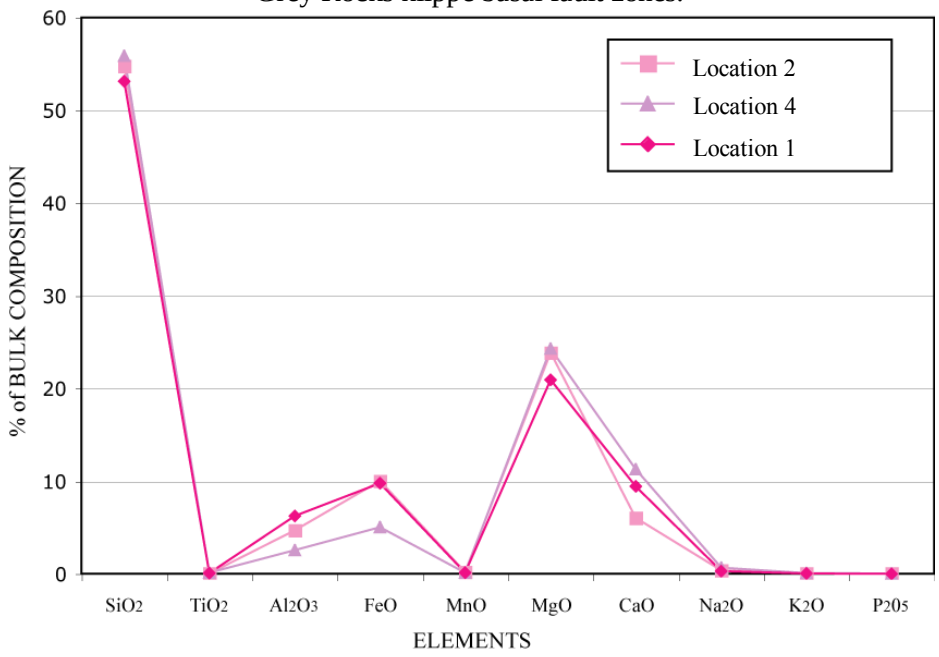

Figure 21. Comparison of A) Grey Rocks shear zone mylonite with samples from the upper (Dc: GR-6) and lower (Oum: UM-2) plate limits. Colored area defines values between upper and lower plate values. Shear zone incorporates both upper and lower plate components resulting in a bulk analysis that lies within the two compositional limits. B) Comparison of mylonite samples from Location 1 (Fig. 2) at the base of Grey Rocks klippe and Locations 2 and 4 (Fig. 2) from the base of Horse Heaven Meadows klippe. Mylonite samples are similar in composition indicating a uniformity of mixing within the shear zone.

STRUCTURE

The basal contact between the Grey Rocks, Panther Rock, and Horse Heaven Meadows klippes with the underlying Trinity ultramafic complex is a 9 to ~85 meter thick fault zone, comprised of coarse-grained breccia, foliated breccia, and mylonite. The fault displaces younger Copley Greenstone and metasedimentary units of the Redding terrane over older Trinity ultramafic complex of the Trinity terrane. Foliation in the upper plate is solely observed adjacent to the basal contact (i.e. Location J, I, 1, 2). Locations 1 through 5 are the best exposures of the basal fault zone between the three klippes and the lower plate. Location 1 is located at the base of the Grey Rocks klippe, Locations 2, 3, and 4 are located at the base of the Horse Heaven Meadows klippe, and Location 5 is located near the base of the Panther Rock klippe.

Grey Rocks Klippe Basal Shear Zone

A 9 meter thick shear zone is exposed at the base of Grey Rocks klippe on the southeast side of Grey Rocks ridge in Grey Rocks basin (Location 1, Fig. 2) Here, the fault plane strikes N10W and dips 34SW, and consists of both coherent and foliated zones (Fig. 22). At Location I (Fig. 2), foliation in the greenstone and ultramafic rocks strikes N30W and dips 72NE. Rocks in the fault zone include mylonite, fractured sections of greenstone with quartz intrusions, and a felsic dike.

Coherent greenstone units (SHZ-6) in the fault zone range from 25 cm to 1 meter in thickness and are separated by 5 cm to 15 cm thick layers of micaceous mylonitic shear rocks (SHZ-7). Coherent greenstone units are greenish dark-grey, fine-grained,

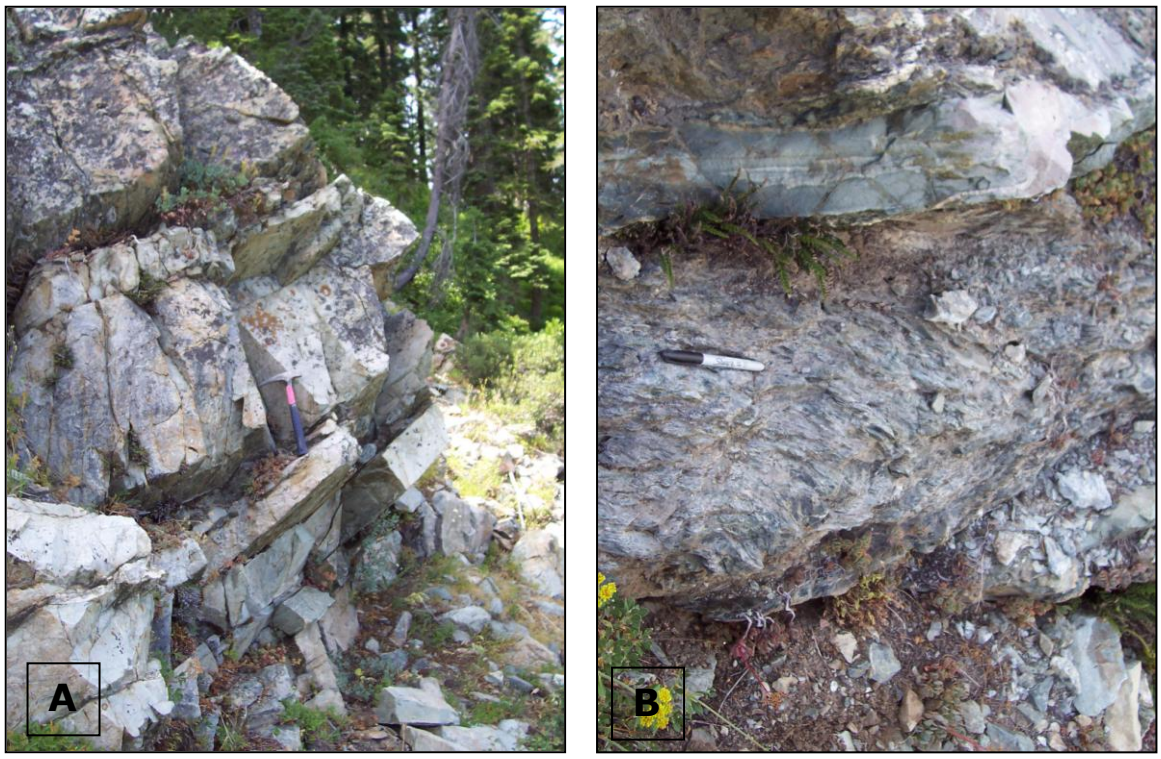

Figure 22: Photographs of Grey Rocks klippe basal shear zone at the fault contact between the greenstone of the Grey Rocks klippe (Dc) and the Trinity ultramafic complex (Ouc). SE margin of Grey Rocks klippe, Location 1 (Fig. 2). Fault zone consists of both sheared and coherent sections of rock within the nine meter thick shear zone. A) Thicker, 28 cm to 1 meter thick, coherent sections of greenstone are separated by thinner layers, 5 to 18 cm, of sheared micaceous mylonite. B) 70 cm thick section of sheared mylonite with Sharpie pen for scale.

fractured, and intruded by multiple sets of offset quartz and calcite veins. The greenstone is comprised of very fine-grained chlorite, quartz, clinozoisite, amphibole, plagioclase degraded to saussurite, and clays. Faint mineral alignment, defined by elongate grains of chlorite and amphiboles, is visible in thin-section (Fig. 23). Foliation in the greenstone unit is solely observed adjacent to the basal fault zone (Location 1, I, and J, Fig. 2).

Incoherent sections are mylonitic, exhibit shear microstructures, and commonly range in thickness from 5 to 15 cm with one section being 1 meter thick (Fig. 24A-D). The 1 meter thick incoherent zone exhibits a strong foliation striking N10W and dipping 43SW. Mylonite is comprised mainly of talc, white micas, serpentine, chlorite, actinolite, and clays. In thin-section, mylonitic foliation is defined by mineral banding, mineral alignment defining a faint s-c fabric, and porphyroclasts of relic hornblendes forming sigma clasts. (A sense of shear was not determined because samples orientation was unclear.)

The sheared rhyolite dike (SHZD-8) has anastomosing and moderately rough foliation. Thin bands of white mica, chlorite, epidote, and quartz flow around the plagioclase crystals creating augins and defining the foliation. Shearing of the dike indicates that dike emplacement may have been syntectonic. Veins cross-cut the foliation perpendicularly and may indicate deformation within an extensional faulting regime.

HORSE HEAVEN MEADOWS KLIPPE BASAL FAULT ZONE

A 3 to ~85-meter thick shear zone is exposed at the base of Horse Heaven Meadows klippe at Locations 2, 3, and 4 (Fig. 2). The klippe forms a convex bowl, with

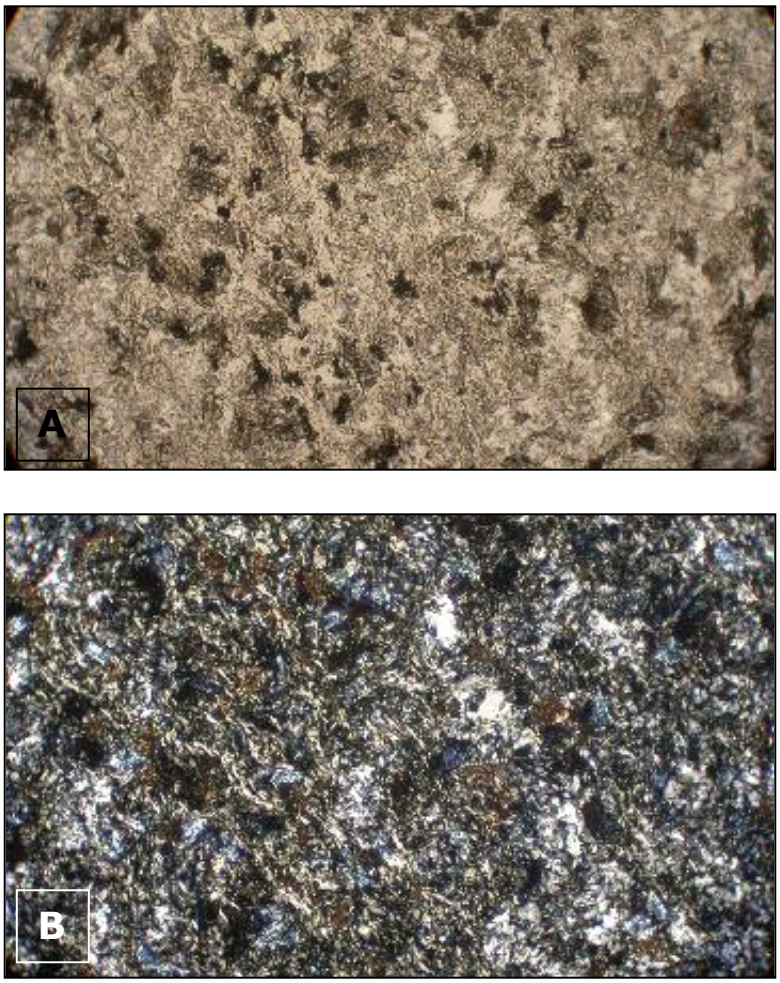

Figure 23: Photomicrograph of coherent greenstone from the Grey Rocks klippe basal shear zone. Sample SHZ-6, Location 1 (Fig. 2), width of image 1.37 mm, A) in plane polarized light and B) in cross polarized light. Sample consists of very fine-grained chlorite, quartz, clinozoisite, amphiboles, and clay. Faint mineral alignment (from upper left corner to lower right corner of image) is defined by aligned chlorite and amphibole crystals.

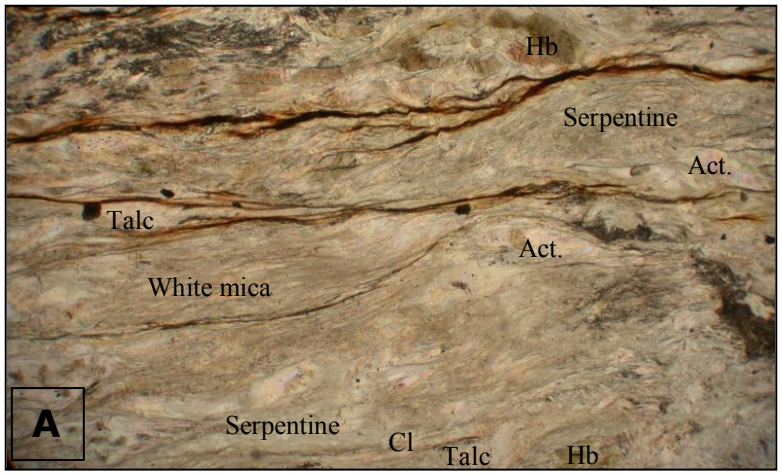

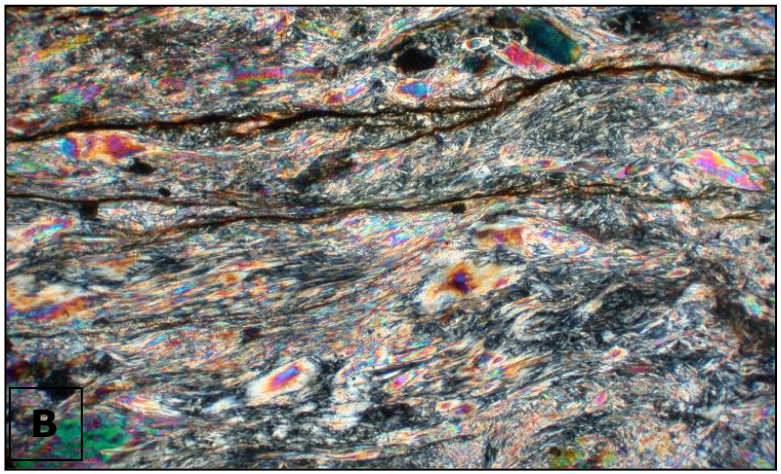

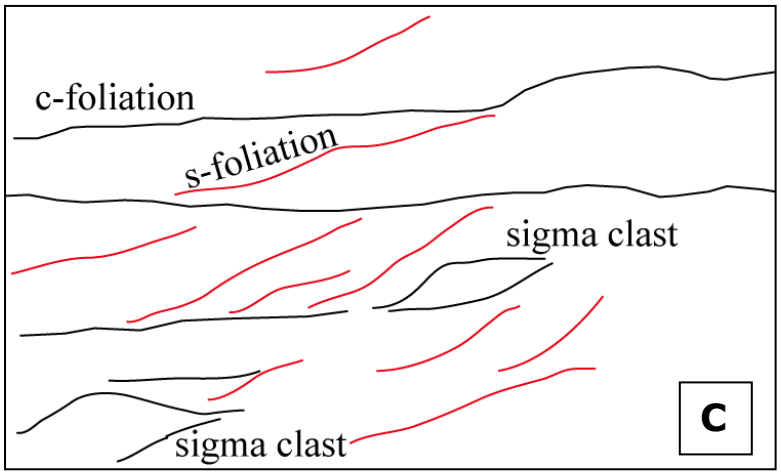

Figure 24: Photomicrograph of mylonite from Grey Rocks klippe basal shear zone (continued on next page), Location 1 (Fig. 2). Sample SHZ-7, width of image 3.2mm, A and D) in plane polarized light, B and E) in cross polarized light, C and F) sketches of A and D. Rock consists of talc, white mica, serpentine, chlorite, hornblende, actinolite. Hornblende altered to actinolite and talc along some s-foliation surfaces. Texture includes mineral banding, s-c fabric, and porphyroclasts of hornblendes forming sigma clasts. A and D are sketches that display s-c foliations and sigma clasts.

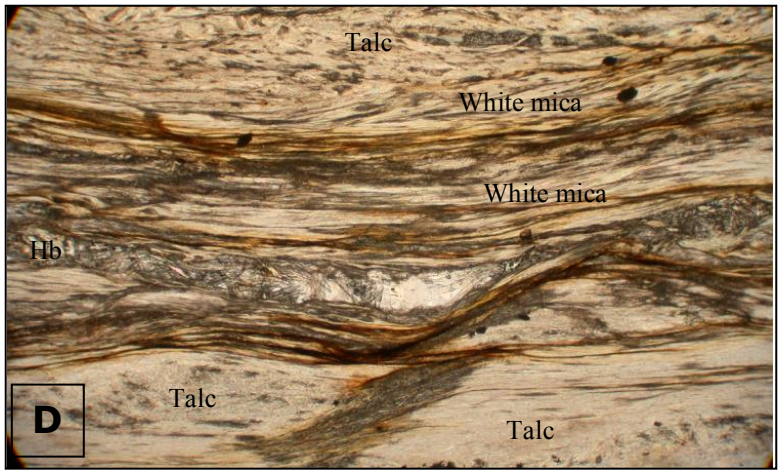
Talc
White mica
White mica
Hb
Talc
Talc
D

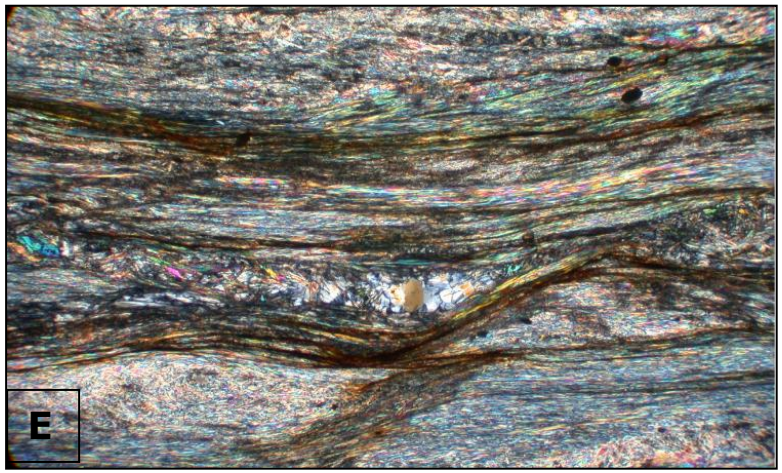
E

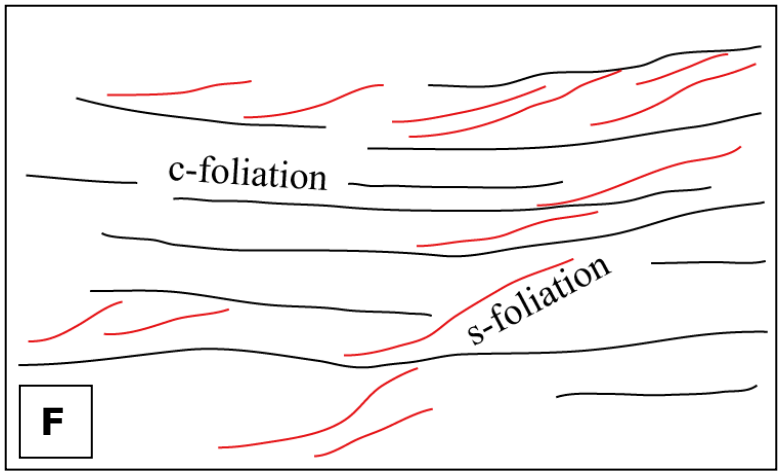
c-foliation
s-foliation
F

the basal fault dipping shallowly to the N-NE. The basal fault zone rocks consist of sheared slate, mylonite, coarse-grained breccia, foliated breccia, and felsic dikes. Foliation in upper plate rocks and increased quartz veins in en echelon patterns are observed solely adjacent to the basal fault.

Location 2) Mile Marker 8.75

Mile Marker 8.75 is a key locality because it is the only place exhibiting direct contact between the Horse Heaven Meadows klippe and the Trinity ultramafic complex (Fig. 25A-B). This location has been described and was previously interpreted as a conformable depositional contact (Boudier et al., 1989; Charvet et al., 1990) (Fig. 25C). Based on identification of shear microstructures in both upper and lower plate rocks, the contact is reinterpreted as a fault contact.

The sequence includes upper plate slate of the Horse Heaven Meadows klippe, fault mylonite, fault breccia, two dikes, and lower plate serpentinized peridotite (Fig. 7B and Fig. 25). The slate directly overlies the fault zone mylonite. The basal fault between the upper plate slate and the ultramafic rocks is defined by mylonitic foliation that strikes N41E and dips 35NW. Fault breccia is juxtaposed with the slate/mylonite block on either side by two younger oblique normal faults. Two felsic dikes approximately 1 to 1.3 meters thick intrude the fault breccia on the western side of the outcrop, striking parallel to the younger faults.

Near the basal fault, the blocky, dark reddish grey, fine-grained slate has two pervasive cleavage planes striking N80E and dipping 25N and striking N26W and dipping 21SW. Bedding was not determined.

25A.

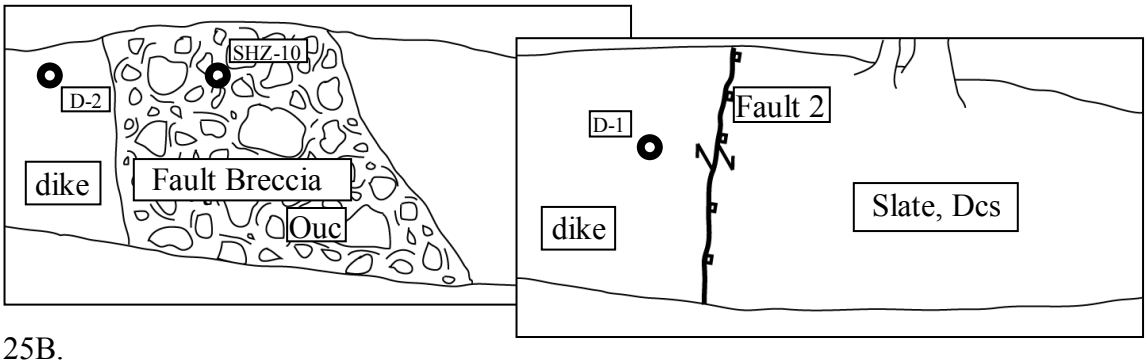

25B.

Figure 25: Interpretations of the basal fault contact between upper plate metasedimentary rocks and lower plate ultramafic rocks of the Trinity terrane at the SE margin of the Horse Heaven Meadows (Location 2, Fig. 2).
A) Photo mosaic of Location 2, continued on next page. View is to the NW. Outcrop is approximately 17 meters wide. Eastern edge continues on next page. Inset is a photo of foliated mylonite at the direct contact between the slate (Dcs) and Trinity ultramafic complex (Ouc). Hammer for scale.
B). Interpretive sketch of 25A photo mosaic showing sample locations.
C) Previously published interpretation of Location 2 as a sedimentary sequence conformably overlying altered peridotite (Charvet and others, 1990).

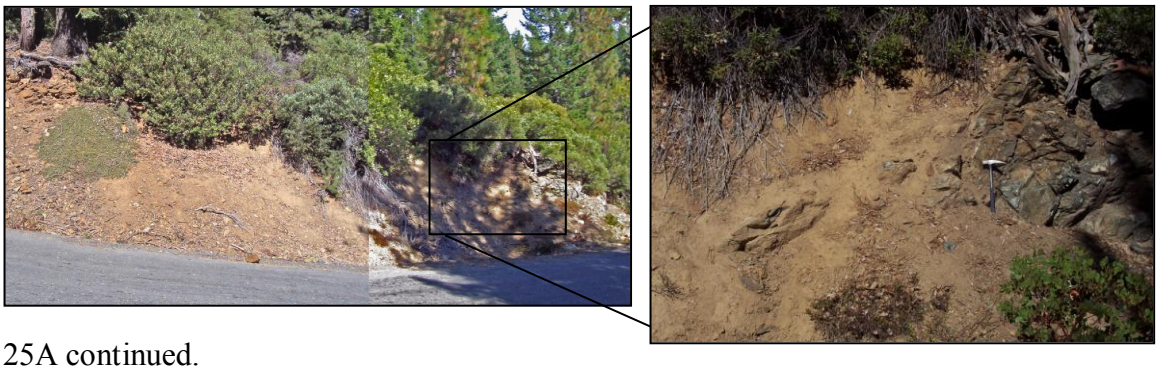

25A continued.

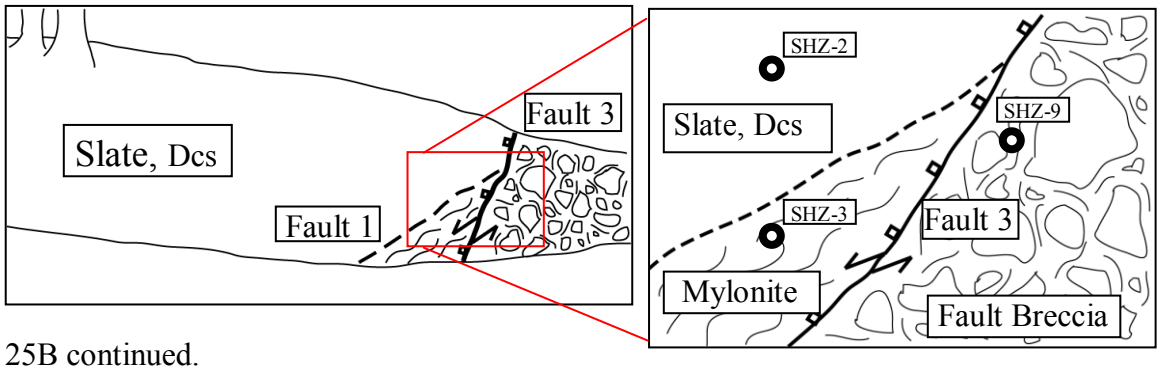

25B continued.

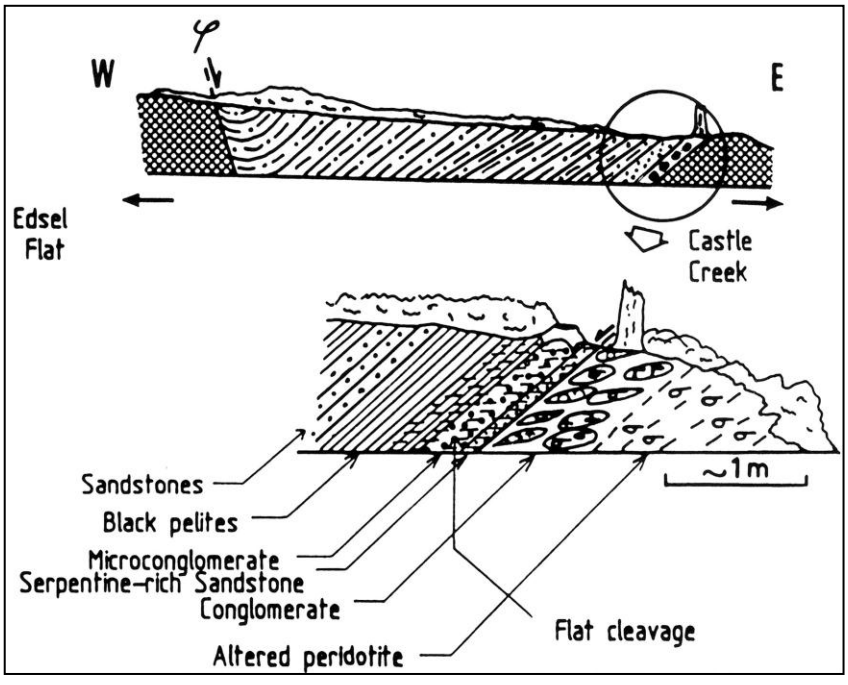

25C.

Microstructures within the upper plate slate, visible in thin-section, include sigma clasts, s-(flattening) foliation, c-(shear) foliation, and thin quartz veins oriented either parallel to foliation, or, more commonly, cutting obliquely across foliation (Fig. 26). Both the rough s and c-foliations are defined by shape-preferred orientation of fine-grained crystals of actinolite, chlorite, and epidote. The sigma clasts are replaced by fine-grained chlorite-actinolite-epidote group minerals, and have actinolite and chlorite "tails".

Several episodes of quartz veining have occurred, evident from the web of veins that cut through each other. Quartz veins account for 15 percent of the slate thin section. The offset displayed in several veins represents a change from a ductile deformation regime to a brittle deformation regime.

Directly beneath the upper plate slate is a thin (15 to 25 cm) mylonite zone. The light-green sheared mylonite displays a strong foliation, striking N41E and dipping 35NW. The foliation parallels the contact of mylonite with the slate. Both the mylonite zone (Fault 3) and the upper plate slate are cut by the younger fault (Fault 2, Fig. 25B).

In thin-section, the mylonitic texture is defined by very strong compositional layering into bands, very strong shape-preferred orientation of minerals, and sigma clasts (altered to tremolite and opaque minerals) (Fig. 27). The mylonite consists of fine-grained white mica, serpentine, chlorite, tremolite, and opaque minerals.

The fault breccia, comprising the thicker part of the shear zone, is visible on opposite sides of the younger, oblique-normal faults (Fig. 25A,B). The dark blackish green fault breccia with mafic and felsic clasts is at least 4 meters thick. The fault breccia is comprised of clasts ranging up to boulder size in a serpentine, quartz, chlorite, and

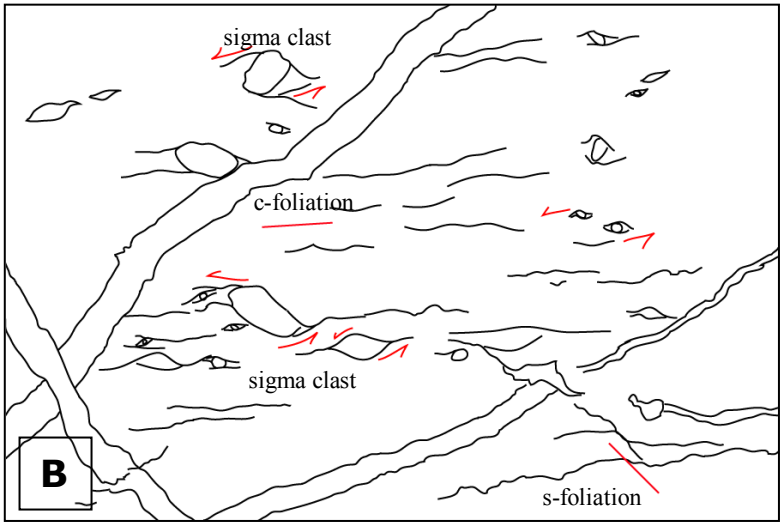

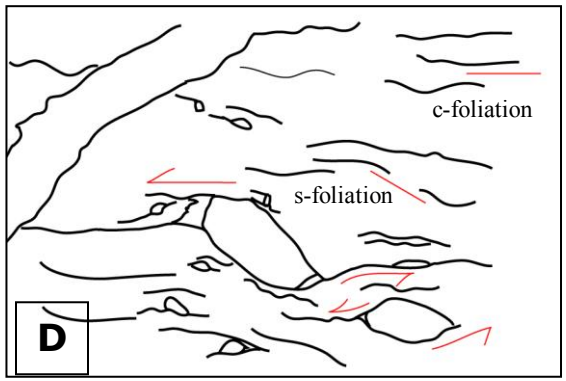

Figure 26. Photomicrograph and sketches of s-c fabric in sheared slate from the shear zone at the base of Horse Heaven Meadows klippe. Sample SHZ-2 is from the SE margin of the klippe, Location 2.
A) Photomicrograph in plane polarized light with field of view 3.2 mm; depicting several cloudy microcrystalline sigma clasts and deformed quartz veins.
B) Sketch of A depicting microstructures and inferred sense of motion. s-fabric, flattening foliation, dips shallowly to the right, and c fabric (shearing) is horizontal.
C) Photomicrograph in plane polarized light with field of view 1.37 mm; depicting a close-up view of a sigma clast. Displays crystal growth in the tails of the clast and alignment of fine-grain minerals.
D) Sketch of C depicting microstructures and sense of motion inferred from features.

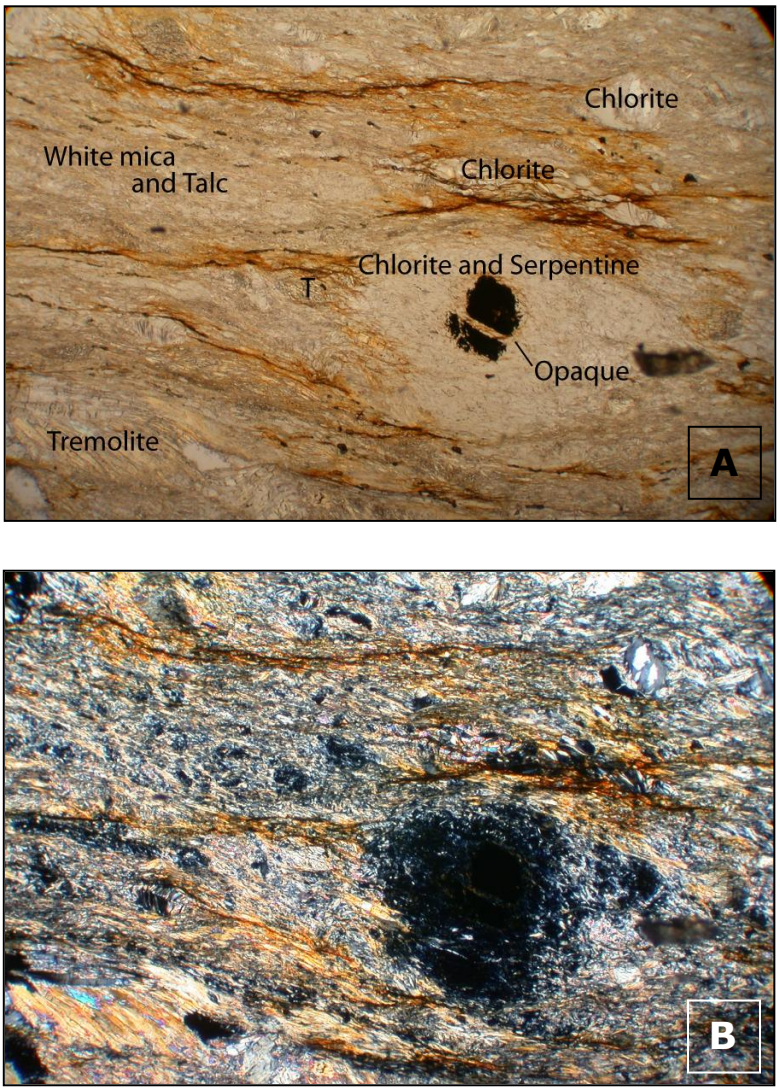

Figure 27: Photomicrographs of mylonite from the fault contact at the SE margin of the Horse Heaven Meadows klippe. Sample SHZ-3, Location 2 (Fig. 2), width of image is 3.2mm, A) in plane polarized light and B) in cross polarized light. Mylonitic unit consists mainly of fine-grained white mica, serpentine, chlorite, tremolite (T), and opaque minerals. Texture includes mineral alignment, sigma clasts, and undulatory extinction in crystals.

Figure 28: Photograph of an angular 20 cm plagiogranite boulder within the fault breccia zone at the base of the Horse Heaven Meadow klippe (Location 2, Fig.2). Sample SHZ-9.

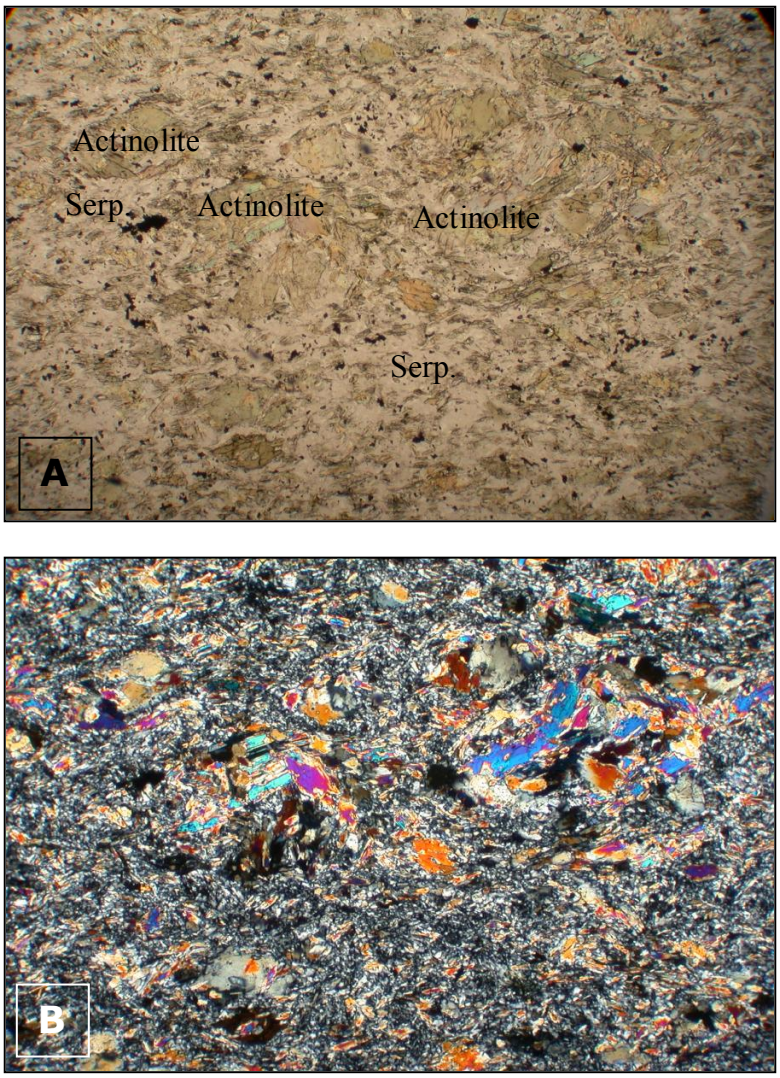

Figure 29: Photomicrographs of a clast within the fault breccia from the basal fault contact between the Horse Heaven Meadows klippe and the Trinity ultramafic complex, Ouc. Sample SHZ-10, Location 2 (Fig. 2), width of image is 3.2 mm, A) in plane polarized light and B) in cross polarized light. Mineralogy includes actinolite, serpentine and fine-grained clays. Anastomosing cleavage planes are defined by the serpentine and clays that flow around the actinolite crystals.

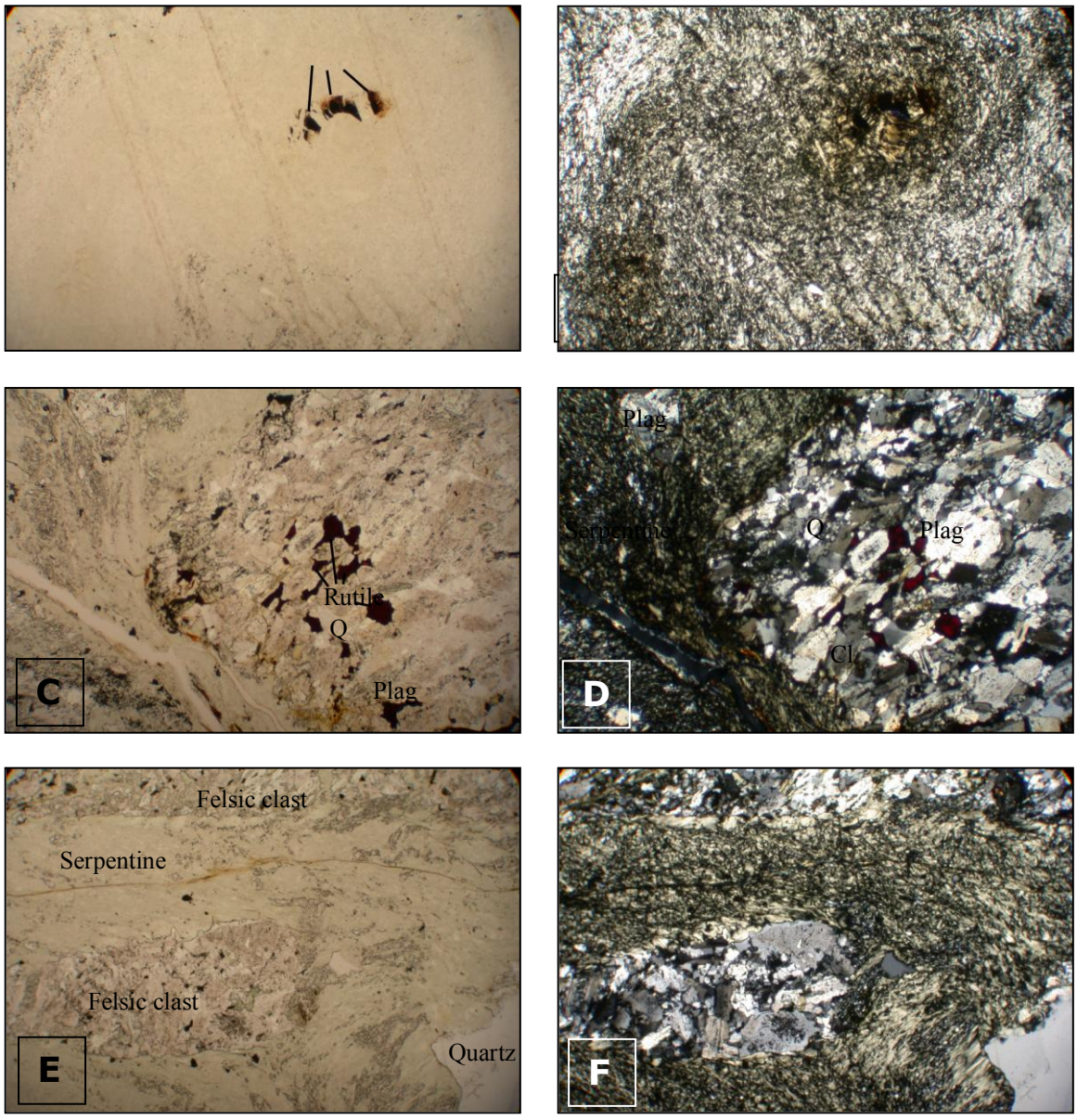

Figure 30: Photomicrographs of fault breccia from the fault zone at the base of the Horse Heaven Meadows klippe. Sample SHZ-9, Location 2 (Fig. 2), width of images are 3.2 mm. Photomicrographs A) in plane polarized light and B) cross polarized light display serpentine matrix with fractured pyrite. Photomicrographs C) in plane polarized light and D) in cross polarized light, display typical angular plagiogranite clasts within the serpentine matrix (Plag-plagioclase, Cl-chlorite, Q-quartz). Photomicrographs E) in plane polarized light and F) in cross polarized light display the serpentine matrix flowing around the plagiogranite clasts.

smectite matrix (Fig. 28). Blocks in the breccia are plagiogranite, amphibolite, and serpentine, (Fig. 29 and Fig. 30). In thin section, the serpentine breccia matrix consists of serpentine around small angular plutonic clasts, creating planar crystal alignment between clasts (Fig. 30). Several clasts exhibit pulled apart clasts with quartz fibers in spaces between fragments (Fig. 30A,B) indicating an extensional deformation regime.

Although the source of the plagiogranite clasts within the fault breccia cannot be uniquely identified, the rock types in the breccia unit occur in the Trinity terrane. Several different generations of plagiogranite are described within the Trinity ultramafic complex (Quick, 1981; Lindsley-Griffin, 1991).

Location 3) Tamarack Creek Junction

Location 3 (Fig. 2), near Tamarack Creek junction with forest road 25, was previously mapped as Devonian Copley Greenstone (Dc) (Irwin, 1994). Many of the greenstone "outcrops" near this area are not actually bedrock but boulder-sized glacial erratics, ranging up to 3-meters in diameter. Based on the composition of rocks along the contact, the contact is reinterpreted here as part of the fault zone breccia that comprises the basal fault of the Horse Heaven Meadows klippe.

In outcrop the foliated fault breccia contains clasts ranging up to 15 cm in diameter and deformed quartz veins within a foliated, fine-grained matrix. The fault zone matrix consists mainly of white mica, talc, and serpentine with some tremolite and chlorite. Clast compositions resemble those at Location 2 (Fig. 2) and consist primarily of plagiogranite, amphibolite, and diorite. Quartz veins are folded and boudinage. A strong foliation is prominant, striking N74W and dipping 68SW (Fig. 31).

Figure 31: Photograph of fault breccia, sample SHZ-5, in outcrop at Location 3 (Fig. 2), at the base of the Horse Heaven Meadows klippe.

In thin-section, the texture includes faint mineral alignment (defined by the serpentine, white mica, and talc), ghost augins, and cracks in the tremolite. The foliation is defined by faint mineral banding and alignment of talc and white mica.

Location 4) Loop Road Contact

The fault contact at Location 4 (Fig. 2) has mylonite and shear zone structures similar to the fault exposures at Locations 2 and 3 (Fig. 2). In outcrop, the mylonite is pale green and fine-grained. The mylonite consists of white mica, talc, fibrous tremolite, opaque minerals surrounded by fine-grained serpentine, and chlorite. In thin-section, a strong foliation is defined by mineral alignment of elongate minerals and by compositional banding of tremolite-rich layers, white mica, and talc. The opaque minerals appear to be replacing pre-existing minerals; they occur in augins with diffuse boundaries.

Panther Rock Klippe

The base of the Panther Rock klippe greenstone is completely obscured by glacial till; however, down-slope of the greenstone approximately 85 meters, a fault breccia zone is exposed. This section of fault breccia represents the basal fault of Panther Rock klippe. The thin remnant of greenstone that comprises the klippe is more extensively altered than the greenstone of the Grey Rocks klippe. The high degree of alteration may be a result of closer proximity to the basal fault.

Location 5: Lower Panther Rock klippe Fault Breccia

A small outcrop of fault breccia can be observed between Panther Rock klippe and Tamarack Creek (Location 5, Fig. 2). The outcrop of fault breccia separates the Panther Rock klippe greenstone from the underlying ultramafic sheet. Similar to the other fault breccias, the fault breccia at Location 5 contains angular plagiogranite, diorite, and amphibolite blocks ranging up to 20 cm in diameter within a serpentine matrix.

High Angle Faults

Younger, high angle normal faults bound the east and west margins of the Grey Rocks and Horse Heaven Meadows klippes, down-dropping the klippes and preserving them. The bounding normal faults tend to strike N-NW along the east and west sides of the Grey Rocks klippe and N, NE, or E along the margins of the Horse Heaven Meadows klippe.

Location P) Grey Rocks Klippe

The younger faults bounding the Grey Rocks klippe are best observed at Location P (Fig. 2) on the eastern side of the klippe. Here, the pegmatitic hornblende gabbro of the Trinity terrane comprises a ridge directly adjacent to the klippe. Although the saddle between the Grey Rocks greenstone and the gabbro ridge is covered, foliated serpentine between upper plate greenstone and the gabbro ridge strikes N9E and dips 61NW. This foliation orientation is similar to the strike and dip of the high-angle bounding fault, as inferred from the map pattern of the faults.

Location 2) Mile Marker 8.75

The best example of high angle normal faults bounding the Horse Heaven Meadows klippe is exposed at Location 2 (Fig. 2) in a road-cut exposure at the southeast margin of the Horse Heaven Meadows klippe (Fig. 25). In the road-cut, two high-angle faults juxtapose fault breccia on either side of a down-dropped segment of the basal shear zone and overlying slate of the Horse Heaven Meadows klippe. The fault surface of the eastern-most fault (Fault 2, Fig. 25A,B) is exposed, striking N42E and dipping 60NW. The fault surface of the western-most fault (Fault 1, Fig. 25A,B) is inferred to be parallel-subparallel to a dike, which strikes N32E and dips 76NW. The amount of displacement on either fault is speculative because of the lack of continuous stratigraphy across either fault; however, based on the location of the rest of the Horse Heaven Meadows klippe and the basal fault, the sliver has been down-dropped at least 15 meters.

The younger faulting may be responsible for tilting the basal shear zone contact and for the highly fractured nature of the metasedimentary rocks in the Horse Heaven Meadows klippe. Other normal faults may be present within the klippe but are hard to distinguish because the metasedimentary rocks have little compositional variation and are also fractured. The irregular basal contact of the Horse Heaven Meadows klippe suggests the presence of many small internal faults within the klippe. Several active landslides and slumps on the eastern border of the klippe occur along the steeply dipping normal faults that bound the klippe (Plate 1).

DISCUSSION

Relationship of Grey Rocks and Panther Rock Klippe Greenstones to the Trinity and Redding Terranes.

Petrologic and geochemical analysis of the greenstones from Grey Rocks and Panther Rock klippes links them with the Copley Greenstone of the Redding terrane (Fig. 19). Based on trace element comparisons of the three units normalized to either MORB or chondrites, samples from the three units are indistinguishable; therefore, the greenstones of Grey Rocks and Panther Rock klippes are interpreted as Devonian Copley Greenstone.

This interpretation conflicts with the previously published interpretations of Brouxel et al. (1988). Although greenstone and slate of the "Grey Rocks outlier" were originally assigned to the Redding terrane (Copley Greenstone) by Irwin (1966) and Wagner and Saucedo (1987), Brouxel and Lapierre (1988) reinterpreted the greenstones of Grey Rocks and Panther Rock klippes as "Trinity pillow basalts." The Trinity terrane pillow basalt unit of Brouxel and Lapierre (1988) also included greenstone at Sanford Pass (near the Carrville Fault area) and at Deer Creek near Mt. Shasta. This interpretation of the greenstones as "Trinity pillow basalts" deposited within the Trinity terrane was based on their geochemical affinity with and proximity to gabbroic plutons and dikes in the Trinity terrane, and the considerable distance between these greenstone units and the Copley Greenstone (Brouxel and Lapierre, 1988; Fig. 25C).

Subsequent mapping of the Sanford Pass/Carrville Fault area by Cashman and Elder (2002) identified greenstone as Copley Greenstone and the basal contact of the greenstone as a fault. Similarly, remapping of the Deer Creek outlier by Goldstein (1997) also identified the Deer Creek outlier as part of the Copley greenstone and the basal contact as a fault.

Relationship of Metasedimentary Rocks in Horse Heaven Meadows and Grey Rocks Klippes to the Redding Terrane.

Metasedimentary rocks in the Horse Heaven Meadows and Grey Rocks klippe have been previously interpreted as a section of Mississippian Bragdon Formation (Charvet et al., 1990). In contrast, based on stratigraphic description comparisons with the Bragdon Formation and the Copley Greenstone, metasedimentary rocks in the Horse Heaven Meadows and Grey Rocks klippes are interpreted here as lenses within the greenstone and are assigned to the Copley Greenstone as Dcs.

The Bragdon Formation is comprised mainly of argillite; however, the formation is characterized by thick lenticular conglomerate beds dominated by rounded clasts of chert, limestone, shale, and sandstone, and, most notably, by lenses of chert pebble conglomerate, (Diller, 1905; Kinkel et al., 1956; Albers and Robertson, 1961). Although clasts in the Bragdon Formation are typically non-volcanic (Diller, 1905), some layers exhibit rounded volcanic clasts that are mixed with rounded sedimentary clasts (Miller and Cui, 1989). In contrast to Bragdon Formation conglomerates, the volcanic breccias and coarse tuffs within the Horse Heaven Meadows and Grey Rocks klippes are comprised solely of angular metavolcanic and single-grain clasts.

The Copley Greenstone has been separated into lithologically distinctive lower and upper sections (Lapierre et al., 1985). The upper section consists primarily of pillow lavas but also contains minor pyroclastic and tuffaceous sedimentary beds (Kinkel et al., 1956; Lapierre et al., 1985). Near Redding, Lapierre et al. (1985) describe "tuffaceous slaty sediments" interbedded with the Copley Greenstone. The southern section of Grey Rocks klippe exhibits a similar relationship of interbedded greenstone and tuffaceous metasedimentary beds.

The lack of conglomerate beds and rounded clasts, lack of limestone, chert, shale, and sandstone clasts in the breccia units and the dominance of volcanic clasts and ash/volcanic glass matrix compositionally distinguishes the metasedimentary and metavolcanic units of the Horse Heaven Meadows and Grey Rocks klippes from the Bragdon Formation and compositionally links the klippes units to the Copley Greenstone. Based on these compositional and spatial relations, the metasedimentary and metavolcanic units of Horse Heaven Meadows and Grey Rocks klippes are interpreted as localized sedimentary deposits within the Copley Greenstone.

Basal Shear Zone Contact of Grey Rocks, Horse Heaven Meadows, and Panther Rock Klippes.

The basal contact between the Grey Rocks, Panther Rock, and Horse Heaven Meadows klippes and the underlying Trinity ultramafic complex is a fault contact (Fig. 32A,B). The conclusion that the basal contacts of the klippes are faults is consistent with prior work that has suggested regional tectonic extensional events (Schweickert and Irwin, 1989; Masson, 2002; Cashman and Elder, 2002). The interpretation of basal fault

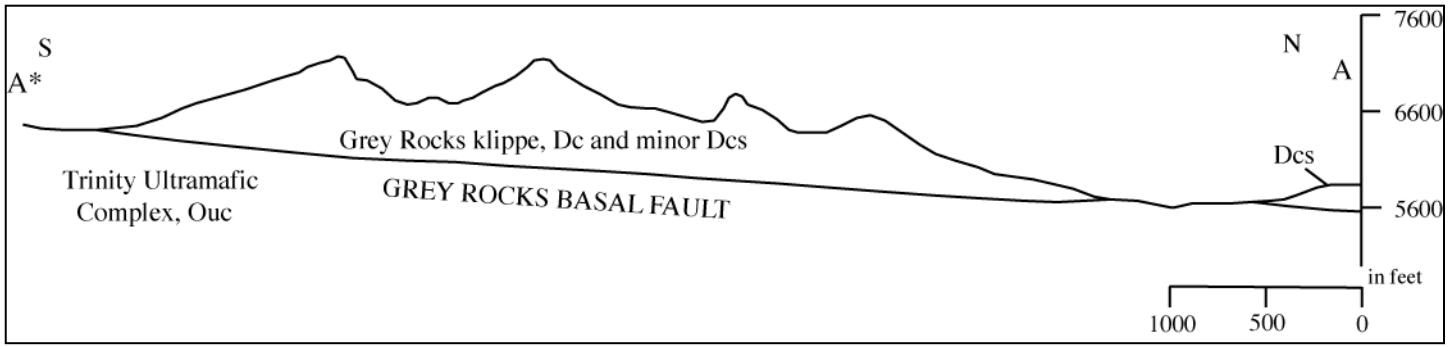

Figure 32A: Cross-section of Grey Rocks klippe depicting shallow tilt of basal fault to the north.

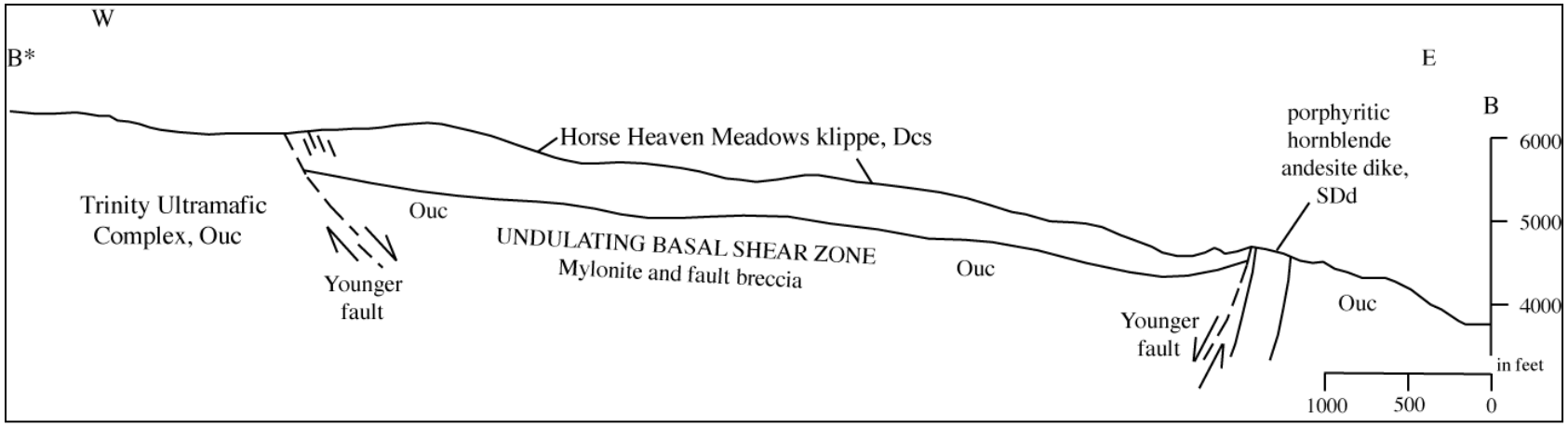

Figure 32B: Cross-section of the Horse Heaven Meadows klippe (Dcs) depicting the undulating basal fault and the high angle faults on the east and west margins of the klippe. (Refer to Figure 2 for locations of transects A-A* and B-B*).

contacts for these greenstone bodies conflicts with the depositional contact interpretation of Grey Rocks, Panther Rock, and Horse Heaven Meadows klippes suggested by Brouxel and Lapierre (1988), Boudier et al. (1989), Charvet et al. (1990), and Wallin and Metcalf (1998).

The basal fault is a low-angle undulatory normal fault that dips shallowly to the N-NE, places younger Redding terrane units over older Trinity terrane units, and has fault zone microstructures that record extensional deformation, (Figure 32B). The shallow, generalized N-NE dip of the Grey Rocks and Horse Heaven Meadows klippes (Figure 32) was determined based on structural relations between the klippes and the underlying Trinity terrane. Fault zone microstructures such as pulled-apart clasts, boudinage quartz veins, and perpendicular to foliation and fault plane quartz veins identify the fault as extensional.

The minimum stratigraphic separation on the fault is 1400 meters based on the correlation of Grey Rocks, Panther Rock, and Horse Heaven Meadows klippes with the upper section of the Copley Greenstone and omission of the massive flows that typify the lower half of the Copley Greenstone. The greenstone pillows and minor metasedimentary and metavolcanic lenses observed at Grey Rocks, Panther Rock, and Horse Heaven Meadows klippe have been correlated with the upper 400 meters of the Copley Greenstone as described by Lapierre et al. (1985) and Kinkel et al. (1956). This correlation and the structural thickness observed in the field identifies an omission of stratigraphy, namely, 1400 meters of massive basalt flows comprising the lower Copley Greenstone.

The basal fault contains mineral assemblages and microstructures that indicate a passage from a deep to shallow pressure and temperature regime during deformation.

Deformation on the fault occurred under greenschist facies conditions evident by greenschist mineral assemblages in deformational microstructures. The mineral assemblages in the Grey Rocks klippe shear zone are albite-epidote-actinolite-chlorite in the greenstone, white mica-epidote-chlorite-albite-quartz in the fault parallel rhyolite dike, and talc-tremolite-antigorite-chlorite in the mylonite, of which all are indicative of metamorphism under greenschist facies conditions (Raymond, 1992). Greenschist facies conditions generally occur at a depth of 10 to 15 km and in temperatures of 300-450^{o}C (Twiss and Moores, 1992). Greenschist facies minerals, chlorite and actinolite, are observed defining foliation in the greenstone of the Grey Rocks klippe shear zone (Location 1, Fig. 2). Chlorite, white mica, and epidote define the foliation that flows around plagioclase crystals in the fault-parallel rhyolite dike. In the mylonite, serpentine, chlorite, and talc minerals are within sigma "tails" and talc, serpentine, white mica, and chlorite define foliation. These metamorphic minerals within the deformational features identify the presence of greenschist metamorphic conditions at the time of formation, and in turn, identify the approximate depth of faulting as ~10 to 15 km.

Although not as indicative of specific pressure/temperature regimes as the mineral assemblages in Grey Rocks klippe shear zone, the basal fault of the Horse Heaven Meadows klippe similarly has some greenschist minerals within the microstructures of fault zone rocks. The mylonite at Location 2 (Fig. 2) has foliation defined by white mica

and serpentine; the slate has actinolite, epidote, and chlorite defining s-c foliations and actinolite and chlorite in sigma "tails".

The passage from a deeper pressure-temperature regime (of greenschist facies) to relatively shallower conditions is marked by a change in deformation behavior. At temperatures and pressures less than 250 ^{o}C and 10 km, the fault zone no longer deformed ductilely through recrystallization of minerals and formation of s-c fabric. Brittle deformational features, such as fault breccia, fractures, and fault perpendicular vein intrusions of quartz and calcite formed within the fault zone.

Although the Grey Rocks, Panther Rock, and Horse Heaven Meadows basal fault zone structures record both brittle and ductile deformation, it is unclear whether the majority of slip on the fault occurred in the brittle or the ductile regime. The regional model for the sequence of events that may have lead to the present-day structural relations of the klippes is depicted in Figure 34. Neither this model nor the present day exposure can completely define the full extent of the pressure-temperature-depth regime history of the faulting. It remains unclear as to whether the majority of the slip occurred prior to uplift and exhumation of the footwall thereby mainly faulting within a ductile regime, or whether the majority of slip accompanied exhumation of the footwall thereby mainly faulting within a brittle regime.

Regional Implications

Schweickert and Irwin (1989) were first to propose a regional extensional faulting event that involved the La Grange Fault, Carrville Fault, and the entire contact between

the Redding and Trinity terrane (Fig. 33 and Fig. 34). The detachment fault interpretation is based on consistencies in the N-NE trend of faults in the Yreka area, spatial relations of younger on older units, the structural omission of units along the La Grange Fault, and orientations of grabens of younger deposits (Schweickert and Irwin, 1989). A"Trinity arch" trends NE and sets the ultramafic center topographically higher than younger units to the north (Yreka terrane) and south (Redding terrane) (Schweickert and Irwin, 1989; Figure 34). Based on the tilt of dated gravels at the La Grange mine (McDonald, 1910; Irwin, 1963), the faulting would be confined to the Oligocene but may have begun in the early Tertiary.

Mapping and petrographic analyses of rocks from Grey Rocks, Panther Rock, and Horse Heaven Meadows klippes support interpretations of a regional extensional faulting event that extended across the eastern Klamath Mountains region (Schweickert and Irwin, 1989; Masson, 2002; Cashman and Elder, 2002). The klippes are located at a midpoint between the breakaway faults of the Yreka/Trinity terrane boundary and the faults of the Redding/Trinity terrane boundary. The importance of the extensional basal fault identified at Grey Rocks, Panther Rock, and Horse Heaven Meadows klippes is that it provides a link between faulting in the north and faulting in the south. These three klippes represent a portion of the upper plate that contain Redding terrane units and record extensional faulting that once extended across the eastern Klamath Mountains region.

Both Redding and Yreka terrane units occur in the upper plate of the extensional fault. In addition to Grey Rocks, Panther Rock, and Horse Heaven Meadows klippes, other Redding and Yreka terrane allochthons with extensional basal faults near Callahan,

Deer Creek, Oregon Mountain, Cecilville, and Richter mine have been interpreted as relating to the same extensional faulting event (Cashman and Elder, 2002). Cashman and Elder (2002) identified allochthons with extensional basal faults with upper plate components of both Redding terrane units (near the Callahan fault and at Deer Creek) and Yreka terrane units (Oregon Mountain, Cecilville, and the Richter mine in southern Scott Valley). Grey Rocks, Panther Rock, and Horse Heaven Meadows klippe have Redding terrane Copley Greenstone and metasedimentary units comprising the upper plate.

Felsic dikes are an additional structural feature similar among all of the allochthons (Cashman and Elder, 2002). The felsic dikes intrude parallel to the basal fault or cross-cut the fault breccia. The felsic dike that intrudes parallel to the shear zone of Grey Rocks klippe is significant in that it contains shear fabric. The shear fabric identifies emplacement as syntectonic. This dike could be used in a future project to identify the exact timing of the faulting event and to test correlation to a Tertiary age as suggested by MacDonald (1910) and Schweickert and Irwin (1989).

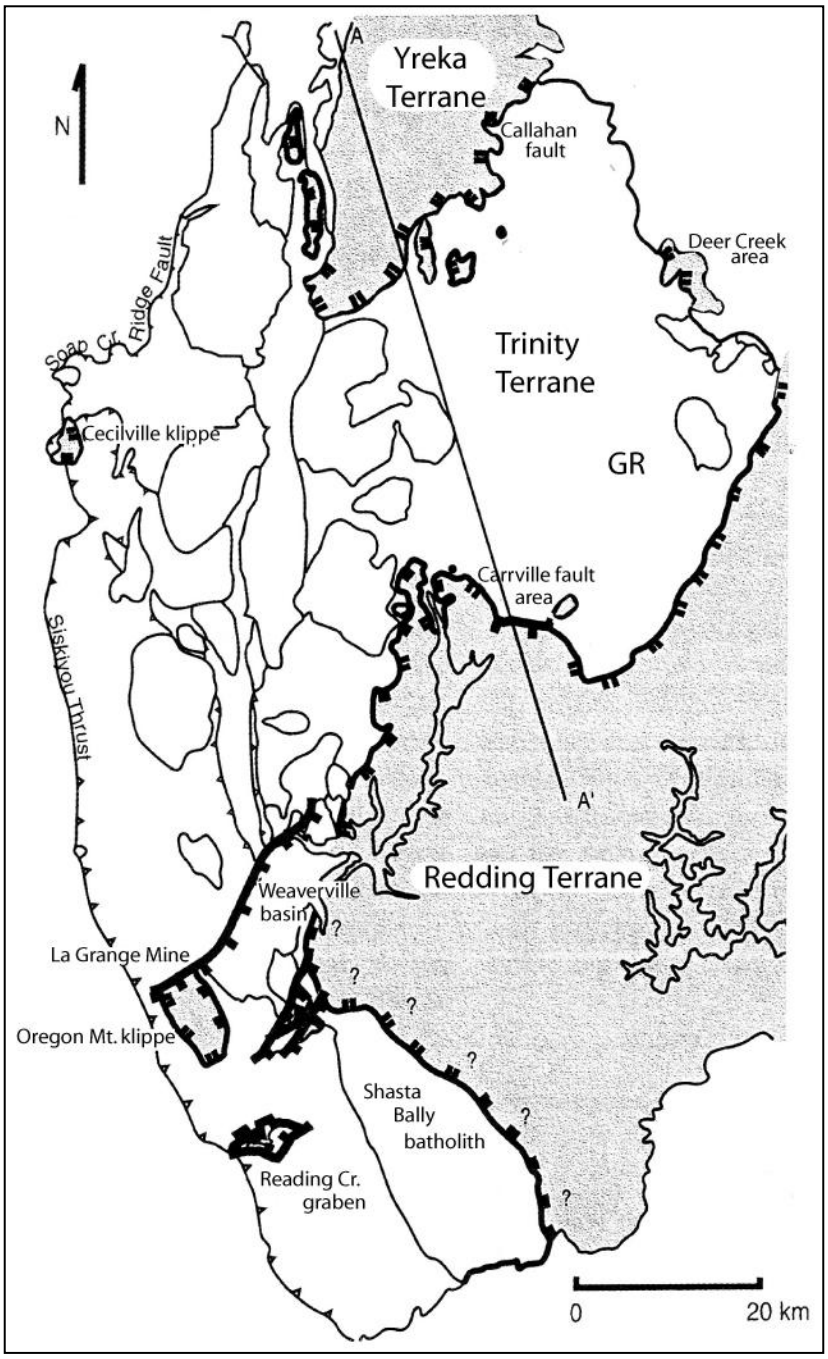

Figure 33: Simplified structural map modified from Schweickert and Irwin (1989) and Cashman and Elder (2002), showing major structural elements supporting a regional detachment fault system. GR represents Grey Rocks area. Cross-section in Figure 34 is along line A-A'.

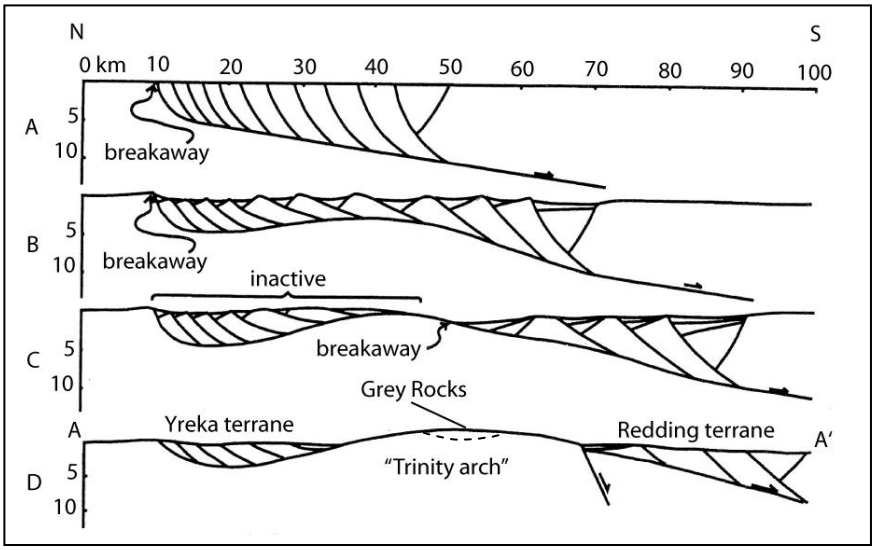

Figure 34: Schematic diagram of cross-sections depicting development of a simplified detachment fault in the EKB, modified from Cashman and Elder (2002). Grey Rocks area is located on the Trinity arch.

.

CONCLUSIONS

The greenstones of the Grey Rocks and Panther Rock klippes are geochemically linked with the Devonian Copley Greenstone of the Redding Terrane, despite the spatial disparity between the outliers and the Redding terrane. The metasedimentary and metavolcanic units of the Horse Heaven Meadows klippe and metasedimentary units of the Grey Rocks klippe comprise localized sedimentary lenses (Dcs) within the Copley Greenstone Formation (Dc). Younger NW-NE trending faults have down-dropped the klippes and preserved them.

The basal fault contacts of the Panther Rock, Grey Rocks, and Horse Heaven Meadows klippes are part of a regional extensional fault system. The basal fault zone strikes N-NW and dips 5-10 degrees to the E-NE. The fault forms a 9 to 85 meter thick zone of deformation, comprised of both mylonite and fault breccia. Although the fault zone structures record both brittle and ductile deformation, the pressure-temperature-depth regime history of faulting remains. Both the present-day structural relations and the regional model are inconclusive as to whether the majority of slip on the fault occurred in the brittle or the ductile regime.

All intrusions within the study area solely intrude footwall rocks of the Trinity ultramafic complex or the fault zone, and are not observed intruding the overlying klippes. A syntectonic rhyolite dike intrudes parallel to the fault zone at Grey Rocks klippe shear zone and two younger felsic dikes cut through the fault breccia at the Horse

Heaven Meadows klippe. Radiometric age dating of these dikes might provide a minimum age for the faulting event.

REFERENCES CITED

Albers, J.P., and Bain, J.H.C., 1985, Regional Setting and New Information on Some Critical Geologic Features of the West Shasta District, California: Economic Geology, v. 80, p. 2072-2091.

Albers, J.P., and Robertson, J.F., 1961, Geology and ore deposits of East Shasta copper-zinc district, Shasta County, California: U.S. Geological Survey Professional Paper 338, 107 p.

Barrow, W.M., and Metcalf, R.V., 2006, A reevaluation of the paleotectonic significance of the Paleozoic Central Metamorphic terrane, eastern Klamath Mountains, California: New constraints from trace element geochemistry and 40Ar/39Ar thermochronology, *in* Snoke, A.W., and Barnes, C.G., eds., Geological studies in the Klamath Mountains province, California and Oregon: A volume in honor of William P. Irwin: Geological Society of America Special Paper 410, p. 393-410.

Boudier, F., Le Sueur, E., and Nicolas, A., 1989, Structure of an atypical ophiolite: The Trinity complex, eastern Klamath Mountains, California: Geological Society of America Bulletin, v. 101, p. 820-833.

Boucot, A.J., Dunkle, D.H., Potter, A., Savage, N.M., and D. Rohr, 1974, Middle Devonian Orogeny in Western North America? A fish and other fossils: Journal of Geology, v. 82, p. 691-708.

Brouxel, M., 1991, Geochemical consequences of flow differentiation in a multiple injection dike (Trinity Ophiolite, N. California), Lithos, v. 26, p. 245-252.

Brouxel, M., and Lapierre, H., 1988, Geochemical study of an early Paleozoic island-arc-back-arc system. Part 1: The Trinity Ophiolite (northern California): Geological Society of America Bulletin, v. 100, p. 1111-1119.

Brouxel, M., Lapierre, H., Michard, A., and Albarede, F., 1987, The deep layers of a Paleozoic arc: Geochemistry of the Copley-Balaklala Series, northern California: Earth and Planetary Science Letters, v. 85, p. 386-400.

Brouxel, M., Lapierre, H., Michard, A., and Albarede, F., 1988, Geochemical study of an early Paleozoic island-arc-back-arc basin system. Part 2: Eastern Klamath, early to middle Paleozoic island-arc volcanic rocks (Northern California): Geological Society of America Bulletin, v. 100, p. 1120-1130.

Brouxel, M., Lecuyer, C., and Lapierre, H., 1989, Diversity of magma types in a lower

Paleozoic island arc—marginal basin system (Eastern Klamath Mountains, California, USA): Chemical Geology, v. 77, p. 251-264.

Cannat, M., and Lecuyer, C., 1991, Epithermal magma chambers in the Trinity peridotite, northern California: Tectonophysics, v. 186, p. 313-328.

Cashman, S.M., and Elder, D.R., 2002, Post-Nevadan detachment faulting in the Klamath Mountains, California: Geologic Society of America Bulletin, v. 114, p. 1520-1534.

Charvet, J, Lapierre, H., Rouer, O., Coulon, C., Campos, C., Martin, P., and Lecuyer, C., 1990, Tectono-magmatic evolution of Paleozoic and early Mesozoic rocks in the eastern Klamath Mountains, California, and the Blue Mountains, eastern Oregon-western Idaho, *in* Harwood, D.S., and Miller, M.M., eds., Paleozoic and early Mesozoic paleogeographic relations: Sierra Nevada, Klamath Mountains, and related terranes: Geological Society of America Special Paper 255, p. 255-276.

Diller, J.S., 1905, The Bragdon Formation: American Journal of Science, v. 4, p. 379-387.

Doe, B.R., Delevaux, M.H., and Albers, J.P., 1985, The Plumbotectonics of the West Shasta Mining District, Eastern Klamath Mountains, California: Economic Geology, v. 80, p. 2136-2148.

Goldstein, H.L., 1997, A continuation of the La Grange fault, eastern Klamath Mountains, California: Arcata, California, Humboldt State University, B.S., thesis, 22 p.

Humphris, S.E., and Thompson, G., 1978a, Hydrothermal alteration of oceanic basalts by seawater: Geochimica et Cosmochimica Acta, v. 42, p. 107-125.

Humphris, S.E., and Thompson, G., 1978b, Trace element mobility during hydrothermal alteration of oceanic basalts: Geochimica et Cosmochimica Acta, v. 42, p. 127-136.

Irwin, W.P., 1960, Geologic reconnaissance of the northern Coast Ranges and Klamath Mountains, California, with a summary of the mineral resources: Sacramento, California Division of Mines Bulletin 179, 80 p.

Irwin, W.P. 1963, Preliminary geologic map of the Weaverville quadrangle, California: US Geological Survey Mineral Investigations Field Studies Map MF-275, scale 1:62,500.

Irwin, W.P., 1966, Geology of the Klamath Mountains province, *in* Bailey, E.H., ed., Geology of northern California: California Divisions of Mines and Geology Bulletin 190, p. 19-38.

Irwin, W.P. 1972, Terranes of the Western Paleozoic and Triassic Belt in the southern Klamath Mountains, California: U.S. Geological Survey Professional Paper 800-C, p. C103-111.

Irwin, W.P., 1981, Tectonic accretion of the Klamath Mountains, *in* Ernst, W.G., ed., The geotectonic development of California--Rubey Volume I: Englewood Cliff, New Jersey, Prentice-Hall, p. 29-49.

Irwin, W.P., 1994, Geologic map of the Klamath Mountains, California and Oregon: U.S. Geological Society Miscellaneous Investigations Series Map I-2148, scale 1:500,000.

Irwin, W.P., and Lipman, P.W., 1962, A regional ultramafic sheet in eastern Klamath Mountains, California: Washington, D.C., U.S. Geological Survey Professional Paper 450-C, p. C18-C21.

Jacobsen, S.B., Quick, J.E., and Wasserburg, G.J., 1984, A Nd and Sr isotopic study of the Trinity peridotite; Implications for mantle evolution: Earth and Planetary Science Letters, v. 68, p. 361-378.

Jensen, L.S., 1976, A new cation plot for classifying subalkalic volcanic rocks: Ontario Geological Survey Miscellaneous Paper 66, 22 p.

Kinkel, A.R., Jr., Hall, W.E., and Albers, J.P., 1956, Geology and base-metal deposits of West Shasta copper-zinc district, Shasta County, California: U.S. Geological Survey Professional Paper 285, 156 p.

Lapierre, H., Albarede, F., Albers, J., Cabanis, B., and Coulon, C., 1985, Early Devonian volcanism in the eastern Klamath Mountains, California: Evidence for an immature island arc: Canadian Journal of Earth Science, v. 22, p. 214-226.

LeBas, M.J., LeMaitre, R.W., Streckeisen, A.L., and Zanettin, B., 1986, A chemical classification of volcanic rocks based on the total alkali-silica diagram: Journal of Petrology, v. 27, p. 745-750.

Lindsley-Griffin, N., 1977, The Trinity Ophiolite, Klamath Mountains, California, *in* Coleman, R.G., and Irwin, W.P., eds., North American ophiolites: Oregon Department of Geology and Mineral Industries, Bulletin 95, p. 107-120.

Lindsley-Griffin, N., 1991, The Trinity complex: A polygenetic ophiolitic assemblage *in* Cooper, J.D. and Stevens, C.H., eds., Paleozoic Paleogeography of the Western United States, Volume II: Pacific Section, Society of Economic Paleontologists and Mineralogists, v. 67, p. 589-607.

Lindsley-Griffin, N., and Griffin, J.R., 1983, The Trinity terrane: An early Paleozoic microplate assemblage, *in* C.H. Stevens, ed., Pre-Jurassic rocks in western North American suspect terranes: Los Angeles, Pacific Section, Society of Economic Paleontologists and Mineralogists, p. 63-75.

Lindsley-Griffin, N., Griffin, J.R., and Wallin, E.T., 1991, Redefinition of the Gazelle Formation of the Yreka Terrane, Klamath Mountains, California: Paleogeographic implications, *in* Cooper, J.D., and Stevens, C.H., eds., Paleozoic paleogeography of the western United States II: Los Angeles, Pacific Section, Society of Economic Paleontologist and Mineralogist, p. 609-624.

Lindsley-Griffin, N., Griffin, J.R., Farmer, J.D., Sivers, E.A., Bruckno, B., and Tozer, M.K, 2006, Ediacaran cyclomedusoids and the paleogeographic setting of the Neoproterozoic—early Paleozoic Yreka and Trinity terranes, eastern Klamath Mountains, California, *in* Snoke, A.W., and Barnes, C.G., eds., Geological studies in the Klamath Mountains province, California and Oregon: A volume in honor of William P. Irwin: Geological Society of America Special Paper 410, p. 411-431.

MacDonald, D.F., 1910, The Weaverville-Trinity Center gold gravels, Trinity County, California: U.S. Geological Survey Bulletin 530, p. 48-58.

Masson, P.H., 2002, Revised geology of the Grey Rocks Outlier, Southeast Klamath Mountains, California: Geological Society of America Abstracts with Programs, v. 34, p. 43.

Mattinson, J.M., and Hopson, C.A., 1972, Paleozoic ages of rocks from ophiolitic complexes in Washington and northern California: Eos: American Geophysical Union Trans., v. 53, p. 543.

Metcalf, R.V., Wallin, E.T., Willse, K.R., and Muller, E.R., 2000, Geology and geochemistry of the ophiolitic Trinity terrane, California: Evidence of middle Paleozoic depleted supra-subduction zone magmatism in a proto-arc setting, *in* Dilek, Y., Moores, E.M., Elthon, D., and Nicolas, A., eds., Ophiolites and oceanic crust: New insights from field studies and the Ocean Drilling Program: Geological Society of America Special Paper 349, p. 403-418.

Miller, M.M., 1989, Intra-arc sedimentation and tectonism: Late Paleozoic evolution of

the eastern Klamath terrane, California: Geological Society of America Bulletin, v. 101, p. 170-187.

Miller, M.M., and Cui, B., 1989, Submarine-fan characteristics and dual sediment provenance, Lower Carboniferous Bragdon Formation, eastern Klamath terrane, California: Canadian Journal of Earth Science, v. 26, p. 927-940.

Miller, M.M., and Harwood, D.S., 1990, Paleographic setting of upper Paleozoic rocks in the northern Sierra and eastern Klamath terranes, northern California, *in* Harwood, D.S., and Miller, M.M., eds., Paleozoic and early Mesozoic paleogeographic relations: Sierra Nevada, Klamath Mountains, and related terranes: Geological Society of America—Special Paper 255, p. 175-192.

Pearce, J.A., 1983, Role of the sub-continental lithosphere in magma genesis at active continental margins, *in* Hawkesworth C.J. and Norry, M.J., eds., Continental basalts and mantle xenoliths. Shiva, Nantwich, p. 230-249.

Potter, A.W., Hotz, P.E., and Rohr, D.M., 1977, Stratigraphy and inferred tectonic framework of lower Paleozoic rocks in the Eastern Klamath Mountains, Northern California, *in* Paleozoic paleontology of the western United States: Pacific Coast Paleogeography Symposium I, Pacific Section, Society of Economic Paleontologists and Mineralogists, no. 7, p. 421-440.

Potter, A.W., Boucot, A.J., Bergstrom, S.M., Blodgett, R.B., Dean, W.T., Flory, R.A., Ormiston, A.R., Pedder, A.E.H., Rigby, J.K., Rohr, D.M., and Savage, N.M., 1990, Early Paleozoic stratigraphic, paleogeographic, and biogeographic relations of the eastern Klamath belt, northern California, *in* Harwood, D.S., and Miller, M.M., eds., Paleozoic and early Mesozoic paleogeographic relations: Sierra Nevada, Klamath Mountains, and related terranes: Geological Society of America Special Paper 255, p. 57-74.

Quick, J.E., 1981, Petrology and petrogenesis of the Trinity Peridotite, an upper mantle diapir in the eastern Klamath Mountains, northern California: Journal of Geophysical Research., v. 86, p. 11837-11863.

Rollinson, H., 1993, Using Geochemical Data: Evaluation, Presentation, Interpretation: London, Longman Scientific & Technical, 352 p.

Schweickert, R.A., and Irwin, W.P., 1989, Extensional faulting in southern Klamath Mountains, California: Tectonics, v. 8, p. 135-149.

Thompson, R.N., 1982, British Tertiary volcanic province: Scott. F. Geology, v. 18, p. 49-107.

Townsend, K., 1995, Petrology of unusual dacite dikes, La Grange Fault, eastern Klamath Mountains, California [B.S. thesis]; Arcata, California, Humboldt State University, 29 p.

Twiss, R.J., and Moores, E.M., 1992, Structural Geology: New York, W.H. Freeman and company, 532 p.

Wagner, D.L., and Saucedo, E.J., 1987, Geologic map of the Weed quadrangle, California: California Division of Mines and Geology, Regional Geologic Map Sheets, Map 4A, scale 1:250,000.

Wallin, E.T., 1990, Petrogenetic and tectonic significance of xenocrystic Precambrian zircon in Lower Cambrian tonalite, eastern Klamath Mountains, California: Geology, v. 18, p. 1057-1060.

Wallin, E.T., Coleman, D.S., Lindsley-Griffin, N., and Potter, A.W., 1995, Silurian plutonism in the Trinity terrane (Neoproterozoic and Ordovician), Klamath Mountains, California, United States: Tectonics, v. 14, p. 1007-1013.

Wallin, E.T., Lindsley-Griffin, N; and Griffin, J.R., 1991, Overview of early Paleozoic magmatism in the eastern Klamath Mountains, California, *in* Cooper J.D., and Stevens, C.H., eds., Paleozoic Paleontology of the western United States II: Los Angeles, Pacific Section, Society of Economic Paleontologists and Mineralogists, v. 67, p. 581-588.

Wallin, E.T., Mattinson, J.M., and Potter, A.W., 1988, Early Paleozoic magmatic events in the eastern Klamath Mountains, northern California: Geology, v. 16, no. 2, p. 144-148.

Wallin, E. T., and Metcalf, R. V., 1998, Supra-subduction zone ophiolite formed in an extensional forearc: Trinity terrane, Klamath Mountains, California: Journal of Geology, v. 106, p. 591-608.

Watkins, R., 1986, Late Devonian to Early Carboniferous Turbidite Facies and Basal Development of the Eastern Klamath Mountains, California: Sedimentary Geology, v. 49, p. 51-71.

Zucca, J.J., Fuis, G.S., Milkereit, B., Mooney, W.D., and Catchings, R.D., 1986, Crustal structure of northeastern California: Journal of Geophysical Research, v. 91, p. 7359-7382.

APPENDIX A:
TABLE OF SAMPLE LOCATIONS, GPS LOCATIONS, MINERALOGY, ROCK TYPE, AND INTERPRETATION.

Appendix A: Table of sample locations, GPS locations, mineralogy, rock type, and interpretation. Page 1 of 7.

Sample Name	Field Map Loc.	Formation	Map Unit	Rock Type	Mineralogy and texture	Interpret-ation	GPS Location				
Upper plate											
SV-1	L	Copley Greenstone metasedimentary and metavocanic	Dcs	pyroclastic breccia	discontinuous, unsorted, angular, polymictic, matrix supported metavolcanic unit. Chlorite, microcrystalline quartz, epidote, and fine-grained clay matix. Clasts range up to cobble size; are volcanic, comprised of 1) epidote and quartz; 2)microcrystalline quartz; 3) microcrystalline quartz with chlorite, plagioclase laths and opaques; and 4) fiberous actinolite, microcrystalline quartz, chlorite, epidote, and saussurite (relict plagioclase). In outcrop, clast boundaries are faint but become more distinguishable in thi section. Blending of clast boundaries due to actinolite and epido overgrowths that have overprinted the unit and original grain boundaries.	Upper plate	none				
SV-2	L	Copley Greenstone metasedimentary and metavocanic	Dcs	pyroclastic breccia		Upper plate					
SV-3	K	Copley Greenstone metasedimentary and metavocanic	Dcs	Coarse tuff	glass-rich matrix-supported unit with fine-grained, poorly sorted angular to subrounded clasts. Fine-grained matrix composed of chlorite, micas, volcanic glass, and fine-grained clays. Clasts consist of volcanic glass; single grains of subhedral and microcrystalline quartz; and subhedral relict grains now compris of actinolite.	Upper plate	UTM	10 T	5 45	449 576	21 80
SV-4	S	Copley Greenstone metasedimentary and metavocanic	Dcs			Upper plate	none				
SV-5	S	Copley Greenstone metasedimentary and metavocanic	Dcs			Upper plate	none				
SV-6	G	Copley Greenstone metasedimentary and metavocanic	Dcs	Tuffaceous medium pebble breccia	massive, unsorted, angular, polymictic, clast-supported volcanic unit with a fine-grained clay, quartz, and chlorite matrix. Large sections of matrix have recrystallized into chlorite, replacing original volcanic glass. Clasts range in size up to 0.75 cm.; have volcanic textures; have compositions of 1) microcrystalline quart 2) aligned fine-grained plagioclase, epidote, and chlorite; and 3) single grain clasts of quartz, plagioclase, and chlorite.	Upper plate	UTM	10 T	5 45	475 516	29 92

Appendix A: Table of sample locations, GPS locations, mineralogy, rock type, and interpretation. Page 2 of 7.

Sample Name	Field Map Loc.	Formation	Map Unit	Rock Type	Mineralogy and texture	Interpret-ation	GPS Location				
GR-1	T	Copley Greenstone	Dc	Greenstone pillows	chlorite; plagioclase with sparrow-tail edges altering to epidote group minerals and cloudy clays; microcrystalline quartz; opaque minerals; clinozoisite; relict clinopyroxene altering to actinolite and chlorite; fine-grained clays. Intergranular texture.	Upper plate	UTM	10 T	5 45	449 538	38 4
GR-2	T	Copley Greenstone	Dc	Greenstone pillows		Upper plate	UTM	10 T	5 45	449 538	38 4
GR-3	T	Copley Greenstone	Dc	Greenstone pillows		Upper plate	UTM	10 T	5 45	449 538	38 4
GR-4	V	Copley Greenstone	Dc	Greenstone pillows		Upper plate	UTM	10 T	5 45	457 537	56 59
GR-5	V	Copley Greenstone	Dc	Greenstone pillows		Upper plate	UTM	10 T	5 45	457 537	56 59
GR-6	H	Copley Greenstone	Dc	Greenstone pillows		Upper plate	UTM	10 T	5 45	45 518	463 88
PR-1	F	Copley Greenstone	Dc	Greenstone float	radial, fibrous actinolite; chlorite;plagioclase, fine-grained microcrystalline and larger quartz; euhedral clinozoisite; square 0.5mm relict pyroxenes altering to chlorite; fine-grained clays. Aphanitic texture with overprint of alteration minerals.	Upper plate	UTM	10 T	5 45	429 572	7 89
PR-2	F	Copley Greenstone	Dc	Greenstone pillows		Upper plate	UTM	10 T	5 45	428 571	32 58
PR-3	F	Copley Greenstone	Dc	Greenstone pillows		Upper plate	UTM	10 T	5 45	428 571	32 58
PR-4	F	Copley Greenstone	Dc	Greenstone pillows		Upper plate	UTM	10 T	5 45	428 571	32 58
PR-5	F	Copley Greenstone	Dc	Greenstone pillows		Upper plate	UTM	10 T	5 45	427 570	84 91
PR-6	F	Copley Greenstone	Dc	Greenstone pillows		Upper plate	UTM	10 T	5 45	427 570	84 91
PR-7	F	Copley Greenstone	Dc	Greenstone pillows		Upper plate	UTM	10 T	5 45	427 570	84 91

Appendix A: Table of sample locations, GPS locations, mineralogy, rock type, and interpretation. Page 3 of 7.

Sample Name	Field Map Loc.	Formation	Map Unit	Rock Type	Mineralogy and texture	Interpret-ation	GPS Location				
COP-1		Copley Greenstone	Dc	Greenstone flow		Upper plate	UTM	10 T	5 45	389 971	60 62
COP-3		Copley Greenstone	Dc	Greenstone flow		Upper plate	UTM	10 T	5 44	369 981	83 73
COP-4		Copley Greenstone	Dc	Greenstone flow		Upper plate	UTM	10 T	5 44	369 981	83 73
COP-5		Copley Greenstone	Dc	Greenstone flow		Upper plate	UTM	10 T	5 45	389 971	60 62
COP-6		Copley Greenstone	Dc	Greenstone flow		Upper plate	UTM	10 T	5 44	368 982	29 96
COP-7		Copley Greenstone	Dc	Greenstone flow		Upper plate	UTM	10 T	5 44	368 983	12 27
COP-8		Copley Greenstone	Dc	Greenstone flow		Upper plate	UTM	10 T	5 44	368 982	29 96
COP-9		Copley Greenstone	Dc	Greenstone flow		Upper plate	UTM	10 T	5 45	495 402	63 71
COP-10		Copley Greenstone	Dc	Greenstone flow		Upper plate	UTM	10 T	5 45	495 402	63 71
COP-11		Copley Greenstone	Dc	Greenstone flow		Upper plate	UTM	10 T	5 45	495 402	63 71

Appendix A: Table of sample locations, GPS locations, mineralogy, rock type, and interpretation. Page 4 of 7.

Sample Name	Field Map Loc.	Formation	Map Unit	Rock Type	Mineralogy and texture	Interpret-ation	GPS Location				
Fault Rocks											
COP-12		Copley Greenstone	Dc	Greenstone		Upper plate	none				
COP-13		Copley Greenstone	Dc	Greenstone		Upper plate	none				
C0P-14		Copley Greenstone	Dc	Greenstone		Upper plate	none				
D-1	2		Dike	rhyolite	dike consisting mainly of microcrystalline to <0.4 mm quartz, anorthoclase feldspar, and <0.5 mm poikilitic plagioclase with epidote group inclusions. Some plagioclase crystals exhibit mantling, myrmekite texture, and grid like twinning. Secondary minerals include chlorite, saussurite, and reddish brown opaques. Aphanitic texture. Displays chilled margins.	Post-tectoni with shear zone	UTM	10 T	5 45	479 556	66 89
D-2	2		Dike	allotriomorphic granular grano-diorite	dike consisting mainly of <0.5 mm quartz, 1 to 1.25 mm mantled poikilitic plagioclase with epidote group inclusions, and minor orthoclase feldspar; minor amounts of chlorite, saussurite, and reddish brown opaques.	Post-tectoni with shear zone	UTM	10 T	5 45	479 556	66 89
SHZ-1	4	Copley Greenstone metasedimentary and metavocanic	Dcs	Slate	Slate	Upper plate	UTM	10 T	5 45	466 574	94 84
SHZ-2	2	Copley Greenstone metasedimentary and metavocanic	Dcs	Slate	Slate, actual composition of the matrix was too fine-grained to determine from thin-section analysis alone. S-C foliation, sigma clasts, aligned minerals, and deformed quartz veins. Foliation defined by aligned elongate fine-grained minerals of actinolite, chlorite, epidote. Sigma clasts are microcrystalline clasts with intergrown epidote group minerals. Quartz veins account for 15% of volume, intrude parallel or oblique to foliation. In outcrop, slat has two pervasive cleavage planes (bedding was not determined) striking N80E and dipping 25N and striking N26W and dipping 21S.	Upper Plate	UTM	10 T	5 45	479 556	66 89

Appendix A: Table of sample locations, GPS locations, mineralogy, rock type, and interpretation. Page 5 of 7.

Sample Name	Field Map Loc.	Formation	Map Unit	Rock Type	Mineralogy and texture	Interpret-ation	GPS Location				
SHZ-3	2	Fault Rocks (mapped as part of Trinity terrane)	Oum	mylonite	consists mainly of fine-grained white mica, serpentine, chlorite, tremolite, and opaque minerals. Texture defined by very strong compositional layering, very strong shape-preferred orientation o minerals, and sigma clasts. In outcrop, displays a strong foliation striking N41E and dipping 35N.	Lower plate	UTM	10 T	5 45	479 556	66 89
SHZ-4	4	Fault Rocks (mapped as part of Trinity terrane)	Oum	mylonite	consists of white mica, talc, fibrous tremolite, opaque minerals surrounded by serpentine, and chlorite. Strong foliation and mineral alignment of elongate minerals and by compositional banding of tremolite rich layers, white mica, and talc. Opaque minerals form augins with diffuse boundaries. In outcrop, mylonit is pale green, fine-grained.	Lower plate	UTM	10 T	5 45	466 574	94 84
SHZ-5	3	Fault Rocks (mapped as part of Trinity terrane)	Oum	fault breccia	consists mainly of white mica, talc, and serpentine with some tremolite and chlorite. Clasts are mainly plagiogranite, amphibole and diorite. Quartz veins are folded and boudinage. Texture includes faint mineral alignment (defined by the serpentine, white mica, and talc), ghost augins, and cracks in the tremolite. Strong foliation is prominant in outcrop, stiking N74W and dipping 68 In thin-section, the foliation is harder to differentiate because of the fine-grain nature of the sample; however, faint mineral banding comprised primarily of talc and white mica define alignment.	Lower plate	UTM	10 T	5 45	452 559	25 06
SHZ-6	1	Copley Greenstone	Fault	Greenstone	very fine-grained chlorite, quartz, clinozoisite, and fine-grained clays and amphiboles. Faint mineral alignment defined by elongat grains of chlorite and amphibole. Highly fractured. Several different quartz veining events, chlorite and quartz sections between fractured sections of rock, and some calcite along vein edges.	Upper plate	UTM	10 T	5 45	479 519	30 19

Appendix A: Table of sample locations, GPS locations, mineralogy, rock type, and interpretation. Page 6 of 7.

Sample Name	Field Map Loc.	Formation	Map Unit	Rock Type	Mineralogy and texture	Interpret-ation	GPS Location				
SHZ-7	1	Fault Rocks (mapped as part of Trinity terrane)	Fault	mylonite	comprised mainly of talc, white micas, serpentine, chlorite, actinolite, and fine grained clays. Exhibits mineral banding, mineral alignment defining a faint s-c fabric, and porphyroclasts o relic hornblendes forming sigma clasts. Relict hornblende altered to actinolite. Outcrop exhibits strong foliation striking N10W ar dipping 43SW.	Lower plate	UTM	10 T	5 45	479 519	30 19
SHZD-8	1		Dike	rhyolite	consists mainly of strongly aligned, poikilitic plagioclase containing fine-grained epidote group inclusions, and quartz; wi lesser amounts of orthoclase feldspar, chlorite, fine-grained white micas, fine-grained clays, and saussurite. Anastomozing and moderately rough foliation, defined by thin bands of white mica and quartz, flows around the plagioclase crystals creating augens Veins intersect the foliation perpendicularly.	Intrusive/ cogenetic with Shear zone	UTM	10 T	5 45	479 519	30 19
SHZ-9	2	Fault Rocks (mapped as part of Trinity terrane)	Oum	Fault breccia	comprised of a serpentine fault breccia with felsic and mafic clasts ranging up to boulder size in a serpentine, quartz, chlorite, and smectite matrix. Matrix consists of serpentine flows around angular plutonic clasts, creating planar crystal alignment. Clasts are plagiogranite, amphibolite, and serpentine. Exhibits pulled apart clasts with quartz fibers between fragments.	Lower plate	UTM	10 T	5 45	479 556	66 89
SHZ-10	2	Fault Rocks (mapped as part of Trinity terrane)	Oum	Fault breccia		Lower plate	UTM	10 T	5 45	479 556	66 89

Appendix A: Table of sample locations, GPS locations, mineralogy, rock type, and interpretation. Page 7 of 7

Sample Name	Field Map Loc.	Formation	Map Unit	Rock Type	Mineralogy and texture	Interpret-ation	GPS Location				
Lower Plate											
D-3	4	Trinity terrane	SDd	porphyritic hornblende andesite	porphyritic pluton with euhedral hornblende up to 3 mm in lengt (altered to fine-grain amphiboles, chlorite, and calcite); euhedral mm plagioclase (altered to saussurite and fine-grained clay); and minor cubic pyrite. The fine-grained groundmass consists of microcrystalline quartz, plagioclase, chlorite, and small laths of clinozoisite.	Lower plate	UTM	10 T	5 45	466 574	94 84
D-4		Trinity terrane	Ogd			Lower plate	none				
UM-1		Trinity terrane	Oum			Lower plate	UTM	10 T	5 45	420 565	23 73
UM-2	A	Trinity terrane	Oum	serpentinized peridotite	dark to blackish green serpentinized peridotite. Complete psuedomorphic alteration to serpentine and magnetite, forming serpentinite. Opaque minerals, faintly aligned in hand sample, preserve original grain boundaries and idiomorphic granular texture.	Lower plate	UTM	10 T	5 45	462 517	77 52
UM-3	B	Trinity terrane	Oum	serpentinized peridotite		Lower plate	UTM	10 T	5 45	454 579	50 65
UM-4	B	Trinity terrane	Oum	serpentinized peridotite		Lower plate	UTM	10 T	5 45	454 579	50 65